PB-224 202

ABSORPTION OF SO2 BY ALKALINE SOLUTIONS IN VENTURI SCRUBBER SYSTEMS

WEST VIRGINIA UNIVERSITY

JULY 1973

DISTRIBUTED BY:

NTIS
National Technical Information Service
U. S. DEPARTMENT OF COMMERCE

PB 224 202

EPA-650/2-73-003

July 1973

Environmental Protection Technology Series

ABSORPTION OF SO_2 BY ALKALINE SOLUTIONS IN VENTURI SCRUBBER SYSTEMS

Reproduced by
NATIONAL TECHNICAL
INFORMATION SERVICE
US Department of Commerce
Springfield, VA 22151

Office of Research and Monitoring
U.S. Environmental Protection Agency
Washington, D.C. 20460

170

BIBLIOGRAPHIC DATA SHEET

1. Report No. EPA-650/2-73-003

2.

3. Recipient's Accession No. PB-224 202

4. Title and Subtitle

Absorption of SO_2 by Alkaline Solutions in Venturi Scrubber Systems

5. Report Date July 1973

6.

7. Author(s)

C.Y. Wen and S. Uchida

8. Performing Organization Rept. No.

9. Performing Organization Name and Address

Department of Chemical Engineering
West Virginia University
Morgantown, West Virginia 26505

10. Project/Task/Work Unit No.

11. Contract/Grant No.

Grant No. 800781

12. Sponsoring Organization Name and Address

EPA, Office of Research and Development
NERC-RTP, Control Systems Laboratory
Research Triangle Park, North Carolina 27711

13. Type of Report & Period Covered

Final

14.

15. Supplementary Notes

16. Abstracts

The report describes studies of SO2 absorption from flue gases by water and alkaline solutions in venturi scrubber processes, including recycle of the scrubbing liquor. It proposes mathematical models describing the process momentum, heat, and mass transfer for SO2-H2O, SO2-NaOH-H2O, SO2-CaO-H2O, and SO2-CaCO3-H2O systems. The momentum, heat, and mass balances describe the performance of the processes taking place in the venturi scrubber. It generates a set of first-order, nonlinear, ordinary differential equations, relating total pressure, liquid velocity, SO2 concentration in the liquid, etc. along the axial direction. It solves these equations numerically for performance profiles, used to examine the effects of such operating variables as liquid flow rate and the concentration of alkali in the liquid phase on the absorption rate. It analyzes data from various size holding tanks and proposes mathematical models for the lime/limestone slurry process holding tanks. Finally, it combines these models to simulate the venturi/holding-tank system with closed-loop recycling of the liquor. It examines the sensitivities of such operating variables as the recycling liquor rate and the alkali makeup rate on the absorption. It qualitatively discusses such practical problems as oxidation of sulfite to sulfate and scaling of the solids. The calculated results using these models show good agreement with experimental data obtained by several investigators.

17. Key Words and Document Analysis. 17a. Descriptors

Air Pollution	Calcium Oxides
Sulfur Dioxide	Calcium Carbonates
Absorption	Limestone
Washing	Slurries
Flue Gases	Scaling
Water	Oxidation
Circulation	
Mathematical Models	
Sodium Hydroxide	

17b. Identifiers/Open-Ended Terms

Air Pollution Control
Stationary Sources
Alkaline Solutions
Venturi Scrubbers

17c. COSATI Field/Group 13B, 7A, 7B

18. Availability Statement

Unlimited

19. Security Class (This Report) UNCLASSIFIED

20. Security Class (This Page) UNCLASSIFIED

21. No. of Pages ~~157~~ 170

22. Price $4.75

FORM NTIS-35 (REV. 3-72)

USCOMM-DC 14952-P72

EPA-650/2-73-003

ABSORPTION OF SO_2 BY ALKALINE SOLUTIONS IN VENTURI SCRUBBER SYSTEMS

by

C. Y. Wen and S. Uchida

Department of Chemical Engineering
West Virginia University
Morgantown, West Virginia 26505

Contract No. EHS-D-71-20
Grant No. 800781
Program Element No. 1A2013

EPA Project Officer: Robert H. Borgwardt

Control Systems Laboratory
National Environmental Research Center
Research Triangle Park, North Carolina 27711

Prepared for

OFFICE OF RESEARCH AND MONITORING
U. S. ENVIRONMENTAL PROTECTION AGENCY
WASHINGTON, DC 20460

July 1973

i9

This report has been reviewed by the Environmental Protection Agency and approved for publication. Approval does not signify that the contents necessarily reflect the views and policies of the Agency, nor does mention of trade names or commercial products constitute endorsement or recommendation for use.

ABSTRACT

Studies of SO_2 absorption from flue gases by water and alkaline solutions in venturi scrubber processes which include recycle of the scrubbing liquor are made. Mathematical models are proposed which describe the momentum, heat and mass transfer in the processes for systems of SO_2-H_2O, SO_2-NaOH-H_2O, SO_2-CaO-H_2O, and SO_2-$CaCO_3$-H_2O.

The momentum, heat and mass balances describe the performance of the processes taking place in the venturi scrubber. A set of first-order, nonlinear, ordinary differential equations are generated relating total pressure, liquid velocity, SO_2 concentration in the liquid, etc. along the axial direction. These equations are numerically solved to give performance profiles which are used to examine the effects of the operating variables such as the liquid flow rate and the concentration of alkali in the liquid phase on the absorption rate.

Data obtained from various sizes of holding tanks are analyzed and mathematical models for the holding tanks for the lime and limestone slurry processes are proposed.

Finally these models are combined to simulate the venturi-holding tank system with closed-loop recycling of the liquor. The sensitivities of some operating variables such as the recycling liquor rate and the alkali make-up rate on the absorption are examined.

Practical problems such as oxidation of sulfite to sulfate and scaling of the solids are qualitatively discussed.

The calculated results using these models show good agreement with experimental data obtained by several investigators.

In this investigation it was found that:

1. A significantly large amount of heat and mass transfer takes place near the liquid nozzle in the venturi scrubber.

2. The operation of the venturi scrubber is practically isothermal except in the zone extending a few centimeters from the liquid injection nozzle.

3. The dissolution of lime into weak acid solutions can be explained by a shrinking core model.

4. The performance of the holding tank in the limestone slurry process can be approximated by an equilibrium stage model in which the tank is assumed to be in dynamic equilibrium with the surroundings.

TABLE OF CONTENTS

Chapter Page

ABSTRACT iii

TABLE OF CONTENTS v

LIST OF FIGURES ix

LIST OF TABLES xiii

I. INTRODUCTION 1

A. Description of Lime/Limestone Slurry Scrubbing Process 2

B. Scope of Investigation 4

II. LITERATURE REVIEW 8

A. Mechanics of Venturi Scrubber Operation 8

(1) Pressure drop in a venturi scrubber 8

(2) Mean diameter of liquid droplets 12

B. Theory of Gas Absorption 16

(1) Gas absorption without chemical reaction 17

(2) Gas absorption with chemical reaction 20

(3) Gas absorption in a venturi scrubber 20

III. THEORETICAL DEVELOPMENT 25

A. Reaction Mechanism and Thermodynamics of Various Systems 26

(1) SO_2-H_2O system 26

(2) SO_2-Alkaline solution system . 27

(3) CO_2-Alkaline solution system . 30

(4) SO_2-Limestone slurry system . . 32

B. Development of Performance Equations for a Venturi Scrubber 35

(1) Pressure drop 36

(2) Equation of motion of liquid droplet 38

(3) Heat and mass transfer in a venturi scrubber 42

(4) Performance equations in dimensionless forms 44

(5) Gas-phase heat and mass transfer coefficients 46

(6) Rate of gas absorption into spherical droplet 47

C. Dissolution of Lime and Limestone in a Holding Tank 51

(1) Properties and behavior of lime in acid solution 52

(2) Model for dissolution of lime in a holding tank 54

(3) Properties and behavior of limestone in SO_2 scrubbing liquor . 57

(4) Model for simulation of a holding tank in limestone process . 64

D. Overall Operation of Venturi Scrubber System with a Closed-Loop 70

IV. RESULTS AND DISCUSSION 76
  A. Simulation of Performance of Venturi Scrubbers 76
    (1) Description of the experiments. 76
    (2) Pressure drop in a venturi scrubber 80
    (3) Momentum, heat and mass transfer 80
  B. Simulation of the Holding Tank Performance 92
    (1) Holding tank for the lime slurry process 92
    (2) Holding tank for the limestone slurry process 96
  C. Performance of Venturi-Holding Tank Systems with Closed-Loop Recycle of the Scrubbing Slurry 100
    (1) Lime slurry process with a closed-loop recycle of the scrubbing liquor 100
    (2) Limestone slurry process with a closed-loop recycle of the scrubbing liquor 102
  D. Scaling and Oxidation in Lime/Limestone Processes 106
V. CONCLUSIONS AND RECOMMENDATIONS 114
NOMENCLATURE 119
BIBLIOGRAPHY 129

APPENDICES

  A. Enhancement Factor for Gas Absorption with Instantaneous Chemical Reaction into a Liquid Drop . . . 137

B. Derivation of Equation (105) . . . 144

C. The Rate of Gas Absorption Accompanied by Instantaneous Irreversible Reaction in a Liquid Droplet in a Venturi Scrubber--A Numerical Solution 147

D. Comments on the Physical and Chemical Properties used in the Mathematical Models of the Scrubbing Processes 151

LIST OF FIGURES

Figure		Page
1	Three Basic Process Routes for SO_2 Scrubbing by Lime/Limestone Slurry	3
2	Solubility of SO_2 in Water vs. SO_2 Partial Pressure	28
3	Comparison of Experimental Data on Rate of SO_2 Absorption with Values based on Penetration Theory	29
4	Correlation of Instantaneous Unsteady State Drag Coefficient with Reynolds Number	41
5	Concentration Profile of SO_2 in a Droplet (SO_2-H_2O System: constant interfacial concentration)	49
6	Equilibrium Concentration of Total Calcium at 50°C and its concentration in Outlet Liquor from Holding Tank vs. Liquor pH	60
7	Equilibrium Concentration of Total Sulfate at 50°C and its Concentration in Outlet Liquor from Holding Tank vs. Liquor pH	61
8	Equilibrium Concentration of Total Sulfite at 50°C and its Concentration in Outlet Liquor from Holding Tank vs. Liquor pH	62
9	Equilibrium Concentration of Total Carbonate at 50°C and its Concentration in Outlet Liquor from Holding Tank vs. Liquor pH	63
10	Material Balance Around a Holding Tank	66

11 pH of Limestone Slurry vs. Vapor Pressure of CO_2 at 50°C 69

12 Mass Transfer Coefficient for CO_2 Evolution in the Holding Tank vs. Liquor Flow Rate 71

13. Venturi-Holding Tank System with Closed-Loop 73

14 (a) Logic Diagram for Simulation of Venturi-Holding Tank Recycling System (Lime Slurry Process) 74
(b) Logic Diagram for Simulation of Venturi-Holding Tank Recycling System (Limestone Slurry Process) 75

15 (a) Dimensions of Venturi Scrubber used by Harris et al.
(b) Dimensions of Flooded Disc Scrubber (FDS) used by Gleason et al . 77

16 Dimensions of Venturi Scrubber used by Johnstone et al 79

17 Comparison of Calculated Pressure Drop in EPA Venturi Scrubber and Flooded Disc Scrubber with Experimental Data 82

18 Pressure Profile in Venturi Scrubber used by Johnstone et al. 83

19 Velocity and Sulfur Concentration Profiles along Axial Distance in EPA Venturi Scrubber 85

20 Temperature Profiles of Gas and Liquid along Axial Distance in EPA Venturi Scrubber 87

21 Profiles of Cumulative Absorption Rate in Venturi Scrubber (Experiment of Johnstone et al) 88

22 Comparison of SO_2 Removal Rate in the Venturi Scrubber Calculated with Experimental Data Obtained by Johnstone et al. 89

23 Concentration Profile of SO_2 in a Droplet (EPA Venturi: H_2O-SO_2 System) 90

24 Concentration Profiles of SO_2 and NaOH in a Droplet (EPA Venturi: $NaOH-SO_2-H_2O$ System) 91

25 Comparison of Calculated SO_2 Removal % with Experimental Data 93

26 Comparison of Calculated Concentration of $Ca(OH)_2$ in Solution from Holding Tank with Data Obtained by Gleason et al. 95

27 Comparison of the Values of Calculated pH of Outlet Liquor from Holding Tank with Experimental Data (Limestone Slurry Process) 97

28 Comparison of Calculated Values of Concentrations of Total Calcium and Sulfite in Outlet Liquor from Holding Tank with Experimental Data (Limestone Slurry Process) 98

29 Comparison of Calculated Values of Concentrations of Total Sulfate and Carbonate in Outlet Liquor from Holding Tank with Experimental Data (Limestone Slurry Process) 99

30 Performance of a Venturi-Holding Tank System with a Closed-Loop Recycling of Slurry (Lime Slurry Process) 101

31 Comparison of Calculated SO_2 Removal % with Experimental Data Obtained by Epstein et al. (42) (Limestone Slurry Process) 104

32 Performance of a Venturi-Holding Tank System with a Closed-Loop Recycling of Slurry (Limestone Slurry Process) . . 106

A-1 Concentration Profile across the Gas-Liquid Interface with Instantaneous Reaction. The Dashed Line Indicates the Approximate Concentration Gradient across the Fluid Film in the absence of Chemical Reaction (APPENDIX A) . . 138

D-1 pH Values of $Ca(OH)_2$ Solutions of Varying Concentration and Temperature (APPENDIX D) 155

LIST OF TABLES

Table		Page
1	Correlation for Pressure Drop in Venturi Scrubber	11
2	Empirical Equations for Droplet Diameter and Their Applicable Ranges	13
3	Experimental Conditions used in the Three Experiments	81
4	Experimental Conditions of Holding Tanks used in Four Experiments . . .	94
D-1	Ionic Velocities U at Infinite Dilution, 18°C	153
D-2	Solubility of Lime in Water Expressed As CaO or $Ca(OH)_2$ at Different Temperatures	154
D-3	pH of Lime Solution at 25°C	156

I. INTRODUCTION

In recent years considerable effort has been devoted to investigating the ever-growing problem of acid gas and dust pollution of the atmosphere. Especially the problem of atmospheric pollution by sulfur dioxide emission has stimulated a large amount of research and development of methods for removing the pollutant from waste gases (8, 13, 23, 42, 50, 70, 95, 98, 99, 100, 104, 111, 116, 117, 118). Many types of processes have been proposed such as the oxidation or reduction of SO_2 in a gas stream to produce sulfuric acid or sulfur, the adsorption on activated carbon or other adsorbents, the absorption by various types of solids and liquid followed by the regeneration of the absorbents, and the absorption by slurry of lime or limestone followed by discarding the loaded absorbent.

Although SO_2 is not recovered in a useful form in the lime/limestone processes, these processes have the outstanding advantages of relative simplicity, lowest investment, and freedom from the problems of marketing a by-product. For these reasons they are being favored by the electric power industry as one of the best solutions to the SO_2 emission problem for use in the immediate future.

The application of the lime/limestone slurry scrubbing process is not only suitable to the power industry but also to the other types of plants that emit SO_2 such as smelters, refineries, and sulfuric acid plants.

In this chapter, a general description of the lime/limestone slurry scrubbing processes and the purpose of this investigation are given.

A. Description of Lime/Limestone Slurry Scrubbing Process

There are three major process routes for SO_2 scrubbing by lime/limestone slurry as shown in Figure 1. The advantages and disadvantages of these methods are as follows:

Method (a). Limestone Slurry Process: This is the simplest of the lime/limestone processes and seems to be the one favored by the power industries at present time. The main drawback is that limestone is not as reactive as lime and only sparingly soluble in water. This necessitates both the usage of more limestone than that required stoichiometrically and large equipment size. The limestone used must be ground to fine powder in order to promote high reactivity and better utilization.

Method (b). Lime Slurry Process: Lime, which is much more reactive and is more alkali than limestone, can be used to improve the scrubbing efficiency. Although

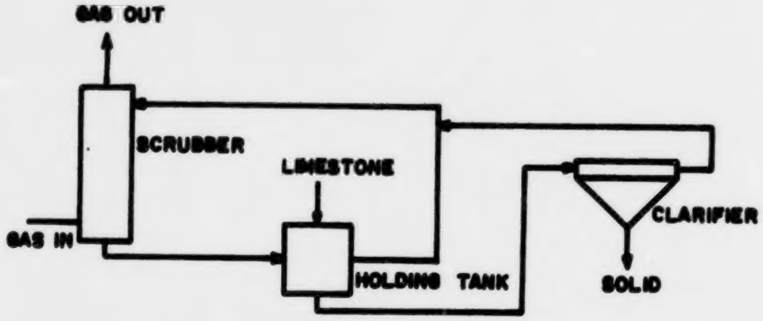

Method (a). Limestone Slurry Process

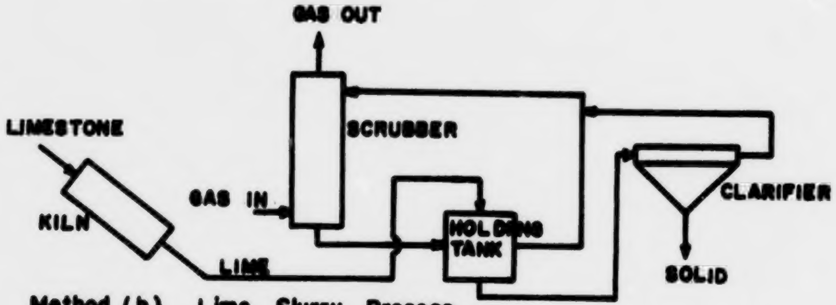

Method (b). Lime Slurry Process

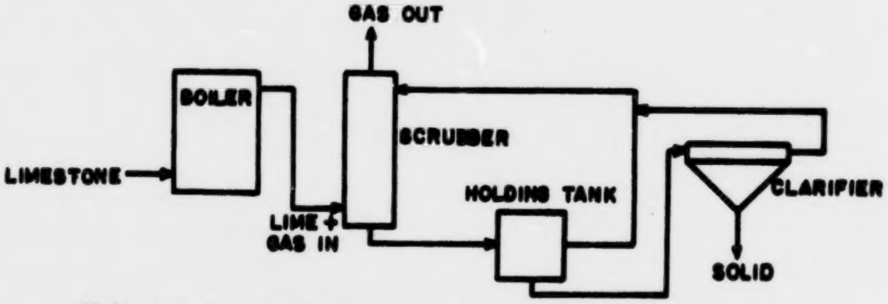

Method (c). Limestone Injection to Boiler Process

Figure 1. Three Basic Process Routes for SO_2 Scrubbing by Lime/Limestone Slurry

smaller operating costs are required due to low recirculation rate of the lime slurry, the cost of calcination of limestone to produce lime may be expensive. Use of lime may also increase the problem of scale formation in the scrubber.

Method (c). Limestone Injection to Boiler Process: The cost of calcination of limestone is a major disadvantage in lime slurry process. It can be reduced by injecting the limestone into the boiler furnace. The limestone injected into the boiler is calcined and the gas then carries the lime into the scrubber. Boiler fouling, overburning of limestone, inactivation of the lime, increased scaling in the scrubber are among the main problems that endanger this approach. This method is not applicable to some plants such as refineries, sulfuric acid plants or smelters.

There are several advantages and disadvantages for each of the methods described. The best process has to be selected by an overall consideration of the process including such factors as the economics of operation, reliability and availability of lime/limestone.

B. Scope of Investigation

To successfully design processes for the removal of pollutants from flue gases requires the understanding of the physical and chemical phenomena taking place in the scrubbing equipment. Although there are many types of scrubbers and process schemes, the present investigation is confined to a venturi-type scrubber combined with a holding tank for recycling the scrubber liquor. This combination is similar to Method (a) described above.

The venturi scrubber was originally developed for the purpose of dust and mist separation. It usually consists of a body, nozzle and diffuser. When a liquid is injected into a high velocity gas stream near the nozzle, the liquid becomes highly dispersed, a large surface area of the liquid is exposed for gas-phase contacting in the diffuser. High rates of heat and mass transfer in the atomization zone have been noted(3, 27, 44, 65, 66, 101, 121). This observation led to the development of the venturi atomizer which has found important applications in gas absorption, evaporation and aerosol collection. However, the theoretical principles and the design criteria have not been completely analyzed and the experimental data available in the literature have not yet been generalized.

Due to practical, as well as economical, consideration, most commercial wet scrubbing processes must be based on a closed-loop system in which the loaded liquor from the scrubber is regenerated and recycled within the process and not discharged from the process. To accomplish this, the venturi scrubber is combined with a mixing/

holding tank which regenerates the degenerated liquor with fresh feeds of lime or limestone. (See Figure 13)

The mechanisms of dissolution of lime or limestone into acid solutions such as recycling liquor in the limestone process are so complex that they are not fully understood. The elucidation of the dissolution mechanisms or performance of the holding tank is necessary for the overall design of a venturi-holding tank scrubber system.

The main objective of the study is to understand the thermodynamics and the kinetics of the system involved, and to elucidate the mechanical and hydrodynamic characteristics of the system so as to simulate the performance of heat and mass transfer in the venturi scrubber and the holding tank for various reaction systems.

Various theories of the gas absorption, with and without chemical reactions, which appear in the literature (21, 32, 33, 47, 48, 56, 71, 88, 90, 94, 96, 105, 106, 110, 114, 122, 124) are used in interpreting the phenomena in the venturi scrubber, and based on the experimental and pilot plant scale operating data (8, 13, 23, 42, 50, 98, 116) the rate-controlling mechanism for dissolution of solid lime and limestone into the recycling slurry is studied. The important mathematical models for a venturi scrubber and a holding tank will be developed and their inter-relationships will be briefly discussed. These models are based on the phenomenological observation of the actual process operations with some assumptions to simplify the evaluation of the model.

Finally, simulations of the venturi-holding tank system are performed using the proposed mathematical models. The overall efficiencies of the scrubber-holding tank systems are discussed and sensitivities of operating variables on the SO_2 removal efficiency are also investigated.

It is hoped that the information presented here can be used to find the best design of these processes.

II. LITERATURE REVIEW

Despite the many industrial applications of atomization techniques, little quantitative information on the performance of venturi scrubbers can be found in the literature. In designing and controlling of the performance of a wet scrubber, it is necessary to know the mechanism of atomization, to estimate the total pressure drop across the venturi scrubber, and to evaluate the amount of heat and mass transferred between the liquid droplets and the gas in the venturi scrubber. The auxiliary equipment associated with the wet scrubber such as the holding tank etc. must also be designed. The following is a review of the literature pertaining to the pressure drop in a venturi scrubber, atomization, gas absorption and the efficiency of venturi atomizers as gas absorbers.

A. Mechanics of Venturi Scrubber Operation

(1) Pressure drop in a venturi scrubber

The overall pressure drop across the venturi scrubber is an important practical factor which must be considered in the design of the scrubber since most of the operating costs are associated with the power consumed in overcoming the venturi's relatively high pressure drop.

The pressure drop for a gas flowing through a venturi scrubber can be estimated by considering the effects of friction along the wall of venturi scrubber and the acceleration of the injected liquid. Frictional losses depend largely upon the geometry to the scrubber and must be determined experimentally. Acceleration losses which are frequently predominant in the scrubber pressure drop, are fairly insensitive to the scrubber geometry and in most cases are predictable theoretically.

Several correlations for the pressure drop in a venturi scrubber available in the literature are summarized in Table 1.

Some of experimental data on the pressure drop in venturi scrubbers have been reported (12, 20, 39, 42, 49, 50, 82, 125). Matrozov's correlation (82) is probably the first to appear in the form of an equation. In 1963, Gieseke (49) performed experiments with a small scale venturi scrubber and found that the experimental data could be correlated by a plot of two quantities: that is, the product of the Euler number and the ratio of the volume flow rate of liquid to that of gas versus the axial distance divided by the product of the drop diameter and the square root of the Reynolds number. The computed pressure drops were about ten percent lower than the experimental values. This seems to be caused by neglecting the friction loss at the wall of the venturi scrubber.

Boothroyd (12) also measured the pressure drop of gaseous suspensions of fine particles flowing through a duct and found that the total pressure drop could be represented by the summation of several individual losses as shown in Table 1.

Recently Volgin et al. (125) presented an empirical correlation consisting of only one term which tends to zero in a dry venturi scrubber. Gleason and McKenna (50) also presented an empirical correlation for pressure drop in a flooded disc scrubber using a sodium carbonate solution.

Most of the pressure drop correlations discussed above were experimentally obtained on relatively small scale equipment. Therefore they are not applicable to different types or sizes of venturi scrubbers unless the values of the coefficients or the powers involved in these correlations are adjusted.

Calvert (24) and Boll (11) developed equations which seem to be applicable to a general type of venturi scrubber. Calvert derived a pressure drop equation by applying Newton's law to obtain the force required to change the momentum of the liquid flowing at a given rate. This equation does not contain a term accounting for the frictional losses at the wall of the venturi scrubber; however, this term becomes negligibly small at a high liquid rate in comparison with the term associated with

Table 1. Correlation for Pressure Drop in Venturi Scrubber

Investigator	Correlation
Matrozov (82)	$\Delta P_1 = \Delta P_d + 18 w^{1.08} m_o^{0.63}$
Geiseke (49)	$\Delta P = \frac{1}{g_c S \varepsilon}\left\{M_g \Delta v_g + M_L \Delta v_L + \frac{\Delta M_L}{2}(v_{g1} + v_{g2} - v_{L1} - v_{L2})\right\}$
Boothroyd (12)	$\Delta P_m = \Delta P_t + \Delta P_{as} + \Delta P_{ag} + \Delta P_{\rho s} + \Delta P_{\rho g}$
Volgin et al. (125)	$\Delta P_2 = 2.22 \times 10^{-2} w^2 q^{0.26} L^{0.143}$
Calvert (24)	$\Delta P_3 = 4 \times 10^{-7} v_g^2 q$
Gleason et al. (50)	$\Delta P_4 = 5.23 \times 10^{-9} v_g^2 (0.264F + 73.8)$
Boll (11)	$-\frac{\Delta P_{oz}}{\rho_g} = \frac{v_{go}^2 - v_g^2}{2g_c} + \frac{m}{g_c}\int_o^t v_g \left(\frac{dv_d}{dt}\right) dt$ $+ \frac{(m+1)}{2g_c}\int_o^t \frac{f v_g^2 v_d}{D_e} dt + \frac{1}{2g_c}\int_{z_o}^{z_1} \frac{f v_g^2}{D_e} dz$

the acceleration losses. Boll's equation is substantially the same as Gieseke's correlation except that the former takes the wall friction into consideration. This equation has been derived by taking a momentum balance on the gas and the liquid in a venturi scrubber and gives the pressure distribution within the venturi scrubber.

(2) Mean diameter of liquid droplets

Various correlations are available in the literature (51, 59, 68, 72, 81, 84, 89, 127, 129) to estimate the mean diameter of liquid droplets from various types of atomizers under different operating conditions. These correlations are applicable only to the specified type of atomizers within a certain range of operating conditions and fluid properties. These conditions include such variables as the volume ratio of gas and liquid, relative velocity of the gas and the liquid, type of nozzle, surface tension, viscosity of the liquid etc. Therefore, the number of correlations for droplet size applicable to a specific type of venturi atomizer is rather limited. These correlations are summarized in Table 2. In using one of these correlations to estimate the droplet diameter, it is important to select a proper correlation which takes these factors into consideration. Applicabilities of various correlations in terms of the range

Table 2. Empirical Equations for Droplet Diameter and Their Applicable Ranges

INVESTIGATOR	EQUATION*	APPLICABLE RANGE		
		v_{ro}[cm/sec]	(M_g/M_L)[-]	μ_L[poise]
Nukiyama and Tanasawa (89)	$D_{32}=58{,}500\,\frac{\sqrt{\sigma}}{v_{ro}\sqrt{\rho_L}}$ $+597\,\left(\frac{\mu_L}{\sqrt{\sigma\rho_L}}\right)^{0.45}\cdot\left(1000\frac{L_o}{G_o}\right)^{1.5}$	10,000 to sonic velocity	1.8 to 15	0.01 to 0.46
Mugele (84)	$\frac{D_{32}}{D_n}=A\left(\frac{D_n\rho_L v_{ro}}{\mu_L}\right)^{B}\cdot\left(\frac{\mu_L v_{ro}}{\sigma}\right)^{C}$ (A, B, C,; constants)	10,000 to sonic velocity	1.8 to 15	--
Gretzinger and Marshall (51)	$D_m=2{,}600\left[\left(\frac{M_L}{M_g}\right)\cdot\left(\frac{D_n v_{go}\rho_g}{\mu_g}\right)\right]^{0.4}$	10,000 to sonic velocity	1 to 15	0.01 to 0.30

Table 2. (continued)

INVESTIGATOR	EQUATION*	APPLICABLE RANGE		
		v_{ro} [cm/sec]	(M_g/M_L) [-]	μ_L [poise]
Wigg (129)	$D_m = 20{,}000 \left(\frac{\mu_L}{\rho_L}\right)^{\frac{1}{2}} \cdot M_L^{0.1} \left(1+\frac{M_L}{M_g}\right)^{\frac{1}{2}} \cdot \frac{D_n^{0.1} \sigma^{0.2}}{\rho_g^{0.3} v_{ro}}$	8,000 to 35,000	0.5 to 20.2	0.032 to 0.45
Kim and Marshall (68)	$D_m = 5{,}120 \frac{\sigma^{0.41} \mu_L^{0.32}}{(v_{ro}^2 \rho_g)^{0.57} S_o^{0.36} \rho_L^{0.16}}$ $+18{,}900 \left(\frac{\mu_L^2}{\rho_L \sigma}\right)^{0.17} \cdot \frac{1}{v_{ro}^{0.54}} \left(\frac{M_g}{M_L}\right)^m$ $m = -1$ for $M_g/M_L < 3$ $m = -0.5$ for $M_g/M_L > 3$	7,500 to sonic velocity	0.06 to 40	0.01 to 0.50

* all units are in c. g. s. units

of mass ratio of gas and liquid, relative velocity of gas and liquid, and the viscosity of liquid, which are considered to be among the most important factors, are also indicated in Table 2.

Among these correlations, probably the best known and the most widely used is that of Nukiyama and Tanasawa (89). Analysis of this equation shows that for a ratio of Q_a/Q_L greater than 5,000, the second term has only a slight influence on droplet size. Also, in this correlation the size is determined by the relative velocity of the gas and liquid, the liquid density and surface tension; the nozzle dimensions do not enter the correlation. This correlation is suitable for flows of high relative velocity and of large mass ratio of gas and liquid.

Wetzel (127) studied venturi atomization of a molten wax and a molten metal alloy with room temperature air. His data indicated an inverse variation of the spray particle size with the air-to-liquid mass ratio. The droplet size decreased from 110 to 30 μ when air-to-liquid mass ratio increased from 100 to 300.

Mugele (84) attempted to develop an expression for the maximum and mean droplet size by dimensional analysis. His correlation covers almost the same range as that of Nukiyama and Tanasawa. A similar correlation was subsequently derived by Gretzinger and Marshall (51) which consists of dimensionless groups having the same ranges of applicability as those for Nukiyama and Tanasawa's correlation.

Wigg's correlation (129), which was proposed to explain wax spray experiments, covers a wide range of relative velocity and mass ratio of gas and liquid; however, the viscosity of the wax was substantially higher than that of water and aqueous solutions used in this study.

Kim and Marshall (68) recently developed a correlation which covers wide ranges of the operating variables. Their correlation has a form similar to that of Nukiyama and Tanasawa, but predicts smaller droplet sizes under similar operating conditions. However, Nukiyama and Tanasawa's equation was based on the data obtained by a physical sampling technique which probably introduced some errors due to evaporation and the target effect resulting from the presence of the sample collecting device. Kim and Marshall (68), also, reported that a modified form of their correlation can be used to correlate Wetzel's drop-size data (127) obtained by venturi atomization.

B. Theory of Gas Absorption

Since gas absorption is one of the most common unit operations in the chemical industry, there are voluminous publications by numerous researchers on the theory of diffusion in counter-current equipment and on the performance of packed towers and other devices used in gas absorption. Only a brief review of this field is given in this section.

(1) Gas absorption without chemical reaction

Historically the best known theory of physical absorption, the two-film theory, was proposed by Lewis and Whitman (73) in 1923. This theory has proved to be of great use in understanding the process of diffusion between two fluids, although there appears to be no tangible evidence of an appreciable diffusional resistance at the actual interface of the fluids, or of the validity in the assumption that equilibrium exists at the interface of the two fluids in contact. In the case of mass transfer between gas and liquid, the concentration and the partial pressure of solute component A at the interface are assumed to be related by the equilibrium condition. Thus,

$$C_{Ai} = H_A p_{Ai} \tag{1}$$

Under the steady-state operation, the solute gas A is absorbed into a liquid stream at a rate given by:

$$N_A = k_G (p_A - p_{Ai}) = k_L (C_{Ai} - C_A) \tag{2}$$

This equation, based on the two-film model, gives rise to the so-called "additivity of resistances". Using the relation (1) P_{Ai} and C_{Ai} are eliminated and we obtain:

$$N_A = K_G\,(p_A - p_A^*) = K_L\,(C_A^* - C_A) \qquad (3)$$

where

$$\frac{1}{K_G} = \frac{1}{k_G} + \frac{1}{H_A k_L} \quad , \quad \frac{1}{K_L} = \frac{H_A}{k_G} + \frac{1}{k_L} \qquad (4)$$

$$C_A^* = H_A p_A \quad , \quad C_A = H_A p_A^*$$

The values of mass transfer coefficients must be estimated for a given type of contacting device and a given operating condition. Kinetic theories of gas are sufficiently well established to the point that mass transfer coefficients for most gases can be estimated theoretically (47). There are also many experimental correlations available (48, 88, 96, 106, 114, 124).

For the mass transfer coefficient in the liquid phase, two cases must be considered; gas absorption with and without a chemical reaction in the liquid phase. There are many theories to explain the complex diffusion processes in the liquid phase even for physical absorption since the two-film theory was first proposed.

In 1935, Higbie (56) proposed the penetration theory to explain gas absorption into quiescent liquid under unsteady state conditions. The average rate of gas absorption and the mass transfer coefficient in time o ~ t are functions of time and expressed as follows:

$$N_A = 2\,(C_{Ai}-C_{Ao})\sqrt{\frac{D_A}{\pi t}} \qquad (5)$$

$$k_L^o = 2\sqrt{\frac{D_A}{\pi t}} \qquad (6)$$

The exposure time t is determined by the hydrodynamic conditions within the system and is the only parameter required to account for their effect on the mass transfer coefficient k_{LA}.

Applications of the Higbie's penetration theory to gas absorption into agitated liquids where the dissolved gas is transported from the surface to the bulk of a liquid phase by convective motion has been made by Danckwerts(31), Harriott(52), and others (33, 114, 124).

Higbie's model specifies the same time of exposure for all the elements of the surface. However, Danckwerts (31) assumes that the probability of an element of the surface being replaced by fresh liquid is independent of the length of time for which it has been exposed. That is to say, a stationary distribution of the surface ages is assumed in which the fraction of the surface has been exposed to the surface for times between θ and $(\theta + d\theta)$ is $se^{-s\theta}d\theta$. Here s is the fraction of the area of surface which is replaced with fresh liquid in unit time. The average rate of absorption by this model and its mass transfer coefficient are:

$$N_A = (C_{Ai}-C_{Ao})\sqrt{D_A s} \qquad (7)$$

$$k_L^o = \sqrt{D_A s} \qquad (8)$$

Here again, the hydrodynamic conditions within the system, so far as they affect k_{LA}, are accounted for by a single parameter s which has the dimensions of reciprocal time.

Some surface-age distributions other than those of Higbie and Danckwerts have been discussed by Danckwerts(33).

(2) Gas absorption with chemical reaction

When gas absorption is accompanied by a chemical reaction, its rate is accelerated to a certain degree depending upon the type of the reaction. The kinetic theories of simultaneous diffusion and chemical reaction in the liquid phase were first developed by Hatta(55), followed by many investigators. There are a number of theories which have been developed and are associated with different types of reactions and hydrodynamic conditions. Many cases with complicated chemical reactions have been numerically solved (16, 17, 18, 19, 22, 63, 79, 97). The case of gas absorption with an instantaneous second-order chemical reaction is discussed in Appendix A. The details of other models can be found in the literature cited (33, 60, 90, 94, 106, 114).

(3) Gas absorption in a venturi scrubber

Comings et al. (27) found good heat transfer from gas to liquid, with a subsequent rapid vaporization of the liquid when the liquid was introduced in the form of a simple jet into a high-velocity gas streams. Using a venturi atomizer, a smoke cloud was created by vaporizing oil with subsequent condensation to form very small drops. They found that the hot gas was cooled rapidly and very high heat transfer rate was achieved in this type of atomizer. This type of scrubber was considered most suitable when the gas film controls the rate because of stagnant conditions existing within the drops. Pigford et al. (101) on the other hand proved that this type of equipment can also be used even when the liquid film resistance controls the rate such as in the desorption of oxygen from water.

Johnstore and Roberts (66) measured the overall efficiency of a venturi scrubber as a gas absorber and obtained an equation for the efficiency of absorption.

Tassler (121), Feild (44), and Johnstone et al.(65) studied the absorption of sulfur dioxide in alkaline solutions using a venturi scrubber and measured experimentally the amount of sulfur dioxide absorbed at various distances from the point of liquid injection. They found that the average volumetric gas film coefficient, $K_g a$, increased with the liquid feed rate and the gas velocity at a given position in the venturi scrubber, and decreased at a constant liquid rate and gas velocity with increasing distance from the point of liquid injection.

Tassler (121) also studied the performance of a venturi scrubber for the desorption of carbon dioxide from water. The overall transfer coefficient, K_La, was calculated from the experimental data. The values of K_La are higher than those obtained in packed towers under countercurrent operation. However, the values of K_La are smaller than those obtained for the absorption of sulfur dioxide in the same venturi scrubber.

Anderson and Johnstone (3) studied the absorption and subsequent liquid-phase reaction of catalyzed sodium sulfite solutions and the simultaneous absorption of atmospheric oxygen with nitrogen dioxide and with sulfur dioxide by water. They found that in the case of oxygen absorption by sodium sulfite solutions containing 0.01M $CoSO_4$ as a catalyst, the values of K_La close to the liquid injection point are nearly 100 times higher than those for oxygen absorption by pure water. The K_La values decrease rapidly with distance and are nearly equal to those for pure water at 1 inch from the liquid injection point.

Kuznetsov and Oratovskii (69) obtained equations for the rate of gas absorption with chemical reaction in the throat and the divergent section of a venturi scrubber, relating the number of transfer units and the degree of absorption to the principal operating and design parameters of the apparatus. They, also, showed that the liquid to gas ratio had an optimum value, while an increase in the gas velocity could lead either to an increase or to a decrease in the degree of absorption depending on the region in which the process was being conducted, that is, chemical reaction controlling, diffusion controlling or the intermediate region. The equations obtained by Kuznetsov et al. (69) for the number of transfer units in a venturi absorber were investigated by Boyadzhiev (14). The optimal conditions for gas absorption with various types of chemical reactions were also determined by Sazkin and Matrozov (112).

Markant et al. (80) studied the absorption of SO_2 from dilute gas streams by magnesium bisulfite solution and obtained a correlation for the vapor pressure of SO_2 over the magnesium bisulfite-magnesium monosulfite solution for their experimental ranges of temperature and acid composition. A correlation for the effects of magnesium monosulfite concentration, acid strength, and acid temperature on SO_2 absorption efficiency of the venturi scrubber was obtained.

Elenkov and Boyadzhiev (40) obtained experimental data on the absorption of SO_2 in water and aqueous solutions of surfactants in a nozzleless venturi scrubber in the range of $N_{Re} = (1.44 \sim 3.27) \times 10^4$ and a gas throat velocity of $40 \sim 120$ m/ sec.

Volgin et al. (125) studied absorption of SO_2 by ammonium sulfite-bisulfite solution in a venturi scrubber which had a throat with either rectangular (10 x 15 mm) cross section and a length of 13 mm, or cylindrical (20 mm diameter) cross section and a length of 10 mm. They demonstrated that absorption in multi-stage venturi scrubbers are competitive with conventional scrubbers such as packed towers and bubble towers with respect to the pressure drop and the consumption of the electric power and that there is an optimum condition of venturi operation with respect to the pressure loss and the extent of absorption.

Tillman (123) recently studied the performance of a venturi scrubber analytically. The mechanism of particulate collection by water droplets in a venturi scrubber was investigated and the effect of water drop size on collection efficiency, the importance of water flow rate, and the best point for injection of the water have been shown.

Gleason and McKenna (50) performed experiments on SO_2 absorption by sodium carbonate, calcium oxide, and calcium carbonate solutions in a flooded disc scrubber which is a type of venturi scrubber. They obtained extensive data on the SO_2 removal efficiency, pressure drop etc. Princiotta and Epstein (104) recently presented the data on the SO_2 removal efficiency and pressure drop obtained from their commerical size plant.

III. THEORETICAL DEVELOPMENT

Despite many important applications of venturi atomization in various fields of industries, only a few theoretical studies can be found in the literature. Most of these are however restricted to the experimental studies of the efficiency of the particle removal from the gas or on the pressure drop, heat and mass transfer in a venturi scrubber of relatively small size. Therefore, the results do not cover all ranges of the operating conditions which may be encountered in practice.

In this chapter, some theoretical models are developed for purposes of simulation and design of a venturi-holding tank system as a gas absorber. First, reaction kinetics of several systems treated in this study, mechanics of a venturi scrubber operation, and heat and mass transfer taking place in the process are discussed in the following sections. The performance equations describing a venturi scrubber operation are then derived and are used to simulate the SO_2 gas absorption both for open-loop and close-loop operations. Finally, the dissolution of lime and limestone are investigated and simulation models are proposed for holding tanks and the simulation of the venturi-scrubber combined with a holding tank is discussed.

A. Reaction Mechanism and Thermodynamics of Various Systems

In this section, the reaction mechanisms and the thermodynamics for the systems in this study, namely, (1) SO_2 - H_2O system, (2) SO_2 - alkaline solution system, (3) CO_2 - alkaline solution system and (4) SO_2 - limestone system are discussed.

(1) SO_2 - H_2O system

When sulfur dioxide is absorbed into water, the following reactions occur in the liquid phase:

$$SO_2 + H_2O \rightleftharpoons H_2SO_3 \rightleftharpoons H^+ + HSO_3^- \qquad (9)$$

$$HSO_3^- \rightleftharpoons H^+ + SO_3^= \qquad (10)$$

The equilibrium constants for reactions (9) and (10) at 25°C are $K_9 = 1.7 \times 10^{-2}$ g-mole/l and $K_{10} = 6.2 \times 10^{-7}$ g-mole/l, respectively (92). Therefore, the latter reaction can be neglected under normal conditions. The forward and backward reaction rate constants for reaction (9) with respect to SO_2, and H^+ and HSO_3^- are $k_f = 3.4 \times 10^6$ sec^{-1} and $k_b = 2 \times 10^8$ l/g-mole · sec (92). In the light of the data obtained by Lynn et al. (78), Onda et al. (92) and Hikita et al. (57) it appears that the rate of hydrolysis reaction of SO_2 in water is rapid relative to the diffusion process and that the surface of the water film is instantly saturated at the equilibrium concentration upon exposure to gaseous SO_2. Therefore, the absorption of SO_2 in water may be treated as a physical phenomenon. The equilibrium relation of this system is given in Figure 2. The SO_2 absorption rates obtained by two types of contacting devices are compared with the theoretical rate using the equilibrium relation as shown in Figure 3. Good agreement in the comparison tends to validate the mechanism presented above.

(2) SO_2 - Alkaline solution system

In the case of the absorption of SO_2 by alkaline solutions, two additional reactions may occur,

$$SO_2\ (aq) + OH^- \rightleftharpoons HSO_3^- \qquad (11)$$

$$HSO_3^- + OH^- \rightleftharpoons SO_3^= + H_2O \qquad (12)$$

and the equilibrium constants for reactions (11) and (12) are $K_{11} = 1.7 \times 10^{12}$ l/g-mole and $K_{12} = 6.2 \times 10^6$ l/g-mole, respectively.

Experimental data obtained by SO_2 absorption into sodium hydroxide solutions by Onda et al. (92) and Hikita et al. (57) have been correlated in the present study by the penetration theory based on an assumption that the reaction is instantaneous and irreversible as shown in Figure 3. The fact that the rate of SO_2 absorption into the sodium hydroxide solution can be represented by the penetration theory with an instantaneous reaction allows these two reactions to be considered as occurring instantaneously. Thus, from the values of equilibrium constants

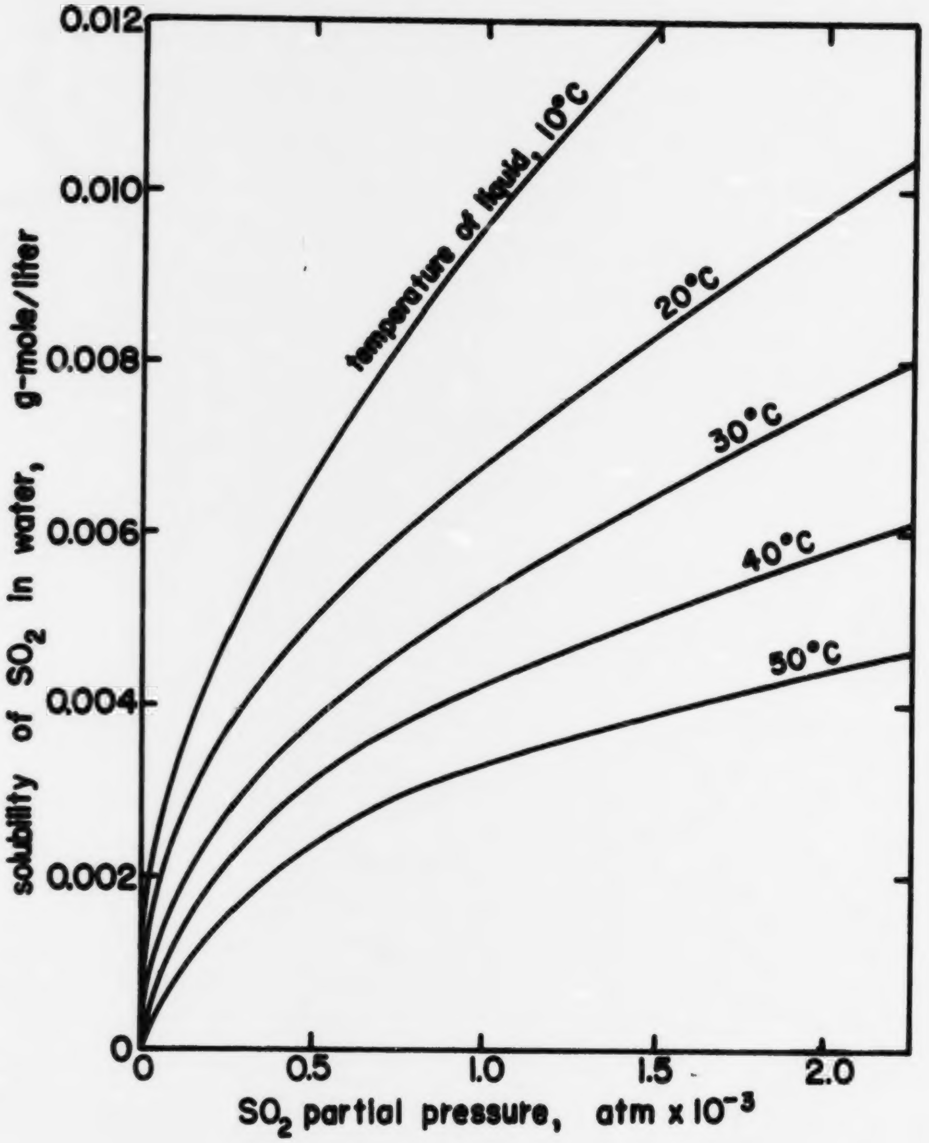

Figure 2. Solubility of SO_2 in Water vs. SO_2 Partial Pressure (93)

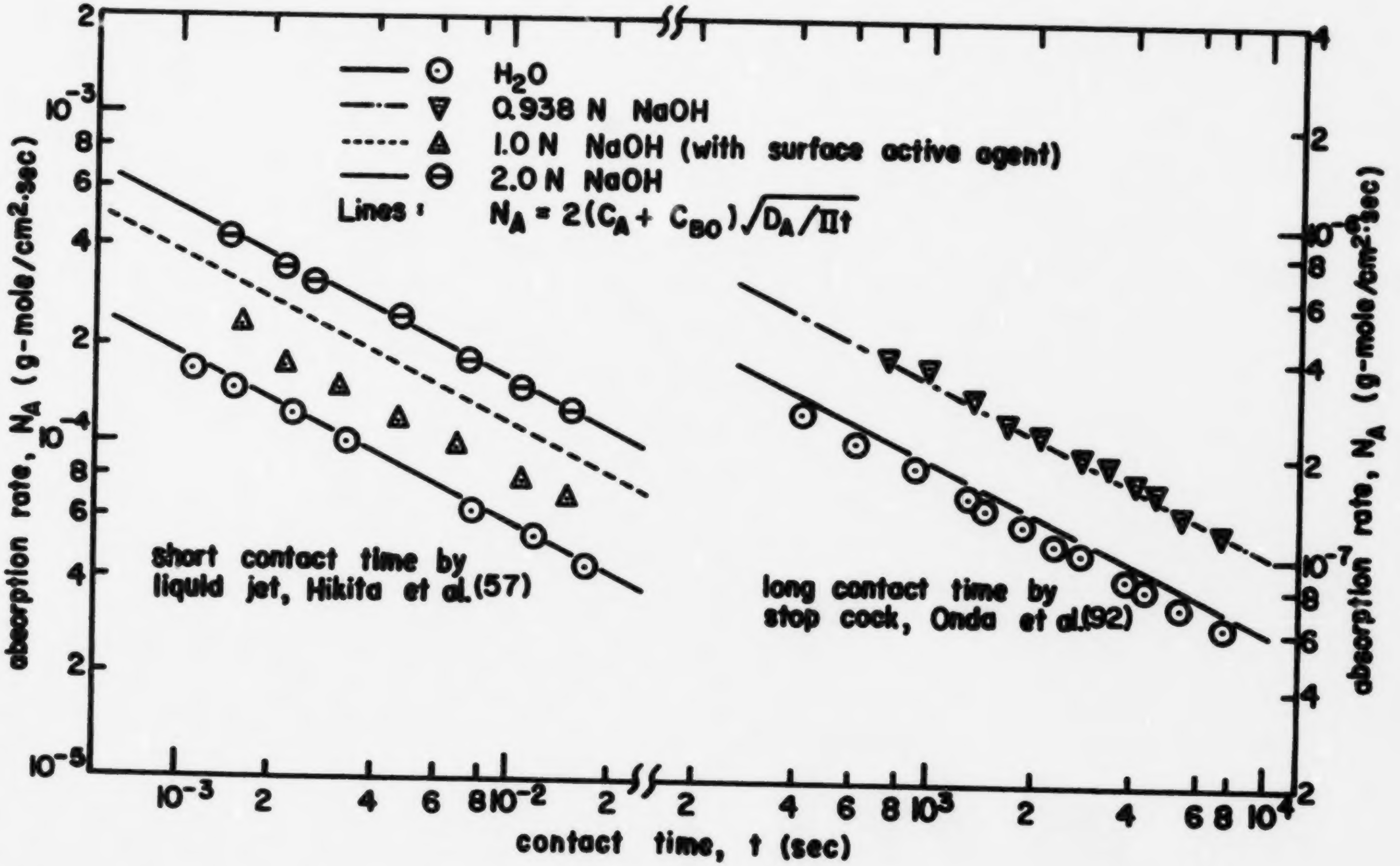

Figure 3. Comparison of Experimental Data on Rate of SO_2 Absorption with Values based on Penetration Theory

for these reactions SO_2 can be considered to react with the hydroxyl ion irreversibly with the overall reaction scheme represented by:

$$SO_2 + 2OH^- \longrightarrow SO_3^= + H_2O \qquad (13)$$

This reaction has the stoichiometric factor (number of OH^- ions reacting with one molecule of $SO_2(aq)$) of two.

(3) CO_2 - Alkaline solution system

The kinetics of the reactions involved in the industrially important processes of the absorption of CO_2 by alkaline solutions are in general rather simple and fairly well understood (5, 28, 33, 35, 41, 86, 108, 109). Three reactions may occur when CO_2 is absorbed by aqueous alkaline solution.

$$CO_2 + OH^- \rightleftharpoons HCO_3^- \qquad (14)$$

$$CO_2 + H_2O \rightleftharpoons HCO_3^- + H^+ \qquad (15)$$

$$HCO_3^- + OH^- \rightleftharpoons CO_3^= + H_2O \qquad (16)$$

Equilibrium constants for reactions (14), (15), and (16) are $K_{14} = 6.1 \times 10^7$ l/g-mole, $K_{15} = 4.5 \times 10^{-7}$ l/g-mole, and $K_{16} = 5.9 \times 10^3$ l/g-mole (33, 99) respectively. Reaction (14) is second-order and its rate constant at 20°C and at infinite dilution is about 6000 l/g-mole · sec (33). Reaction (15) is first-order with respect to the concentration of CO_2 in the solution, with a rate-constant of about 0.02 sec^{-1} at 20°C (33). Thus, in any solution in which the concentration of OH^- is greater than 10^{-4} g-ion/l ($pH > 10$), the rate of reaction of CO_2 by reaction (14) will be greater than 0.6 sec^{-1}. This is more than 30 times as fast as the rate of reaction by (15). When the pH value of the solution is less than 10, reaction (15) becomes important from the reaction rate point of view. However, even in the case of CO_2 absorption in the solution whose pH is lower than 10, from the equilibrium constant for this reaction (15) and experimental data for absorption of CO_2 in water obtained by many investigators, (33, 86, 92) the hydrolysis reaction (15) has no effect on the absorption of CO_2 in weak alkaline or weak acid solutions. That is, the absorption of CO_2 in such solutions can be treated by a physical mechanism. Therefore, reaction (15) is normally neglected in determining the rate of absorption of CO_2.

In a solution of alkali hydroxide such as sodium hydroxide and calcium hydroxide (lime), reaction (14) is followed instantaneously by reaction (16). Thus the overall reaction is:

$$CO_2 + 2OH^- \longrightarrow CO_3^= + H_2O \qquad (17)$$

This reaction is generally treated as a second-order reaction with respect to CO_2 and OH^- and may be considered irreversible as long as the solution is an alkaline solution. The stoichiometric factor for this reaction is two.

(4) SO_2 - Limestone slurry system

Although limestone slurry processes have been often encountered in the industry, very few data are available for the reaction kinetics of SO_2. Possible reaction mechanisms for flue gases containing CO_2 and SO_2 were first proposed by Pearson et al. (95) and Beuschlein et al. (9)

In spite of some apparent disagreements recent works by various investigators have clarified the situation somewhat in regard to the nature and extent of reactions occurring in the limestone slurry process. In this section, the mechanisms of this system are reviewed and discussed in more detail.

The absorption of SO_2 from flue gases by a limestone slurry generally constitutes a three-phase system involving gas, liquid and solid. When SO_2 is absorbed into the limestone slurry, the following chemical reactions take place in the scrubber and the holding tank.

$$SO_2 + H_2O \rightleftharpoons H_2SO_3 \rightleftharpoons H^+ + HSO_3^- \tag{18}$$

$$HSO_3^- \rightleftharpoons H^+ + SO_3^= \tag{19}$$

$$H_2SO_3 + HCO_3^- \longrightarrow HSO_3^- + H_2CO_3 \tag{20}$$

$$CaCO_3(s) \rightleftharpoons CaCO_3(aq) \rightleftharpoons Ca^{++} + CO_3^= \tag{21}$$

$$CaCO_3(aq) + H_2CO_3 \longrightarrow Ca(HCO_3)_2 \tag{22}$$

$$Ca(HCO_3)_2 \rightleftharpoons Ca^{++} + 2HCO_3^- \tag{23}$$

$$CO_2 + H_2O \rightleftharpoons H_2CO_3 \rightleftharpoons H^+ + HCO_3^- \qquad (24)$$

$$HCO_3^- \rightleftharpoons H^+ + CO_3^= \qquad (25)$$

$$Ca^{++} + SO_3^= \longrightarrow CaSO_3 \qquad (26)$$

$$CaSO_3 + \tfrac{1}{2}H_2O \longrightarrow CaSO_3 \cdot \tfrac{1}{2}H_2O\downarrow \qquad (27)$$

$$CaSO_3 + \tfrac{1}{2}O_2 \longrightarrow CaSO_4 \qquad (28)$$

$$CaSO_4 + 2H_2O \longrightarrow CaSO_4 \cdot 2H_2O\downarrow \qquad (29)$$

Gaseous SO_2 from the flue gas is absorbed into the liquid phase, where it is partially ionized according to reactions (18) and (19). Solid calcium carbonate is dissolved by the solution in which it undergoes a reversible reaction with the weakly ionized carbonic acid to form fairly soluble calcium bicarbonate, as shown in reactions (21), (22), and (23). The formation of calcium bicarbonate is favored by the high partial pressure of carbon dioxide in the flue gas according to reaction (24). If the concentration of HCO_3^- ions is high enough in the liquid phase as in the case of limestone slurry process, reaction (20) between $SO_2(aq)$ and bicarbonate ion is considered as one of the possible reactions. This reaction is an exchange reaction between a strong acid and a weak acid. It has been suggested by Bjerle et al. (10) and Nilsson et al. (87) that the key reaction of the SO_2 scrubbing mechanism is this type of reaction. For this reaction (20), the equilibrium constant, K, at 50°C is given as (8) $K = 7.0 \times 10^6$. Experimentally it has been proved (10) that the rate of absorption of SO_2 into limestone slurry can be explained by the irreversible and instantaneous reaction between dissolved SO_2 and HCO_3^- presenting in the liquid. Dissociation reactions (21) and (25) are not considered significant in the limestone slurry since the dissociation constants are very small. Bisulfite ions produced by reaction (20) react as reactions (19) and (26), and some parts of calcium sulfite, then, react with oxygen dissolved in the liquid phase. As the result, calcium sulfite and calcium sulfate combined with water molecules precipitate out of the liquid.

Therefore, the following reaction represents an overall reaction between SO_2 and limestone slurry:

$$\begin{aligned} &CaCO_3(s) + SO_2(g) + \left(\frac{1}{2}+\frac{3}{2}\alpha\right) H_2O(l) + \frac{\alpha}{2} O_2(g) \\ &\longrightarrow (1-\alpha)CaSO_3 \cdot \tfrac{1}{2}H_2O(s) + \alpha CaSO_4 \cdot 2H_2O(s) \\ &+ CO_2(g) \end{aligned} \tag{30}$$

where α is a fraction of calcium sulfite oxidized to calcium sulfate. According to the stoichiometric relation, for every mole of SO_2 absorbed, one mole of limestone is dissolved in the liquid phase, and one mole of calcium salt (calcium sulfite and calcium sulfate) precipitates out of the liquid phase, and consequently one mole of CO_2 is evolved from the liquor. Experimental data from the overall system including a scrubber and a holding tank should satisfy these stoichiometric relations.

Equilibrium relations among the dissolved components in the liquid phase, coexisting solids, and the partial pressures of SO_2 and CO_2 over the limestone slurry have been calculated by Philips (99) and Berkowitz et al. (8)

B. Development of Performance Equations for a Venturi Scrubber

When a liquid is injected into a high velocity gas stream in a venturi scrubber, it is atomized by the formation and subsequent shattering of attenuated, twisted filaments and thin cuplike films. These initial filaments and films provide extremely large surface areas for heat and mass transfer. Later, nearly spherical droplets are formed which have less surface area per unit volume of liquid than do the attenuated films and filaments.

Although the actual process of the atomization of the liquid is very complex, the following representations of atomization are realistic enough so that theoretical treatment can be applied.

(a) Every droplet formed at the point of liquid injection will have a mean diameter that can be calculated by a correlation. Practically no change in the droplet diameter takes place while passing through the venturi scrubber that may be caused by coalescence or shattering of the droplets.

(b) The shape of the droplet is nearly spherical and internal circulation of liquid in the droplet can be neglected so the droplet can be represented by a rigid sphere (61).

(c) Effect of gas compressibility can be neglected.

(d) Deposition or reentrainment of the liquid or from the wall of the scrubber vessel can be neglected.

(e) The variation in gas flow rate due to liquid vaporization is negligibly small.

(f) The amount of SO_2 absorbed is so small compared to the amount of liquor, heat generated due to reaction and solution is negligible.

(g) Sensible heat exchange takes place between gas and liquid streams. However, temperatures within a single liquid droplet is assumed uniform.

(h) Heat loss through the wall of the venturi scrubber is negligible.

(i) There is no dissolution of lime or limestone in the venturi scrubber.

(1) Pressure drop

A differential equation for pressure drop in a venturi scrubber with respect to the axial distance is derived by making a momentum balance in an incremental section of the scrubber (11).

$$d(M_g v_g) + d(M_L v_L) + Sg_c dp_f + Sg_c dp = 0 \qquad (31)$$

Using the relationships:

$$M_g = S\varepsilon \rho_g v_g = \rho_g G_o \sim \text{constant}$$

$$M_L = S\,(1-\varepsilon)\,\rho_L v_L = \rho_L L_o \sim \text{constant}$$

equation (31) is reduced to the following form:

$$\frac{dp}{dz} = -\left\{ \frac{\varepsilon \rho_g v_g}{g_c} \cdot \frac{dv_g}{dz} + \frac{(1-\varepsilon)\rho_L v_L}{g_c} \cdot \frac{dv_L}{dz} + \frac{dp_f}{dz} \right\} \qquad (32)$$

This is a nonlinear, first-order, ordinary differential equation for pressure loss with respect to axial distance of the venturi scrubber.

The last term on the right hand side of equation (32) relates to the friction loss which is generally expressed by the following form under turbulent flow conditions.

$$dp_f = f\,\frac{\rho_m v_g^2}{2g_c} \cdot \frac{dz}{d_e} \qquad (33)$$

where f is a friction factor which depends on the roughness of the wall of the venturi scrubber and the Reynolds number of the gas (83).

In the case of a venturi-type scrubber such as the flooded disc scrubber (FDS) in which there is a sudden expansion or contraction of the gas, an additional pressure loss term is added to equation (32). Pressure losses due to the contraction and the expansion, ΔP_c, and ΔP_e can be calculated by the following equations, respectively $^{(47)}$.

$$\Delta P_c = 0.5 \frac{\rho_g v_{go}^2}{2g_c} \qquad (34)$$

$$\Delta P_e = \frac{\rho_g (v_{go} - v_{g1})^2}{2g_c} \qquad (35)$$

Total pressure drop in the venturi scrubber is therefore obtained as the summation of these losses. That is:

$$\Delta P = \Delta P_a + \Delta P_f + \Delta P_c + \Delta P_e \qquad (36)$$

where ΔP_a is the acceleration loss calculated by the first and the second terms in the right hand side of equation (32).

(2) Equation of motion of liquid droplet

Assuming that the liquid atomizes instantly into the droplet form with a constant mean diameter at the point of entry to the high velocity gas stream, the force balance for a vertically moving droplet yields:

$$\rho_L \left(\frac{\pi d_p^3}{6}\right) \frac{dv_L}{dt} = \rho_L \left(\frac{\pi d_p^3}{6}\right) g - \rho_g \left(\frac{\pi d_p^3}{6}\right) g + C_d \left(\frac{\pi d_p^2}{4}\right) \frac{\rho_g}{2} (v_g - v_L) \left| v_g - v_L \right| \qquad (37)$$

where C_d is the drag coefficient, defined as

$$C_d = \frac{\text{drag}}{(\text{frontal area})\left(\frac{\rho_g (v_g - v_L)^2}{2g_c}\right)} \qquad (38)$$

In general, the dimensional analysis shows that the drag coefficient is a function of various dimensionless groups as follows:

$$C_d = f\,(N_{Re}, N_{Su}, N_{Wt}, N_{Ac}, \rho_g/\rho_L, \mu_g/\mu_L) \qquad (39)$$

The analysis of the droplet motion is so complicated by the gas-liquid droplets interactions particularly in the acceleration region as well as the nature of the droplet that it is practically impossible to obtain a complete trajectory except under rather idealized conditions. For steady motion of solid spheres, C_d becomes a function of Reynolds number alone. The studies on the effects of acceleration, distoration, oscillation and internal motion in the liquid droplets have been summarized by Hughes and Gilliland (61). According to the experimental data obtained by Allen (2) and Cook (29) the drag coefficients in their study are always higher than those for steady motion. Recently Ingebo (62) studied the drag coefficients for droplets and solids in cloud accelerating in airstreams. Diameter and velocity data for individual droplets and solid spheres were obtained with a high-speed camera. An analysis of the data for unsteady momentum transfer from airstreams to clouds of solid spheres, nonevaporating droplets and evaporating droplets gave the following correlation for the drag coefficient.

$$C_d = 27/N_{Re}^{0.84} \tag{40}$$

Equation (40) is said to be applicable for a Reynolds number range of 6 to 400 and a sphere diameter range of 20 to 120 microns. Rapid variation in acceleration and velocity difference with time gave instantaneous drag coefficients between Stokes' law and steady state values. These results are summarized in Figure 4 with the lines obtained from the literature (62).

If the droplet is flowing in the gas-phase under normal pressure the second term on the right hand side of Equation (37) is usually negligible in comparison to the other terms. For vertical motion, equation (37) can be reduced to:

$$\frac{dv_L}{dz} = \frac{g}{v_L} + \frac{3}{4} \cdot \frac{C_d}{d_p} \cdot \frac{\rho_g}{\rho_L} \cdot \frac{(v_g - v_L)\,|v_g - v_L|}{v_L} \tag{41}$$

If the motion is in the horizontal direction, the term due to gravity can be eliminated and the relationship is simplified to:

$$\frac{dv_L}{dz} \quad \frac{3}{4}\,\frac{C_d}{d_p}\,\frac{\rho_g}{\rho_L}\,\frac{(v_g - v_L)\,|v_g - v_L|}{v_L} \tag{42}$$

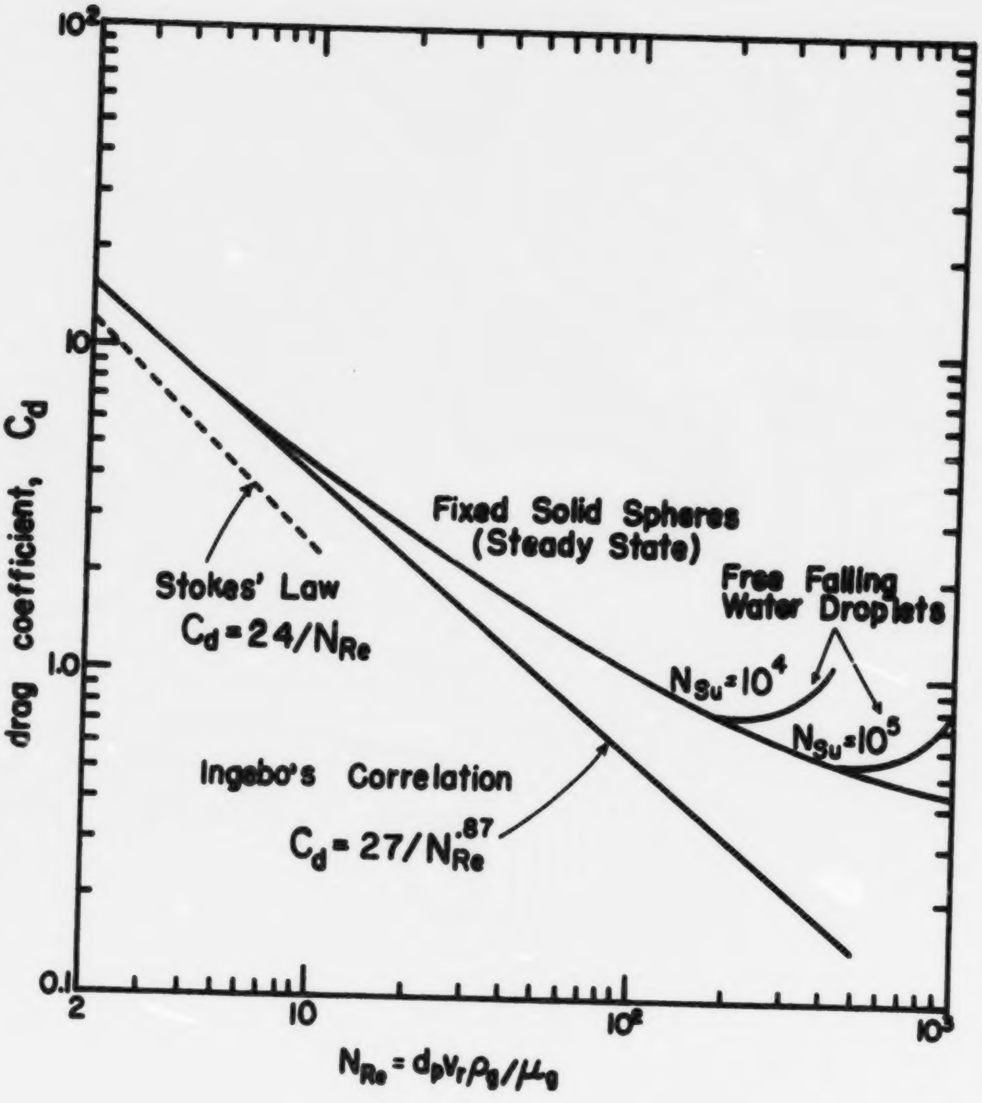

Figure 4. Correlation of Instantaneous Unsteady State Drag Coefficient with Reynolds Number

The average gas velocity at any point in the venturi scrubber is calculated by the following relation:

$$v_g = \frac{G_o}{\varepsilon S} \qquad (43)$$

where ε is a voidage in the scrubber and is related by the following relationship to the velocity of the droplet.

$$v_L = \frac{L_o}{(1-\varepsilon)S} \qquad (44)$$

(3) Heat and mass transfer in a venturi scrubber

The heat and mass balances for gas and liquid stream in an incremental section of a venturi scrubber are:

$$h_G a\ (t_g - t_L)\ dV = (L_m - dL_m)\ C_{PL} dt_L + \beta k_{Gw}\ ap(y_{wi} - y_w)\ dV \qquad (45)$$

$$G_m C_{pg} dt_g = h_G a\ (t_L - t_g)\ dV \qquad (46)$$

$$(L_m - dL_m)(x + dx) - L_m \cdot x = aN_A dV = -(G_m/p) dp_A \qquad (47)$$

$$G_m dy_w = k_{Gw} ap(y_{wi} - y_w) dV = -dL_m \qquad (48)$$

Using the relationships, $x = \overline{C}_A/\rho_M$, $dV = Sdz$, $N_A = k_L \Delta C_A$ and $a = 6(1-\varepsilon)/d_p$ and neglecting dL_m in equations (45) and (47) in comparison with the other terms, the following set of differential equations are obtained:

$$\frac{dt_L}{dz} = \frac{a}{(L_m/S)C_{PL}} \left[h_G(t_g - t_L) - \beta k_{Gw} p \, (y_{wi} - y_w)\right] \qquad (49)$$

$$\frac{dt_g}{dz} = \frac{h_G a}{(G_m/S)C_{Pg}} (t_L - t_g) \qquad (50)$$

$$\frac{dL_m}{dz} = k_{Gw} a S p \, (y_w - y_{wi}) \qquad (51)$$

$$\frac{dp_A}{dz} = - \frac{a p k_L}{(G_m/S)} \Delta C_A \qquad (52)$$

$$\frac{d\bar{C}_A}{dz} = \frac{a \rho_M k_L}{(L_m/S)} \Delta C_A \qquad (53)$$

$$\frac{dy_w}{dz} = \frac{k_{Gw} a p}{(G_m/S)} (y_{wi} - y_w) \qquad (54)$$

And from $v_L = dz/dt$,

$$\frac{dt}{dz} = \frac{1}{v_L} \qquad (55)$$

(4) Performance equations in dimensionless forms

The above differential equations (32), (41), and (49) ~ (55) can be written in dimensionless forms by introducing the following dimensionless variables and coefficients:

$$Z = \frac{z}{z_o} \quad , \quad P = \frac{p}{p_o} \quad , \quad V_L = \frac{v_L}{v_{go}} \quad , \quad V_g = \frac{v_g}{v_{go}} \quad ,$$

$$T_L = \frac{t_L}{t_{go}} \quad , \quad T_g = \frac{t_g}{t_{go}} \quad , \quad L_m' = \frac{L_m}{L_{mo}} \quad ,$$

$$\bar{C}_A' = \frac{\bar{C}_A}{C_{Ao}^* + C_{Bo}} \quad , \quad T = \frac{v_{go}}{z_o} t \quad , \quad P_A = \frac{p_A}{p_{Ao}} \quad ,$$

$$\xi_1 = \frac{\varepsilon \rho_g v_{go}^2}{g_c p_o} \quad , \quad \xi_2 = \frac{(1-\varepsilon)\rho_L}{\varepsilon \rho_g} \xi_1 \quad , \quad \xi_3 = \frac{\rho_m z_o}{\varepsilon \rho_g d_e} \xi_1$$

$$\xi_4 = \frac{g z_o}{v_{go}^2} \quad , \quad \xi_5 = \frac{z_o \rho_g}{d_p \rho_L} \quad , \quad \xi_6 = \frac{C_{pg} G_m}{C_{pL} L_m} \xi_8 \quad ,$$

$$\xi_7 = \frac{G_m \beta}{L_m C_{pL} t_{go}} \xi_{12} \quad , \quad \xi_8 = \frac{h_G a z_o}{(G_m/S) C_{pg}} \quad , \quad \xi_9 = \frac{G_m}{L_{mo}} \xi_{12}$$

$$\xi_{10} = \frac{L_m (C_{Ao}^* + C_{Bo}) p_o}{G_m \rho_M p_{Ao}} \xi_{11} \quad , \quad \xi_{11} = \frac{a \rho_M z_o k_L}{(L_m/S)} \quad ,$$

$$\xi_{12} = \frac{k_{Gw} a p_o z_o}{(G_m/S)}$$

Then,

$$\frac{dP}{dZ} = -\left\{\xi_1 V_g \frac{dV_g}{dZ} + \xi_2 V_L \frac{dV_L}{dZ} + \xi_3 \frac{f}{2} V_g^2\right\} \qquad (56)$$

$$\frac{dV_L}{dZ} = \frac{\xi_4}{V_g} + \xi_5 \frac{3C_d}{4} \cdot \frac{(V_g-V_L)\left|V_g-V_L\right|}{V_L} \qquad (57)$$

$$\frac{dT_L}{dZ} = \xi_6 (T_g-T_L) - \xi_7 (y_{wi}-y_w) P \qquad (58)$$

$$\frac{dT_g}{dZ} = \xi_8 (T_L-T_g) \qquad (59)$$

$$\frac{dL'_m}{dZ} = -\xi_9 (y_{wi}-y_w) P \qquad (60)$$

$$\frac{dP_A}{dZ} = -\xi_{10} P\Delta C'_A \qquad (61)$$

$$\frac{d\overline{C}'_A}{dZ} = \xi_{11} \cdot \Delta C'_A \qquad (62)$$

$$\frac{dy_w}{dZ} = \xi_{12} (y_{wi} - y_w) P \tag{63}$$

$$\frac{dT}{dZ} = \frac{1}{V_L} \tag{64}$$

This set of differential equations is numerically solved by Runge-Kutta-Gill method, which saves computer memories, using given initial conditions at the nozzle point. The heat and mass transfer coefficients and equilibrium relations needed to solve the above set of equations are estimated as discussed below.

(5) Gas-phase heat and mass transfer coefficients

Gas-phase heat and mass transfer to or from a single sphere placed in a moving fluid has been studied by many investigators (46, 107, 120). A correlation having the same form as the Ranz-Marshall equation obtained by Steinberger and Treybal (120) can be used to calculate the gas-phase heat and mass transfer coefficients of the individual droplet in a venturi scrubber:

$$N_{Sh} = N_{Sh,o} + 0.347 (N_{Re} \cdot N_{Sc}^{\frac{1}{2}})^{0.62} \tag{65}$$

where

$$N_{Sh,o} = 2 + 0.569 (N_{Gr} \cdot N_{Sc})^{0.250} \text{ for } (N_{Gr} \cdot N_{Sc}) < 10^8$$

$$N_{Sh,o} = 2 + 0.0254\,(N_{Gr} \cdot N_{Sc})^{\frac{1}{3}}(N_{Sc})^{0.244}$$

$$\text{for } (N_{Gr} \cdot N_{Sc}) > 10^{8}$$

The applicable ranges of this correlation are:

$$1 < N_{Re} < 30{,}000$$

$$0.6 < N_{Sc} < 3{,}000$$

Equation (65) is also used to compute the mass transfer coefficient of water vapor from the surface of a liquid drop into the gas-phase.

(6) Rate of gas absorption into spherical droplet

The rate of gas absorption and the mass transfer coefficient in a stagnant liquid drop for physical absorption can be obtained by solving the following partial differential equation expressing the material balance in the drop.

$$\frac{\partial C_A}{\partial t} = \frac{D_A}{r^2} \cdot \frac{\partial}{\partial r}\left(r^2 \frac{\partial C_A}{\partial r}\right) \qquad (66)$$

$$\left.\begin{array}{llll} \text{I.C.} & : \; t = 0, & 0 < r < r_o & : \; C_A = 0 \\ \text{B.C.I.} & : \; r = 0, & t > 0 & : \; \partial C_A/\partial r = 0 \\ \text{B.C.II.} & : \; r = r_o, & t > 0 & : \; C_A = C_{Ai} \end{array}\right\} \quad (67)$$

This partial differential equation can be solved analytically as follows. By introducing a change of variables, $u = C_A r$, the above equation with initial and boundary conditions are rewritten to:

$$\frac{\partial u}{\partial t} = D_A \left(\frac{\partial^2 u}{\partial r^2}\right) \tag{68}$$

$$\left.\begin{array}{llll} \text{I.C.} & : \; t = 0, & 0 < r < r_o & : \; u = 0 \\ \text{B.C.I.} & : \; r = 0, & t > 0 & : \; u = 0 \\ \text{B.C.II} & : \; r = r_o & t > 0 & : \; u = r_o C_{Ai} \end{array}\right\} \tag{69}$$

The solution of this set of a partial differential equation with modified initial and boundary conditions is given by:

$$u = rC_{Ai} + \frac{2r_o C_{Ai}}{\pi} \sum_{m=1}^{\infty} \frac{(-1)^m}{m} \sin\left(\frac{m\pi r}{r_o}\right) \exp\left(-\frac{D_A m^2 \pi^2 t}{r_o^2}\right)$$

or,

$$\frac{C_A}{C_{Ai}} = 1 + \frac{2r_o}{\pi r} \sum_{m=1}^{\infty} \frac{(-1)^m}{m} \sin\left(\frac{m\pi r}{r_o}\right) \exp\left(-\frac{D_A m^2 \pi^2 t}{r_o^2}\right) \tag{70}$$

The concentration profiles of the dissolved gas in the droplet along the radial direction is shown in Figure 5 with $(D_A t / r_o^2)$ as a parameter.

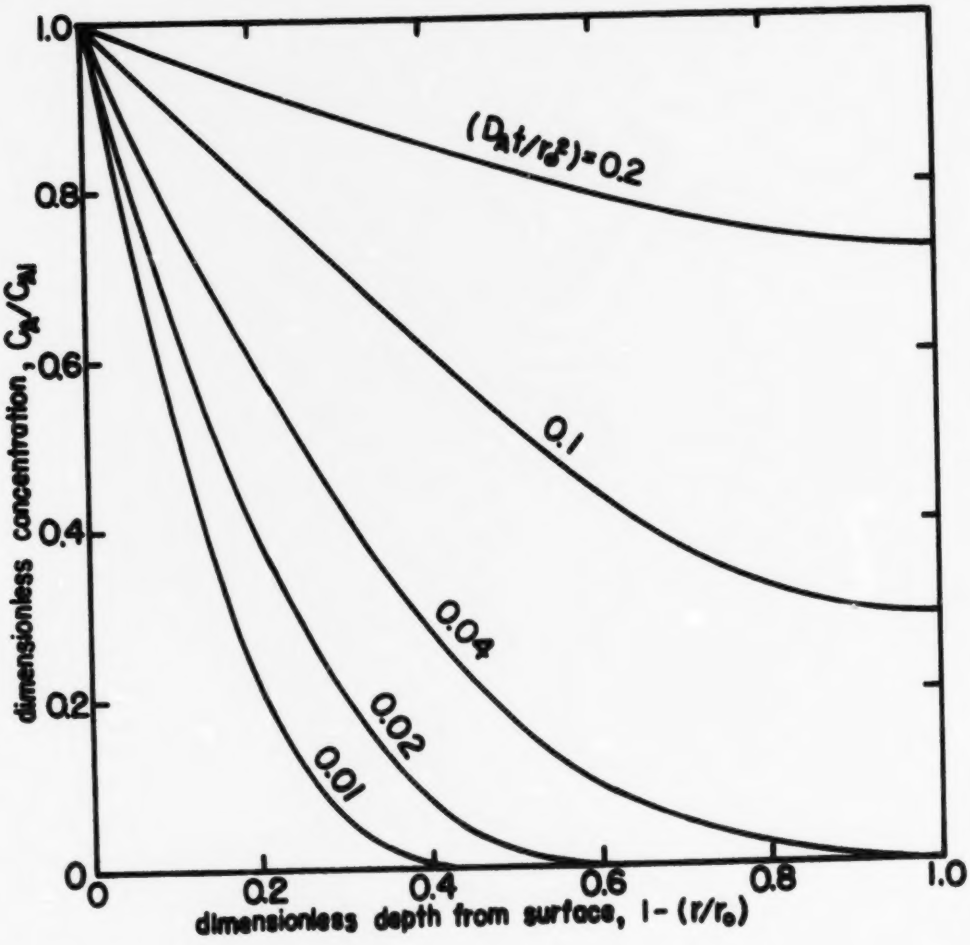

Figure 5. Concentration Profile of SO_2 in a Droplet (SO_2-H_2O System : constant interfacial concentration) (91)

From the definition of the flux of the dissolved gas A at the interface in a unit time, we have,

$$N_A = D_A \left(\frac{\partial C_A}{\partial r}\right)_{r = r_o} \tag{71}$$

Differentiating equation (70) with respect to r, the equation for rate of absorption into the spherical drop at time t is obtained as;

$$N_A = \frac{2D_A C_{Ai}}{r_o} \sum_{m=1}^{\infty} \exp\left(-\frac{D_A m^2 \pi^2 t}{r_o^2}\right) \tag{72}$$

Thus the mass transfer coefficient at time t is given by;

$$k_{Lp} = \frac{2D_A}{r_o} \sum_{m=1}^{\infty} \exp\left(-\frac{D_A m^2 \pi^2 t}{r_o^2}\right) \tag{73}$$

For gas absorption into a stagnant liquid drop with an irreversible, instantaneous reaction such as absorption of SO_2 into alkaline solution, the liquid-phase mass transfer coefficient is given as follows: Assuming both the diffusivities of the gas and the reactant in the liquid are nearly the same (see APPENDIX A), we have

$$k_L = \left(1 + \frac{C_{Bo}}{\gamma C_{Ai}}\right) k_{Lp} \tag{74}$$

where C_{Ai} is the interfacial concentration calculated by:

$$C_{Ai} = \frac{C_A^* - C_{Bo}R}{1+R} \tag{75}$$

where the ratio of the resistance in gas-phase to that in liquid-phase, that is $R = k_{Lp}H_A/k_g$.

The rate of absorption in this case will be:

$$N_A = k_L C_{Ai} = k_L \cdot \Delta C_A \tag{76}$$

When the interfacial concentration, C_{Ai}, changes considerably, or the diffusivities of the gas and the reactant cannot be approximated to have same values, this approach will produce some errors. In that case, a set of partial differential equations obtained from the material balance within a droplet has to be solved numerically (see APPENDIX C). However, in most cases of SO_2 absorption by lime or limestone slurry in a venturi scrubber, the above approach is sufficiently accurate.

C. Dissolution of Lime and Limestone in a Holding Tank

A clear understanding of the dissolution mechanisms of lime and limestone into a weak acid solution that is recycled in the SO_2 scrubbing process is essential in development and efficient operation of the wet scrubbing system.

In this section, studies on the properties and behaviors of lime and limestone in the solution are presented and their reactions and the dissolution into the recycling liquor are analyzed. Based on these analyses, mathematical models which can be used to predict performance of a holding tank are proposed.

For more information on the physical and chemical properties of lime and limestone, see APPENDIX D.

(1) Properties and behavior of lime in acid solution

Lime's effectiveness as an alkali scrubbing liquor largely depends upon its ultimate solubility and the rate of dissolution. Some of the previous studies on the dissolution of lime into various solutions have revealed the following [1, 15, 25, 54].

i. The initial rate of the dissolution is directly proportional to the ultimate solubility of lime.

ii. Particle size exerts some influence over the rate of dissolution. The increase in rate of dissolution is proportional to the increase in the contact area between the solid lime and the solution.

iii. If the lime reacts with an acid that forms a soluble lime salt, the rate of dissolution is increased, the increase over the rate in water being directly proportional to the concentration of acid.

iv. If the lime reacts with an excess of acid that forms an insoluble salt, the particles of lime are crusted over with this insoluble coating (blinding), so that the rate of dissolution decreases.

When lime is dissolved into water, the following reactions take place:

$$CaO + H_2O \rightleftharpoons Ca(OH)_2 \qquad (77)$$

$$Ca(OH)_2 \rightleftharpoons Ca^{++} + 2OH^- \qquad (78)$$

Since reaction (78) is an ionic reaction, it may be considered as a rapid reaction. The previous study on the rate of dissolution of lime (54) shows that the hydrolysis reaction (77) is also very fast and the dissolution process into water may be controlled by the diffusion of the product from the lime particle. Thus, when a solid lime is placed in contact with a liquid, the liquid-solid interface can be considered to be covered by the saturated solution. The solute diffuses from the solid surface through the film of liquid surrounding the solid particle into the main body of the liquid where it is uniformly distributed by the convection currents.

If the excess acid such as sulfuric acid is present in the solution, the following reaction occurs in the liquid film surrounding the particle.

$$Ca(OH)_2 + H_2SO_3 \longrightarrow CaSO_3\downarrow + H_2O \tag{79}$$

(2) Model for dissolution of lime in a holding tank

In order to develop a model for dissolution of lime in a holding tank, the following assumptions are made:

i. The concentration of $Ca(OH)_2$ at interface is considered to reach the saturated concentration immediately.

ii. The dissolution reactions take place only from the surface of the particle rather than from within the particle.

iii. As the dissolution proceeds, the size of the particle shrinks.

iv. All particles are nearly spherical in shape and can be represented by a mean diameter when it is present in the tank.

Applying the particle size shrinking model (71) to the particles in the holding tank, the following equation may be written on the rate of the dissolution:

$$-\frac{1}{4\pi r_p^2} \cdot \frac{dN_B}{dt} = k_s\,(C_{Bs}-C_{Bo}) \tag{80}$$

Introducing the molar density of the solid, ρ_{MB}, into this relation, we obtain;

$$-\frac{dr_p}{dt} = \frac{k_s}{\rho_{MB}}\,(C_{Bs}-C_{Bo}) \tag{81}$$

If the diffusion process in the film around the particle is the controlling step and the relative velocity between the solid and the liquid is small, the following relation is applicable:

$$N_{Sh} = 2.0 \tag{82}$$

that is,

$$k_s = \frac{D_B}{r_p} \tag{83}$$

When the excess acid presents in the solution, k_s is approximated by (90):

$$k_s' = k_s \left(1 + \frac{C_{acid}}{C_{Bs}}\right) \tag{84}$$

Then the equation (81) can be integrated as:

$$\int_{r_p}^{R_p} r_p dr_p = \frac{D_B}{\rho_{MB}} (C_{Bs}-C_{Bo}) \int_o^t dt \tag{85}$$

Therefore, the radius of the solid particle at time t is given by:

$$r_p = \sqrt{R_p^2 - \frac{2D_B}{\rho_{MB}} (C_{Bs}-C_{Bo})\ t} \tag{86}$$

The time required for the complete dissolution, τ, is given by:

$$\tau = \frac{R_p^2 \rho_{MB}}{2D_B(C_{Bs}-C_{Bo})} \tag{87}$$

From the relation of the radius of the particle and the fraction of the dissolution, we have:

$$\frac{\text{volume of particle left}}{\text{total volume of particle}} = 1-X_B = \frac{\frac{4}{3}\pi r_p^3}{\frac{4}{3}\pi R_p^3} = \left(\frac{r_p}{R_p}\right)^3 \qquad (88)$$

Combining equations (86) and (88), we obtain:

$$1 - X_B = \frac{1}{R_p^3}\left[R_p^2 - \frac{2D_B}{\rho_{MB}}(C_{Bs}-C_{Bo})t\right]^{3/2} \qquad (89)$$

If the holding tank can be considered as a complete mixing tank, the exit age distribution function is given by:

$$E(t) = \frac{1}{\bar{t}}e^{-t/\bar{t}} \qquad (90)$$

where

$$\bar{t} = 60\ V_t/F \qquad (91)$$

Thus, the fraction of solid dissolved in the tank has the following relation with the tank characteristics:

$$\begin{aligned} 1 - \bar{X}_B &= \int_0^\infty (1-X_B)E(t)dt \\ &= \frac{1}{R_p^3\bar{t}}\int_0^\tau \left[R_p^2 - \frac{2D_B}{\rho_{MB}}(C_{Bs}-C_{Bo})t\right]^{3/2} e^{-t/\bar{t}}\,dt \end{aligned} \qquad (92)$$

From the material balance of $Ca(OH)_2$ around the holding tank, the following additional relation can be obtained:

$$M\overline{X}_B = 60L_o\,(C_{Bo} - C_{Bi}) \qquad (93)$$

These equations (87), (92), and (93) are solved to obtain the outlet concentration of $Ca(OH)_2$ in the solution.

(3) Properties and behavior of limestone in SO_2 scrubbing liquor

Similar to the case of lime, in order to provide a model for simulation of the dissolution mechanism of limestone into acid solutions such as the recycling liquor in the limestone - SO_2 scrubbing system, experimental data taken under the conditions similar to the field plants are needed. However, only a few studies on the dissolution rate of limestone into several acid solutions have been reported (37, 38, 98). These data were obtained under limited conditions different from the conditions of practical interest. Therefore, it is questionable that these results are useful to simulate the holding tank in the limestone slurry process.

To develop a kinetic model to estimate the rate of dissolution of limestone, it is necessary to know the key reactions contributing to the dissolution as well as to find the ultimate solubility of limestone into the slurry. In the case of limestone, however, not only a number of reactions are taking place simultaneously but also its solubility is strongly dependent upon the partial pressure of CO_2 over the solution or the concentration of carbonate ions in the solution (15, 113).

In pure distilled water in which there is no dissolved CO_2 and which is exposed to a CO_2 - free atmosphere, limestone is virtually insoluble. With an increase in partial pressure of CO_2, the solubility increases steadily to a point where it might be characterized as sparingly soluble. A number of measurements have been made by many researchers (15, 113) on solubilities under varied conditions, such as temperature, partial pressure of CO_2, and in aqueous solutions which contain other soluble salts. Many of the results do not agree with each other, but this is believed to be due to different laboratory procedures, conditions of test, and the quality of the limestone.

Chemical reactions involved in the dissolution of limestone into SO_2 scrubbing liquor are discussed in Section A of this chapter. Besides the complexity of the reaction mechanism, reactions seem to interact with each other making it practically impossible to limit the number of reactions as rate-determining steps.

There is, however, a considerable amount of data on the total concentrations of the key components such as sulfate, sulfite, calcium, and carbonate in the recycling liquor obtained from various SO_2 scrubbing plants (6, 13, 23, 117). It is believed that these components play main roles in the overall reaction in SO_2 - limestone system. This was already discussed in Section A in this chapter. In Figure 6 ~ 9, comparisons of the outlet concentrations of such components with the equilibrium values calculated by computer programs originally developed by Phillips (99), and revised later by Berkowitz et al. (8) are shown against the pH of the liquor leaving the holding tank.

From these figures, we can observe the following facts: In spite of the significant differences in the operating conditions and the design of the holding tank such as residence time and area exposed to the atmosphere, the data seem to indicate that concentrations of each component in the liquor are very close to the equilibrium values. Effect of magnesium components on the equilibrium relations seems significant. Since $MgSO_3$ and $MgSO_4$ are both soluble (18 and 50 g/1, respectively (13)) the magnesium fed with the limestone will inexorably build up in the scrubber liquor. As seen from the figures, most of magnesium in the liquor presents in the form of $MgSO_4$. The rate of building up of magnesium depends upon the operating time, quality of limestone, etc.

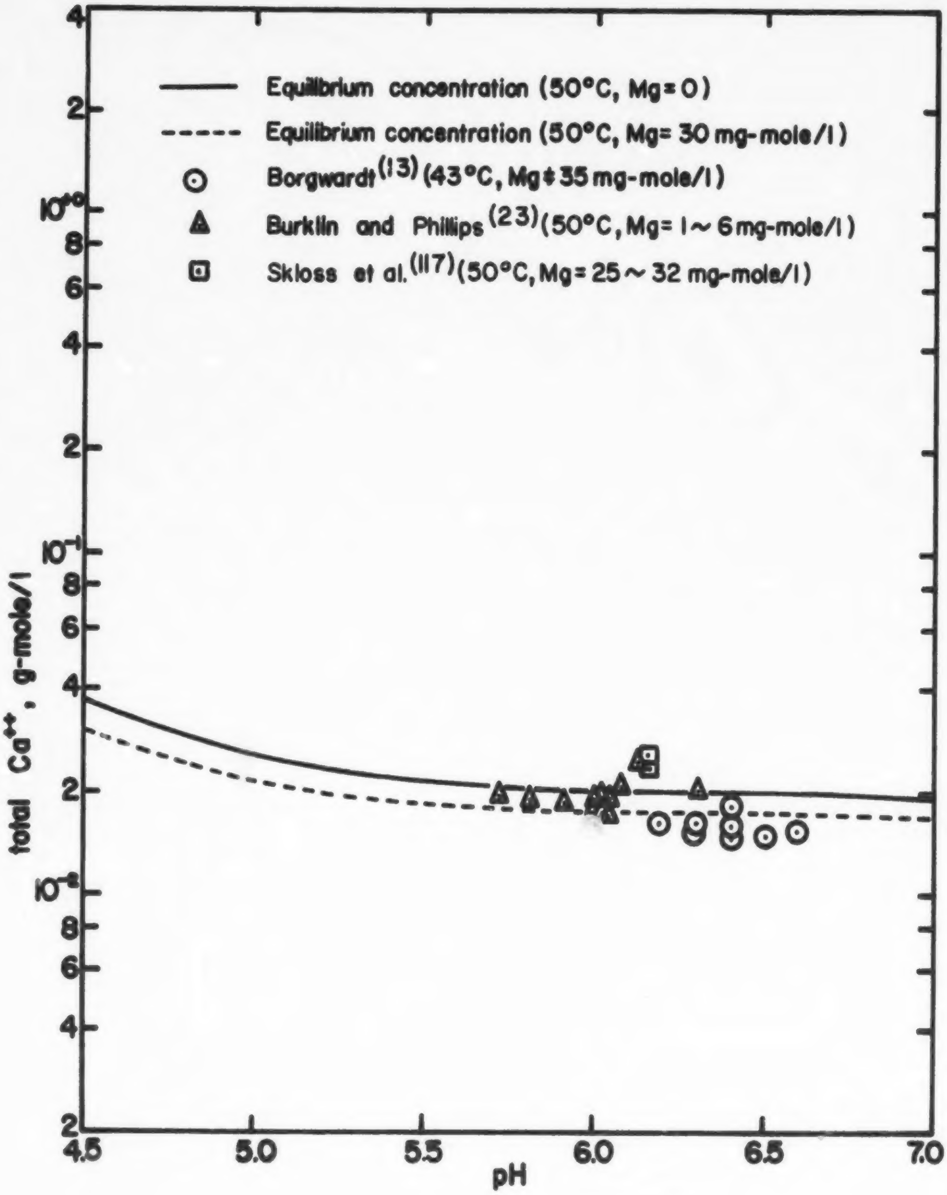

Figure 6. Equilibrium Concentration of Total Calcium at 50°C and its Concentration in Outlet Liquor from Holding Tank vs. Liquor pH.

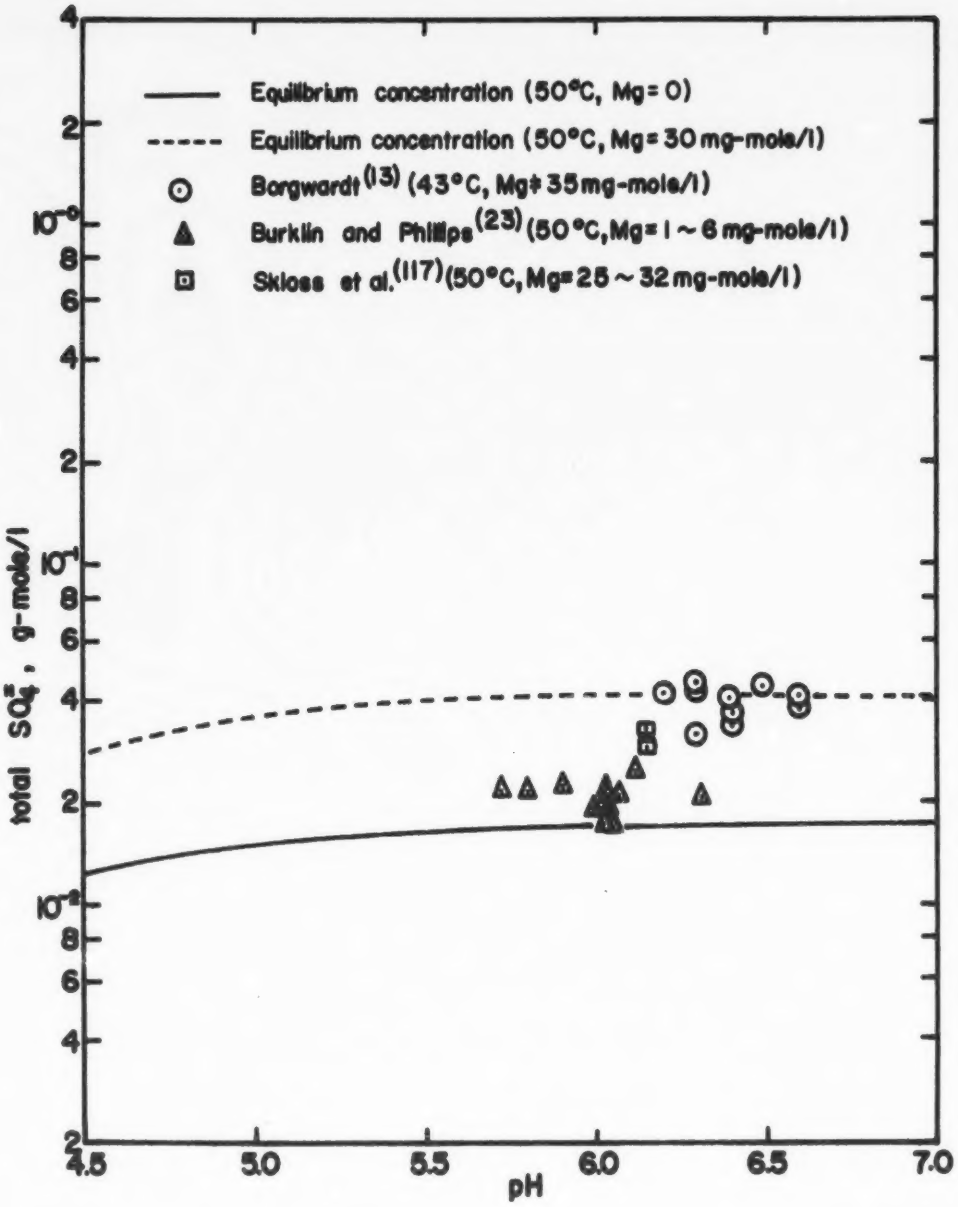

Figure 7. Equilibrium Concentration of Total Sulfate at 50°C and its Concentration in Outlet Liquor from Holding Tank vs. Liquor pH.

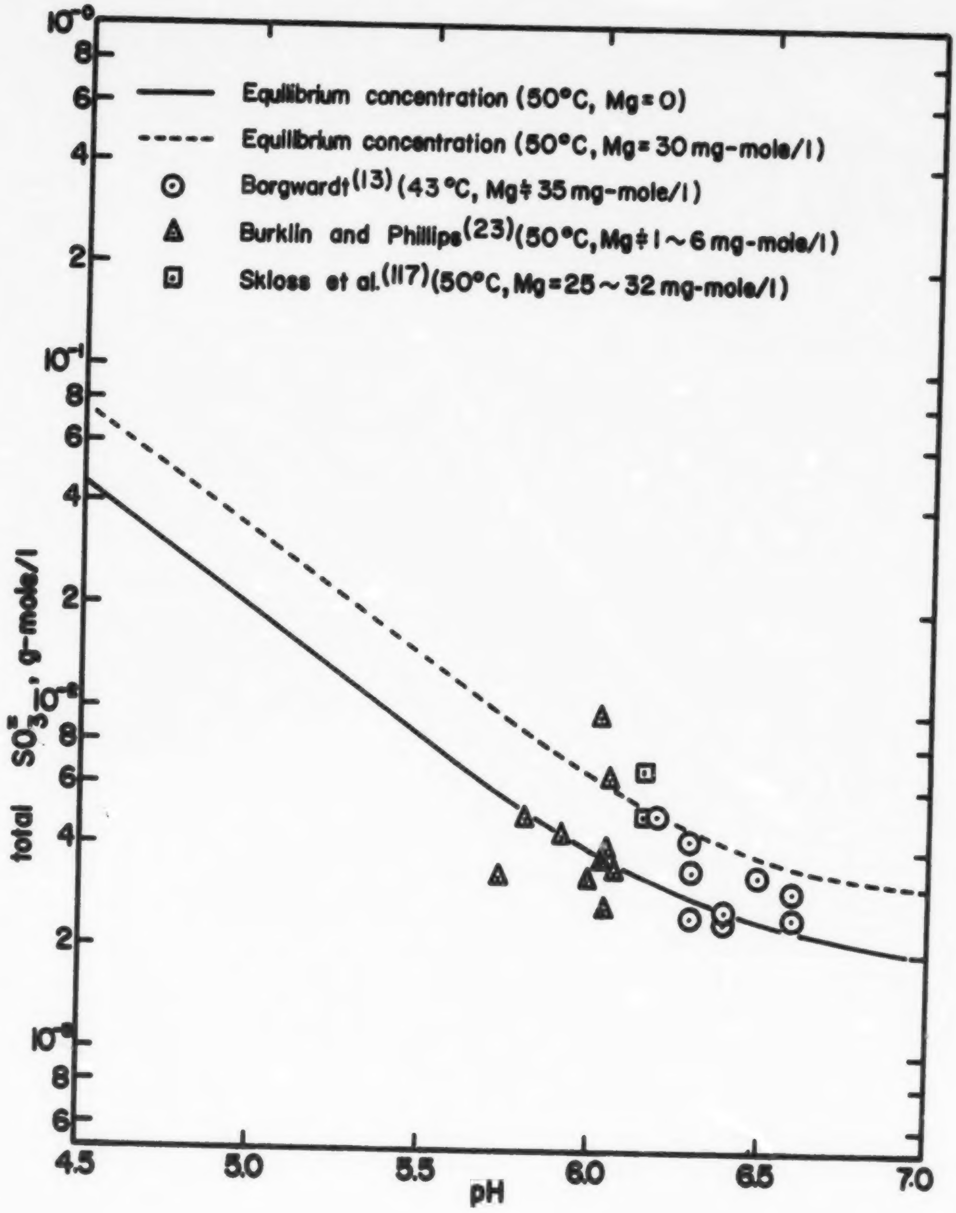

Figure 8. Equilibrium Concentration of Total Sulfite at 50°C and its Concentration in Outlet Liquor from Holding Tank vs. Liquor pH.

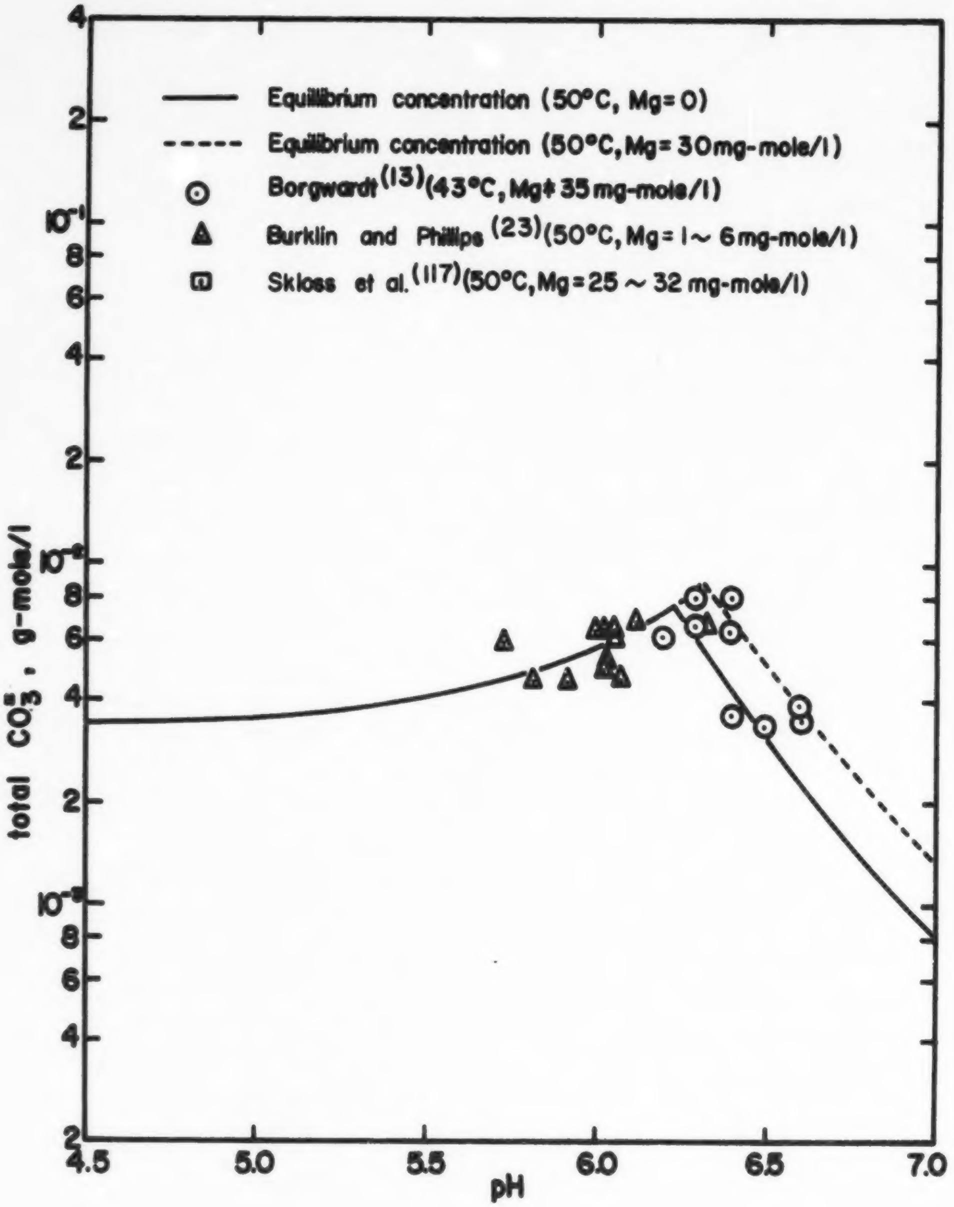

Figure 9. Equilibrium Concentration of Total Carbonate at 50°C and its Concentration in Outlet Liquor from Holding Tank vs. Liquor pH.

(4) Model for simulation of a holding tank in limestone process

As mentioned in the previous section, the dissolution mechanism of limestone into SO_2 scrubbing liquor which may contain various salts and ions in addition to dissolved CO_2 is rather complex and cannot be completely explained by the available data at the present time.

In order to develop a model for simulation of a holding tank in limestone slurry process, the following assumptions are made:

i. The tank is operated under steady state condition and is completely mixed.

ii. The tank is operated very closely as an equilibrium stage, that is, the outlet concentrations of each component are in "dynamic equilibrium" with the gas-phase.

iii. There is an evolution of CO_2 from the liquid in the tank to the gas-phase.

iv. There is no heat transferred between tank and surroundings, and heat of dissolution can be neglected.

With the above assumptions, a schematic flow diagram of a holding tank can be shown as Figure 10.

Taking the material balance around the tank for each component, we obtain:

$$X_1 + T_1 = S_1 \qquad (94)$$

where

$$T_1 \equiv Y_1 + Z_1 \quad \text{and} \quad S_1 \equiv X_1 + Y_1 + Z_1$$

$$X_2 + T_2 = S_2 \qquad (95)$$

where

$$T_2 \equiv Y_2 + Z_2 \quad \text{and} \quad S_2 \equiv X_2 + Y_2 + Z_2$$

$$W = M \qquad (96)$$

$$X_3 + T_3 = M \qquad (97)$$

where

$$T_3 \equiv Y_3 + Z_3$$

$$F\,[Ca]_1 + S_1 + M = F\,[Ca]_2 + S_2 + M \qquad (98)$$

$$F\,[S]_1 + T_1 = F\,[S]_2 + T_2 + T_3 \qquad (99)$$

where

$$[S]_1 \equiv [SO_3]_1 + [SO_4]_1, \quad \text{and} \quad [S]_2 \equiv [SO_3]_2 + [SO_4]_2$$

$$F[CO_3]_1 + X_1 + M = F[CO_3]_2 + X_2 + X_3 + N_{CO_2} \qquad (100)$$

$$X_3/M = X_2/S_2 \qquad (101)$$

The liquor leaving the holding tank is in equilibrium with the gas and solid phases in the tank. It means therefore that there is a pH of the liquor uniquely related to this condition as follows:

$$[Ca]_2 = f_1\,(pH) \qquad (102)$$

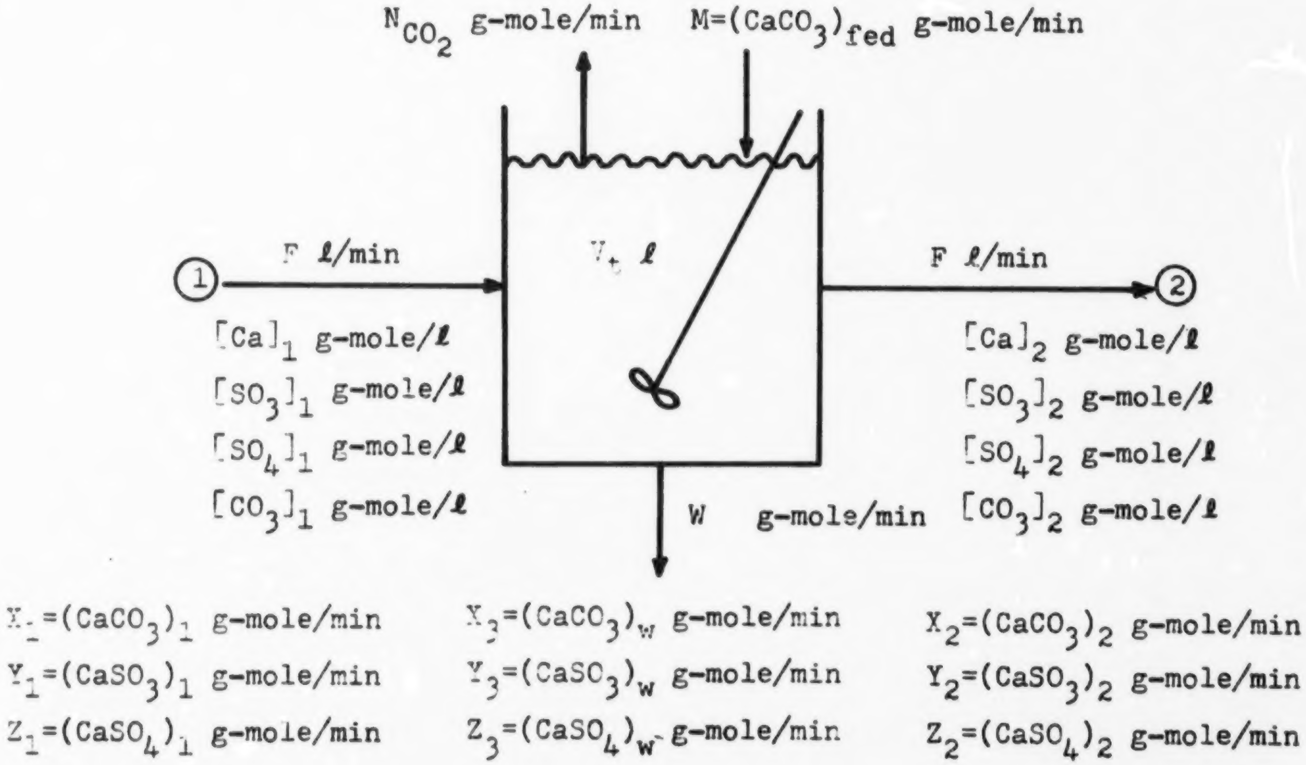
N_{CO_2} g-mole/min
$M=(CaCO_3)_{fed}$ g-mole/min
①
F ℓ/min
V_t ℓ
F ℓ/min
②
$[Ca]_1$ g-mole/ℓ
$[SO_3]_1$ g-mole/ℓ
$[SO_4]_1$ g-mole/ℓ
$[CO_3]_1$ g-mole/ℓ
W g-mole/min
$[Ca]_2$ g-mole/ℓ
$[SO_3]_2$ g-mole/ℓ
$[SO_4]_2$ g-mole/ℓ
$[CO_3]_2$ g-mole/ℓ
$X_1=(CaCO_3)_1$ g-mole/min
$Y_1=(CaSO_3)_1$ g-mole/min
$Z_1=(CaSO_4)_1$ g-mole/min
$X_3=(CaCO_3)_w$ g-mole/min
$Y_3=(CaSO_3)_w$ g-mole/min
$Z_3=(CaSO_4)_w$ g-mole/min
$X_2=(CaCO_3)_2$ g-mole/min
$Y_2=(CaSO_3)_2$ g-mole/min
$Z_2=(CaSO_4)_2$ g-mole/min

Figure 10. Material Balance Around a Holding Tank

$$[S]_2 = f_2\ (\mathrm{pH}) \tag{103}$$

$$[CO_3]_2 = f_2\ (\mathrm{pH}) \tag{104}$$

Thus, there are nine unknowns; $[Ca]_2$, $[S]_2$, $[CO_3]_2$, S_2, T_2, T_3, X_2, X_3, and pH, and nine equations; (95), and (97) ∼ (104). Theoretically it is possible to solve this set of equations but it will require a trial and error method.

It is easier to find the pH of the liquor by using the following relation. The derivation of this equation is shown in APPENDIX B. The pH of the leaving liquor should satisfy:

$$\Delta Ca - \Delta S - \Delta CO_3 + N_{CO_2}/F = 0 \tag{105}$$

where

$$\Delta Ca = [Ca]_1 - [Ca]_2$$

$$\Delta S = [S]_1 - [S]_2$$

$$\Delta CO_3 = [CO_3]_1 - [CO_3]_2$$

The rate of CO_2 evolution from the holding tank may be approximated by:

$$N_{CO_2} = k'_G a V_L (p^{*}_{CO_2} - p^{o}_{CO_2}) \tag{106}$$

N_{CO_2} is a function of pH, operating conditions and the design of the tank. Once the value of $k'_G aV$, which is a function of the operating conditions and the design of the tank, is known, every term in equation (105) becomes a function of pH only. Therefore the pH of the leaving liquor from the tank can be calculated by this equation.

The equilibrium partial pressure of CO_2 over the limestone slurry is shown in Figure 11 against the pH of the liquor. The partial pressure of CO_2 is a strong function of pH of the liquor and also the concentration of magnesium. When pH is less than 6, which is often encountered in the scrubber operation, the equilibrium partial pressure of CO_2 is much higher than the partial pressure of CO_2 in the scrubbing gas. This means that CO_2 may evolve in the scrubber in the limestone slurry process rather than being absorbed. When the pH of the liquor increases above 6, the partial pressure of CO_2 decreases sharply so that the rate of CO_2 evolved from the tank which is represented by equation (106) is reduced if $k'_G aV$ remains constant. Therefore, it is difficult to increase the pH higher than a certain value under normal operating or design conditions.

To find the pH of the outlet liquor by solving equation (105), $k'_G a$ has to be estimated. From the experimental data obtained from the various investigations (13, 23, 117), $k'_G a$ is calculated:

$$k'_G a = (\Delta Ca - \Delta SO_3 - \Delta SO_4 - \Delta CO_3) \frac{F}{V_t \cdot P^*_{CO_2}} \qquad (107)$$

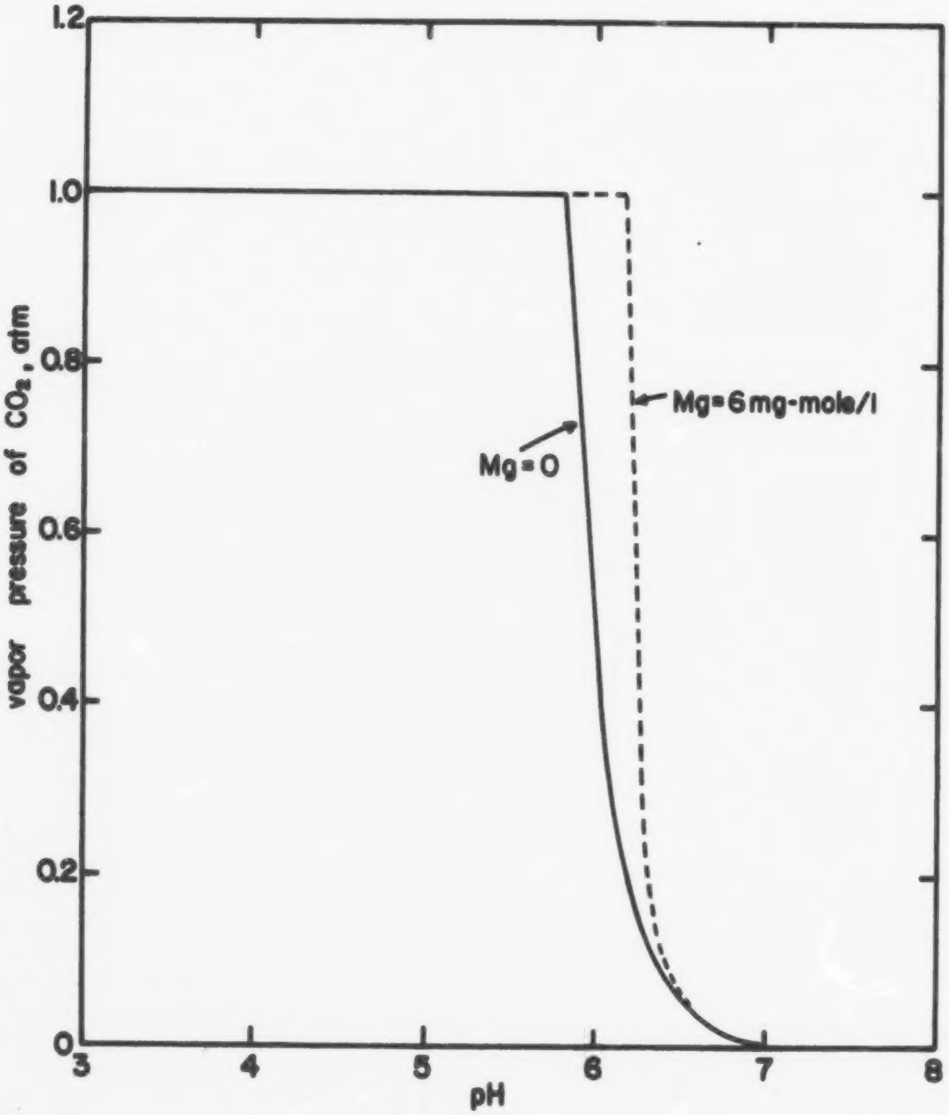

Figure 11. pH of Limestone Slurry vs. Vapor Pressure of CO_2 at 50°C

where $p^*_{CO_2}$ is the equilibrium pressure of CO_2 with the pH of the outlet liquor. The calculated results are shown in Figure 12 versus liquor flow rate. The mass transfer coefficient for CO_2 evolution from the holding tank in limestone slurry process, k'_Ga, slightly increases with the liquor flow rate. The following correlation for k'_Ga can be used to approximate the CO_2 evolution rate in the holding tank.

$$k'_Ga = 0.000211F^{0.263} \tag{108}$$

D. Overall Operation of Venturi Scrubber System with a Closed - Loop

From the practical point of view, most commercial wet scrubbing processes must be based on a closed-loop system in which the loaded liquor from the scrubber is regenerated in a holding tank and recycled within the process and not discharged from the process. Removed sulfur from the scrubbing gas is withdrawn as solid calcium salts from the process.

In this section a procedure of simulation of overall operation of a venturi scrubber with a holding tank and some other auxiliary equipment as shown in Figure 13 is discussed.

Prior to the discussion, the following assumptions are imposed on the venturi-holding tank system.

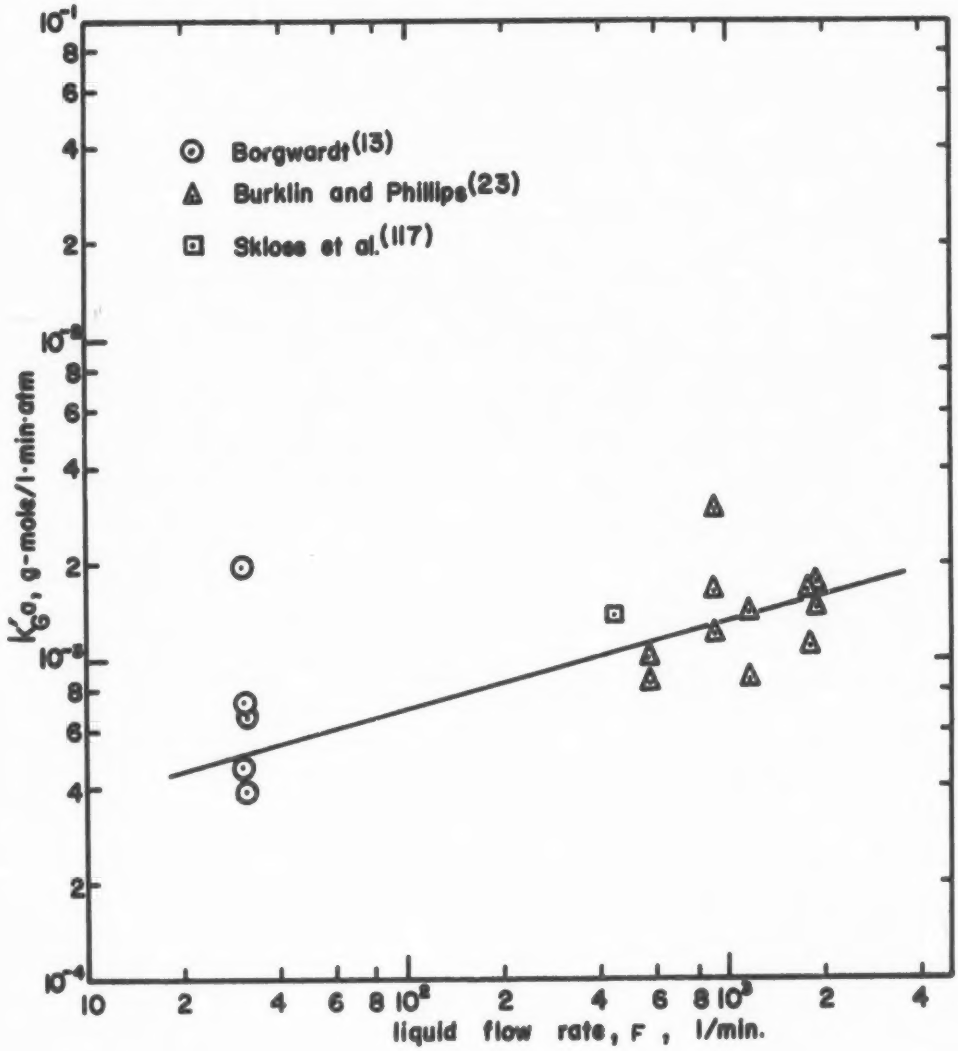

Figure 12. Mass Transfer Coefficient for CO_2 Evolution in the Holding Tank vs. Liquor Flow Rate.

i. There is no dissolution of lime or limestone except in the holding tank.

ii. The holding tank is considered to be completely mixed.

iii. Solid deposit and undissolved solid lime or limestone are removed from the clarifier.

iv. Make-up water is either not required or can be added without significant effect on the process performance, since the loss of the water due to evaporation in scrubber or with solid deposit from the system is negligibly small.

v. The system is under steady-state condition.

vi. Heat is exchanged between the gas-phase and the liquid-phase only in the venturi scrubber. Heat loss from the system through the auxiliary equipment and heat of dissolution of lime or limestone is negligible.

Hence, with the knowledge of given conditions such as the flow rate of recycling liquor, the amount of gas scrubbed, the sulfur-alkali ratio, etc., the steady-state operating conditions in the system can be found as shown in Figure 14(a) and 14(b).

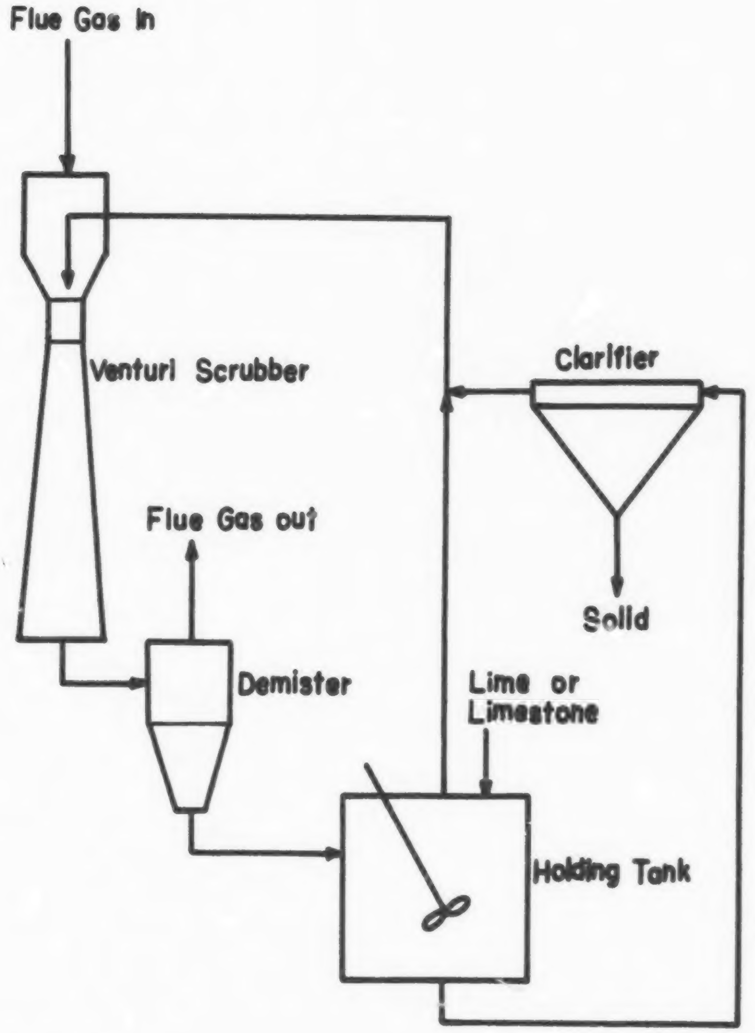

Figure 13. Venturi-Holding Tank System with Closed-Loop

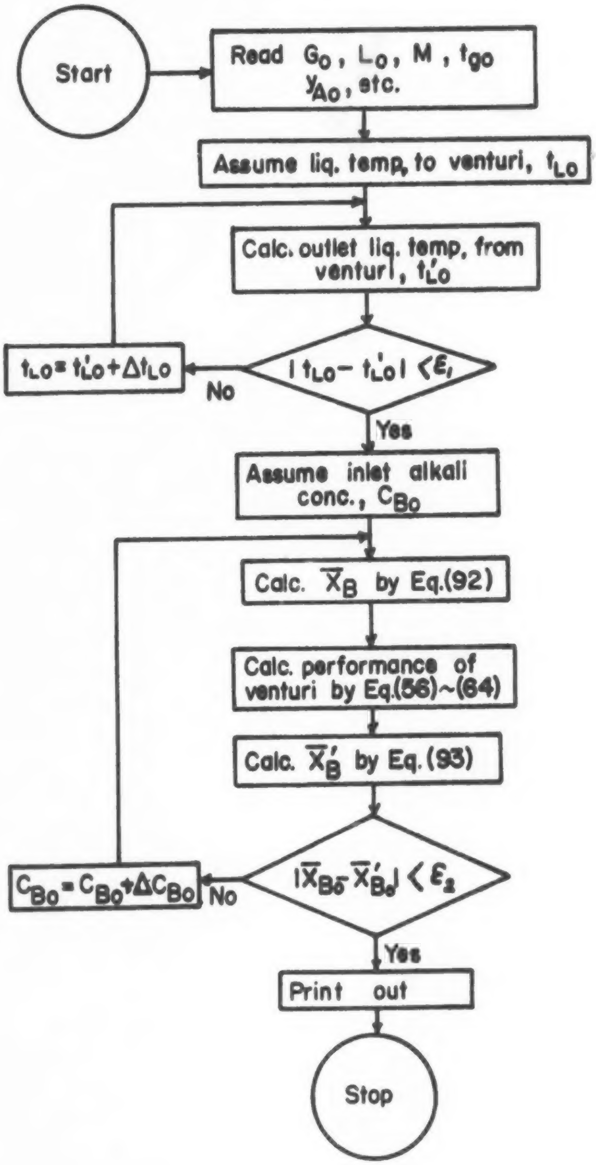
Start
Read G_0, L_0, M, t_{go} y_{A0}, etc.
Assume liq. temp. to venturi, t_{L0}
Calc. outlet liq. temp. from venturi, t'_{L0}
$|t_{L0} - t'_{L0}| < \varepsilon_1$
No
$t_{L0} = t'_{L0} + \Delta t_{L0}$
Yes
Assume inlet alkali conc., C_{B0}
Calc. $\overline{X}_B$ by Eq.(92)
Calc. performance of venturi by Eq.(56)~(64)
Calc. $\overline{X}'_B$ by Eq.(93)
$|\overline{X}_{B0} - \overline{X}'_{B0}| < \varepsilon_2$
No
$C_{B0} = C_{B0} + \Delta C_{B0}$
Yes
Print out
Stop

Figure 14 (a). Logic Diagram for Simulation of Venturi-Holding Tank Recycling System (Lime Slurry Process)

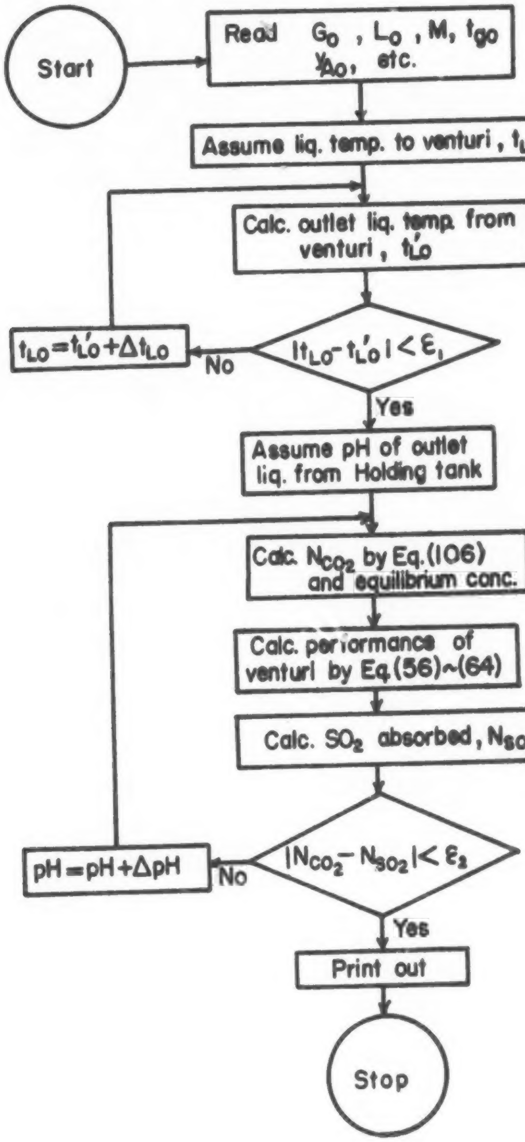
Start
Read G_o , L_o , M, t_{go} y_{Ao}, etc.
Assume liq. temp. to venturi, t_{Lo}
Calc. outlet liq. temp. from venturi, t'_{Lo}
$|t_{Lo}-t'_{Lo}| < \varepsilon_1$
No
$t_{Lo}=t'_{Lo}+\Delta t_{Lo}$
Yes
Assume pH of outlet liq. from Holding tank
Calc. N_{CO_2} by Eq.(106) and equilibrium conc.
Calc. performance of venturi by Eq.(56)~(64)
Calc. SO_2 absorbed, N_{SO_2}
$|N_{CO_2}-N_{SO_2}| < \varepsilon_2$
No
pH=pH+ΔpH
Yes
Print out
Stop

Figure 14 (b). Logic Diagram for Simulation of Venturi-Holding Tank Recycling System (Limestone Slurry Process)

IV. RESULTS AND DISCUSSION

In order to verify the mathematical models developed in the last chapter, a series of simulations of various venturi scrubbers and holding tanks are performed and the results are compared with experimental data. These simulations are conducted independently for venturi scrubbers and holding tanks, and then an overall simulation of a venturi-holding tank in which the scrubbing liquor is recycled is conducted. The sensitivity of the scrubbing efficiency on several operating variables is also investigated.

A. Simulation of Performance of Venturi Scrubbers

In this section, simulations of the experiments of SO_2 absorption by various solutions in several venturi scrubbers conducted by Harris et al. (53, 85), Gleason et al. (50), and Johnstone et al. (44, 65) are discussed.

(1) Description of the experiments

Harris et al. (53, 85) studied SO_2 absorption by water and NaOH solution in a venturi scrubber whose dimensions are shown in Figure 15-(a) (EPA venturi scrubber). The liquid was injected to the convergent section of the venturi scrubber where it was immediately atomized into small liquid droplets. The pressure drop across the

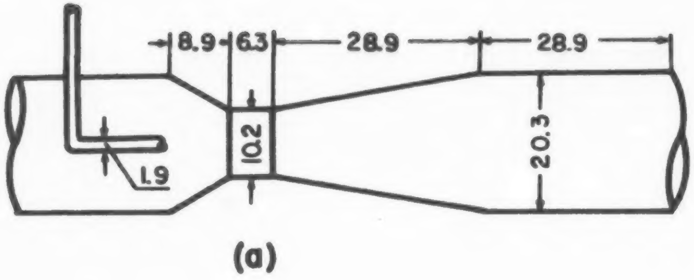

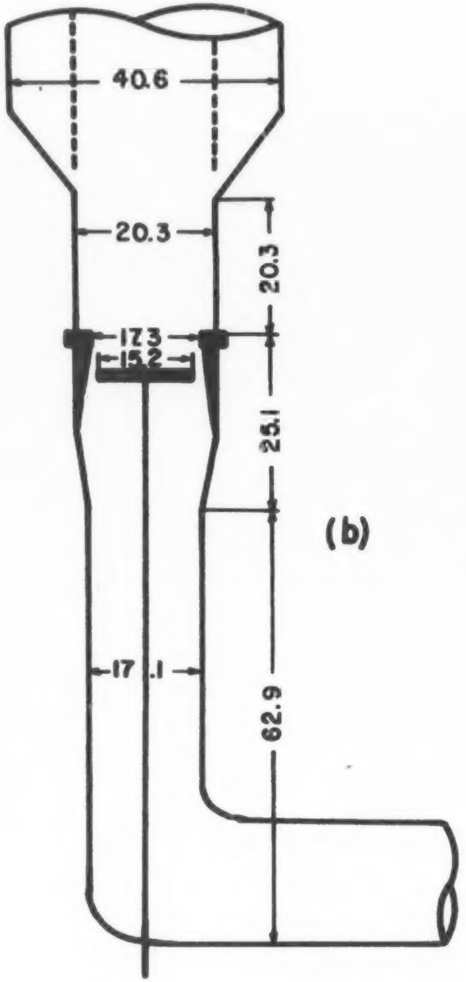

Figure 15. (a) Dimensions of Venturi Scrubber used by Harris et al. (53, 85) (EPA Venturi Scrubber)

(b) Dimensions of Flooded Disc Scrubber (FDS) used by Gleason et al. (50)

venturi scrubber and the difference in partial pressures of SO_2 at inlet- and outlet- points were measured.

Gleason et al. (50) investigated the absorption of SO_2 by water and lime and limestone slurries in a flooded disc scrubber (FDS). The FDS has a movable disc near the throat (126) as shown in Figure 15-(b). Vertical movement of the disc in the converging throat provides a means for varying the area of the annulus. This allows flexibility with respect to maintaining a fixed pressure drop under varying process operating conditions due to scaling, change in gas flow rate, etc. Also the moveable disc can be adjusted to give a desired efficiency with varying the velocity at the throat. Gleason et al. (50) also used a flooded disc scrubber in combination with a packed tower connected through a holding tank. The concentration of SO_2 in the scrubbing gas at the inlet and outlet of the FDS, pressure drop across the FDS and the pH at several points in the system were measured.

The last case of SO_2 absorption in a venturi scrubber is a series of experiments conducted by Johnstone et al. (44, 65). The dimensions of their scrubber are shown in Figure 16. As mentioned in CHAPTER II, they measured the total pressure and the rate of absorption at several points along the length of the venturi scrubber for water-SO_2 and NaOH solution - SO_2 systems.

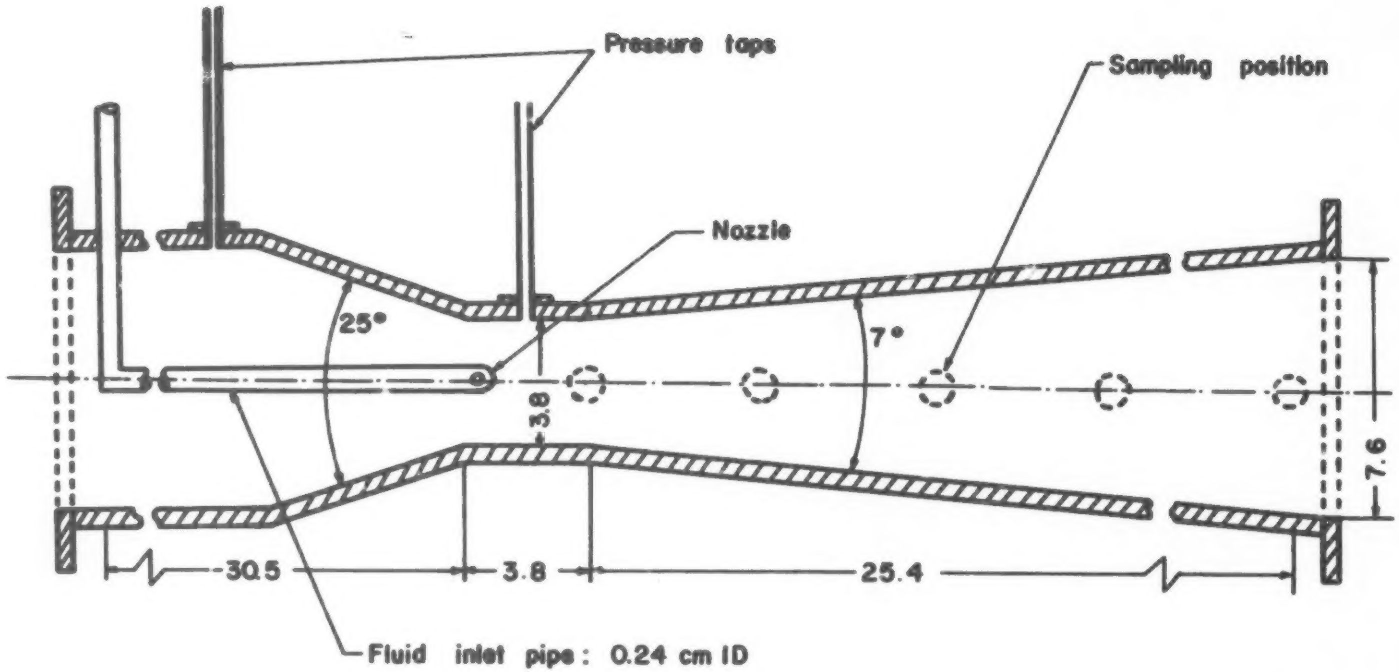

Figure 16. Dimensions of Venturi Scrubber used by Johnstone et al.(44, 65) (in cm.)

The operating conditions in these experiments are summarized in Table 3.

(2) Pressure drop in a venturi scrubber

In Figures 17 and 18, the calculated pressure drops are compared with experimental data, showing good agreement between the two. Application of the pressure drop correlations for venturi-type scrubbers listed in Table 1 to the experiments described above shows that none of the correlations could predict the pressure drop without changing the coefficients or powers in the equations except Calvert's equation and Boll's equation. Calvert's and Boll's equations are basically the same as equation (32). Calvert's equation predicted the pressure drop fairly accurately in the case of the flooded disc scrubber, while it gave higher values for the venturi scrubber used by Harris et al.$^{(53, 85)}$.

The change in the static pressure along the venturi scrubber was predicted closely by equation (32) for the venturi scrubber used by Johnstone et al. as shown in Figure 18. It is advantageous to use equation (32) since it can predict accurately the pressure profile within a venturi scrubber.

(3) Momentum, heat and mass transfer

Figures 19 through 24 are examples of calculated results for venturi scrubbers of Harris$^{(53)}$ and Johnstone et al.$^{(44, 65)}$. The velocity profiles of the gas and

Table 3. Experimental Conditions used in the Three Experiments

Experiment	Harris et al. (53,85)	Gleason et al. (50)	Johnstone et al. (44,65)
Gas rate, m^3/min (Gas rate, ACFM)	25.5 ~ 34.0 900 ~ 1,200	25.5 (900)	7.1 ~ 13.6 250 ~ 480
Liquid rate, /min (Liquid rate, GPM)	38 and 57 (10 and 15)	30 ~ 60 (8 ~ 16)	0.11 ~ 1.14 (0.03 ~ 0.30)
Gas velocity, m/sec	60 ~ 70	30 ~ 43	100 ~ 200
Inlet gas temp °C Outlet gas temp°C	120 ~ 160 25	180 ~ 190 49	---
Pressure drop cm-H_2O	20 ~ 30	13 ~ 25	---
SO_2 inlet conc. ppm	2,000	1,000 ~ 2,000	1,520
SO_2 removal %	32 ~ 64 11 (for H_2O)	40 ~ 50 14 (for H_2O)	1.5 ~ 15
Solution	H_2O, NaOH soln.	H_2O CaO slurry	NaOH soln.

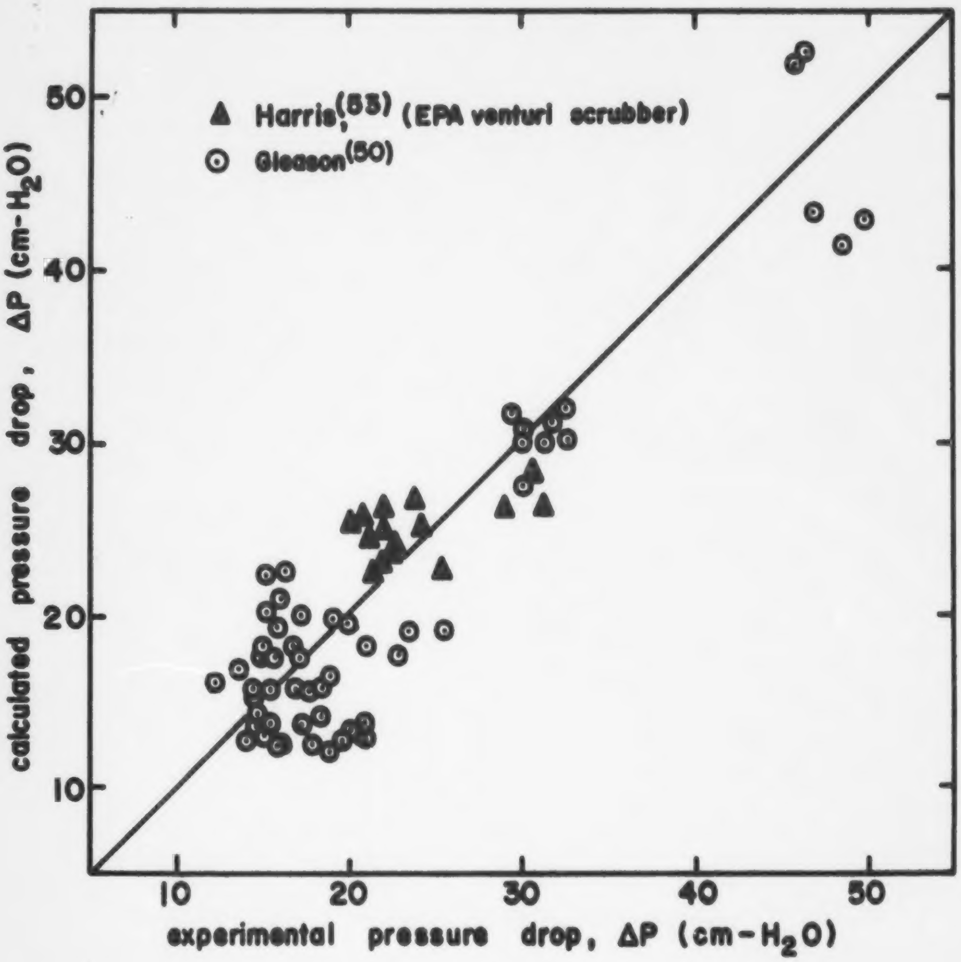

Figure 17. Comparison of Calculated Pressure Drop in EPA Venturi Scrubber and Flooded Disc Scrubber with Experimental Data

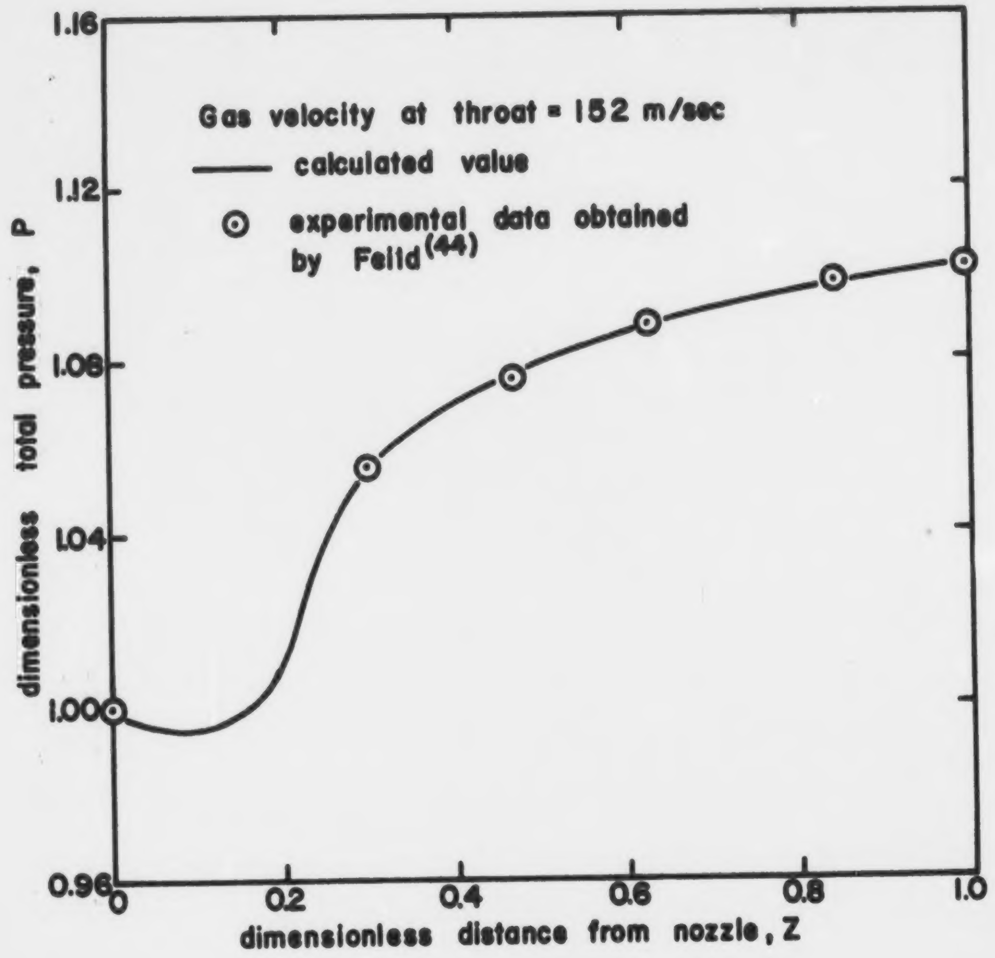

Figure 18. Pressure Profile in Venturi Scrubber used by Johnstone et al.$^{(44, 65)}$

the liquid, the concentration profile of sulfur dioxide absorbed in the liquid-phase and the temperature profiles in the gas and liquid along the axial direction in the EPA venturi scrubber are presented in Figures 19 and 20. The operating conditions and experimental data covered are:

Gas flow rate = 30.3 m^3/min
Liquid rate = 37.85 /min
Inlet gas temperature = 154°C
Outlet gas temperature = 43°C
Inlet SO_2 concentration = 2000 ppm
Outlet SO_2 concentration = 1160 ppm
Pressure drop = 21 cm H_2O

Figure 19 shows that in the EPA venturi, the velocity of the liquid reaches its maximum value after the throat of the venturi while the gas velocity reaches maximum in the throat section. The liquid velocity exceeds the gas velocity when the gas velocity decreases sharply due to the expansion of the venturi duct after the throat. The contraction and the expansion of the venturi duct seems to be desirable not only for atomization of the liquid but also for heat and mass transfer between the gas and the liquid as the result of the high relative velocity induced.

From the concentration profiles of sulfur dioxide absorbed in the liquid phase it is seen that a large amount of absorption takes place near the point of the

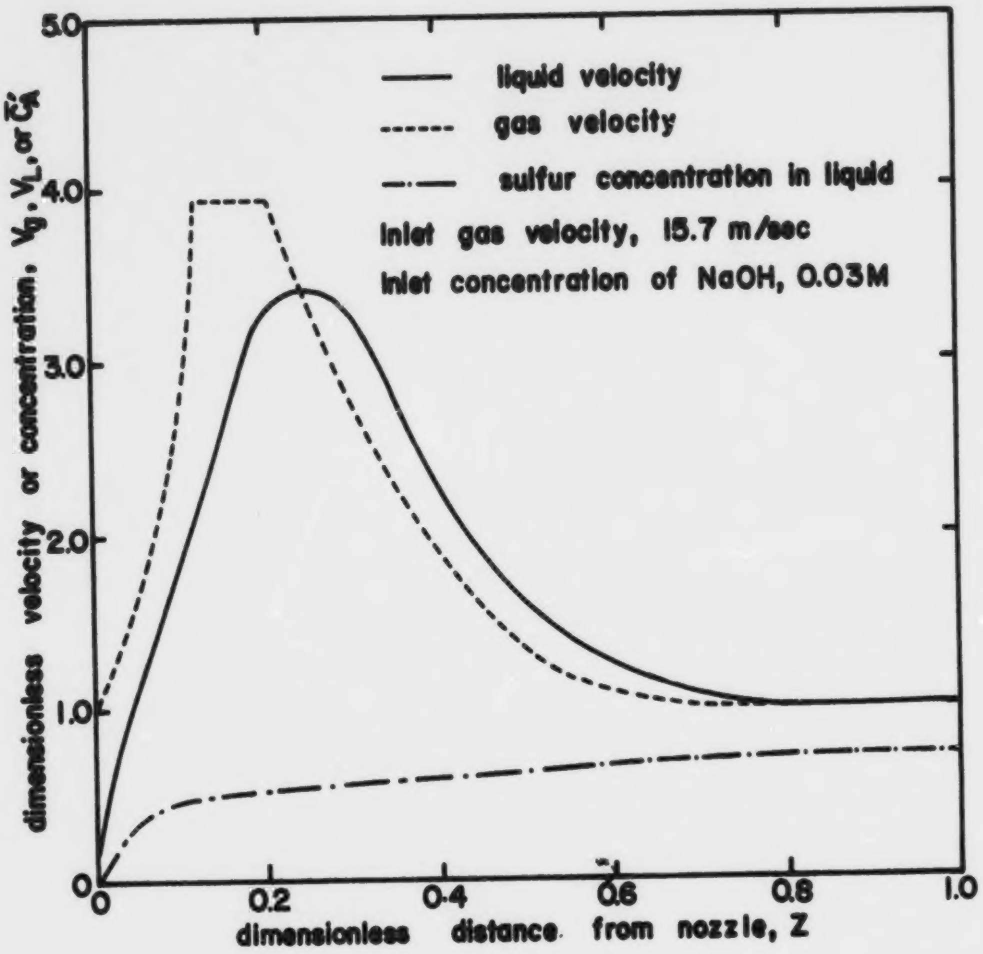

Figure 19. Velocity and Sulfur Concentration Profiles along Axial Distance in EPA Venturi Scrubber (53)

liquid injection. This is principally due to the following three factors in this region: the small transfer resistances, large concentration difference, and relatively long residence time of the liquid droplets.

The temperature profiles of the gas and the liquid shown in Figure 20 indicate that the temperatures of both the liquid and the gas approach the same value rather quickly. Thus venturi scrubbers can be considered to be highly efficient heat transfer devices.

The performance of the FDS can be seen to be nearly the same as the EPA venturi scrubber.

Figures 21 and 22 are comparisons of calculated values of the absorption rate along the venturi as a function of the liquid rate based on the experimental data obtained by Johnstone et al.(44, 65). The cumulative absorption rate in Figure 21 and total absorption rate in Figure 22 increases with liquid rate almost proportionally. The calculated values show satisfactory agreement.

Figures 23 and 24 show the concentration profiles of SO_2 and alkali within a liquid drop in two typical cases with the distance from the point of the liquid injection as a parameter. For the SO_2 - H_2O system, the concentration of SO_2 within the liquid drop is almost in equilibrium at the outlet point as shown in Figure 23. In Figure 24 the concentrations of SO_2 and NaOH within

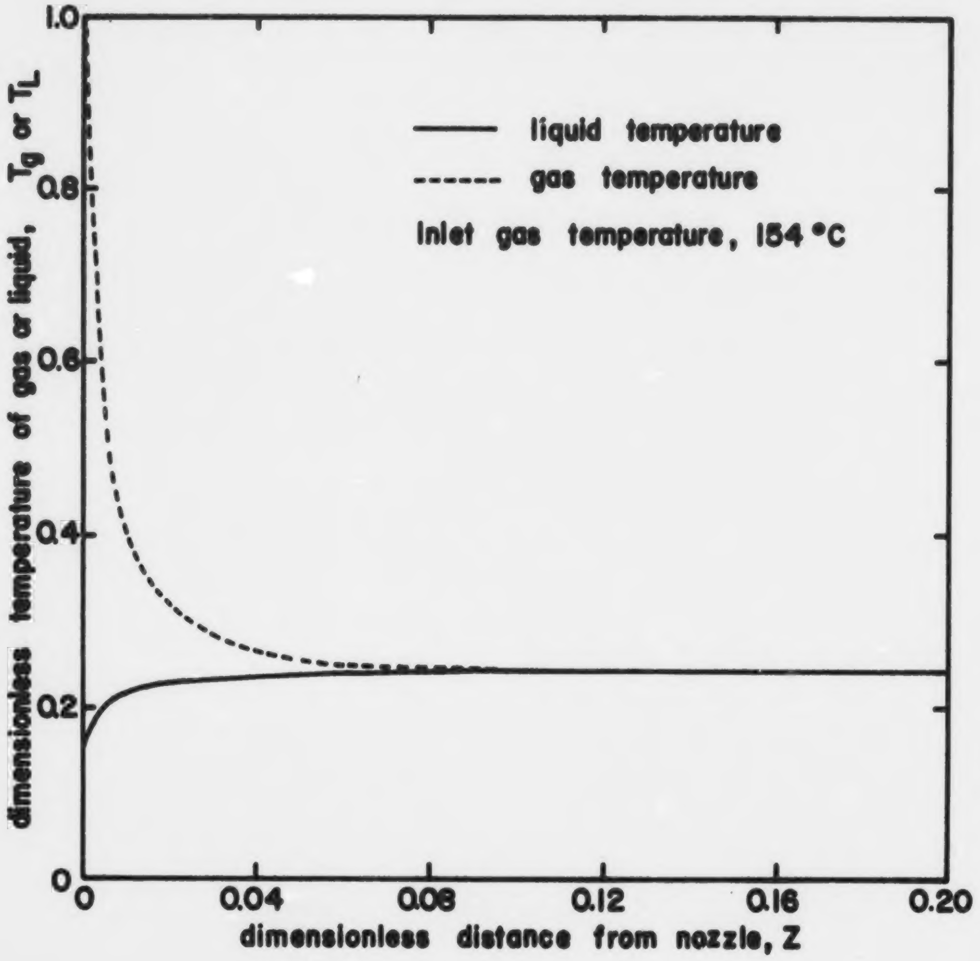

Figure 20. Temperature Profiles of Gas and Liquid along Axial Distance in EPA Venturi Scrubber (53)

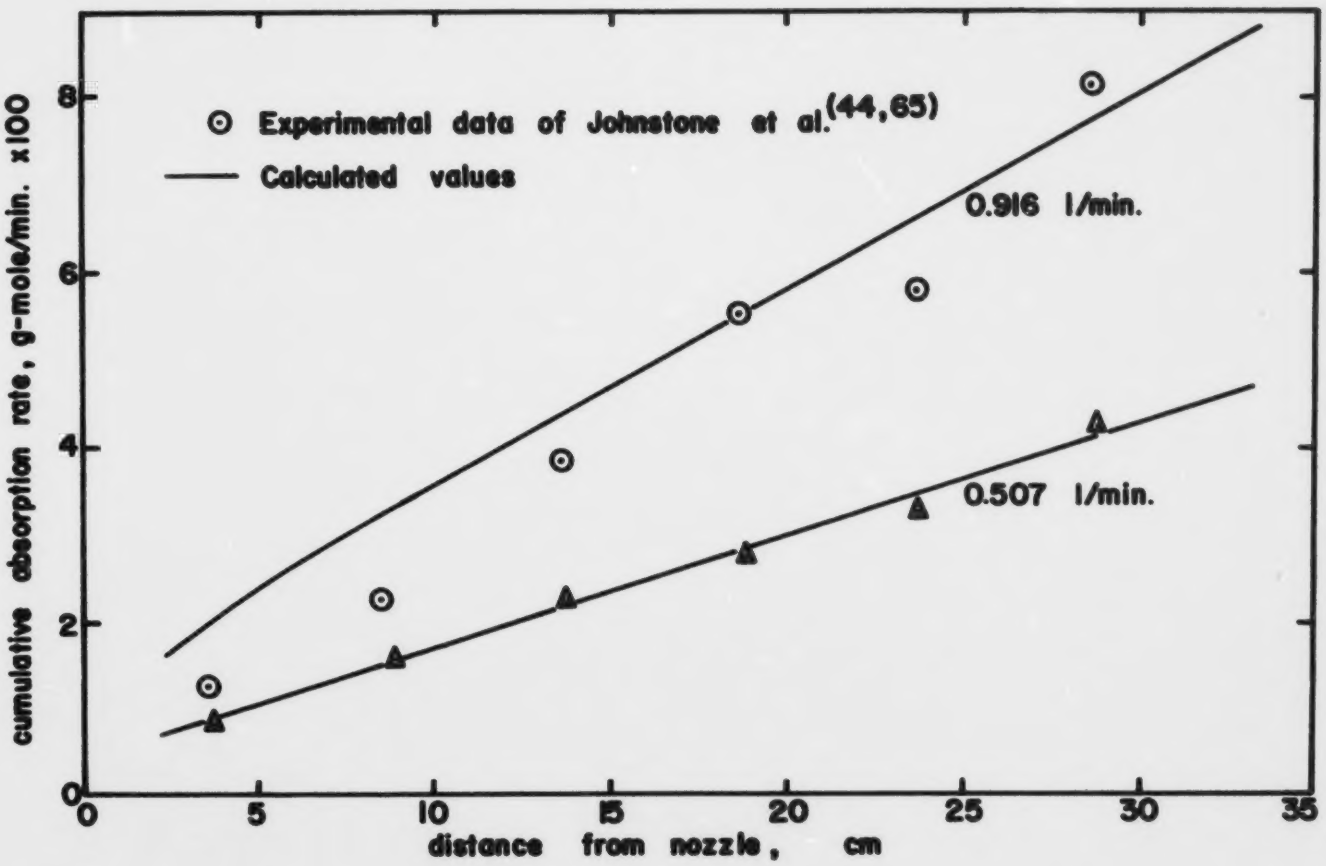

Figure 21. Profiles of Cumulative Absorption Rate in Venturi Scrubber (Experiment of Johnstone et al.)(44, 65)

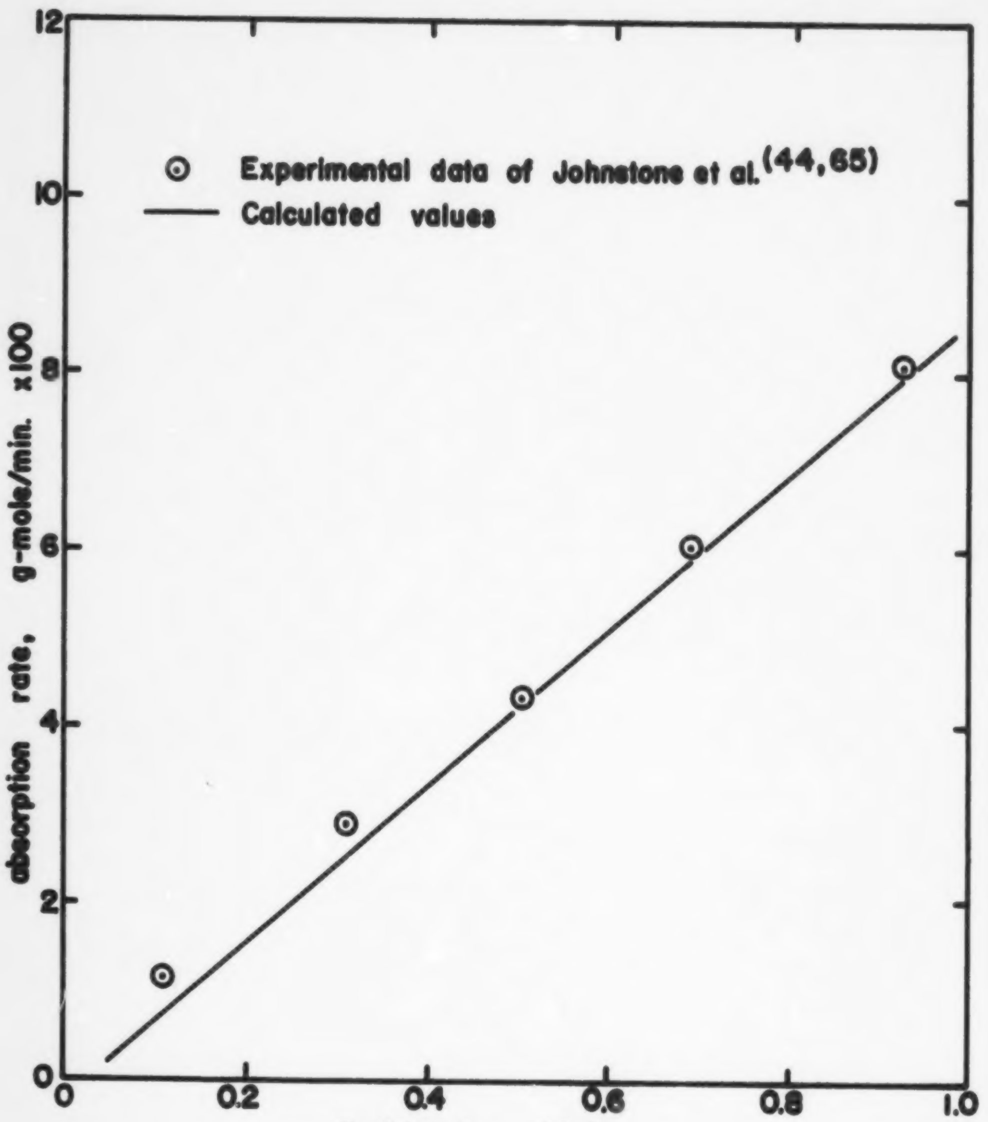

Figure 22. Comparison of SO_2 Removal Rate in the Venturi Scrubber Calculated with Experimental Data Obtained by Johnstone et. al. (44, 65)

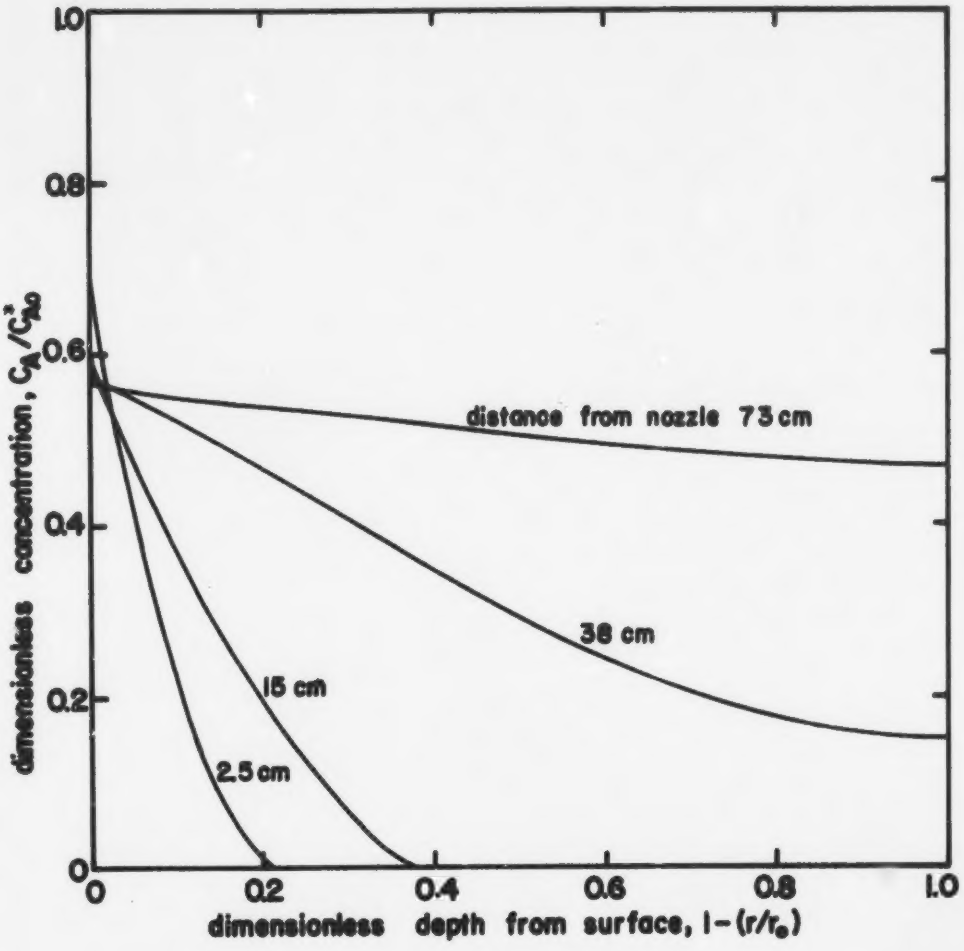

Figure 23. Concentration Profile of SO_2 in a Droplet (EPA Venturi: $H_2O - SO_2$ System)

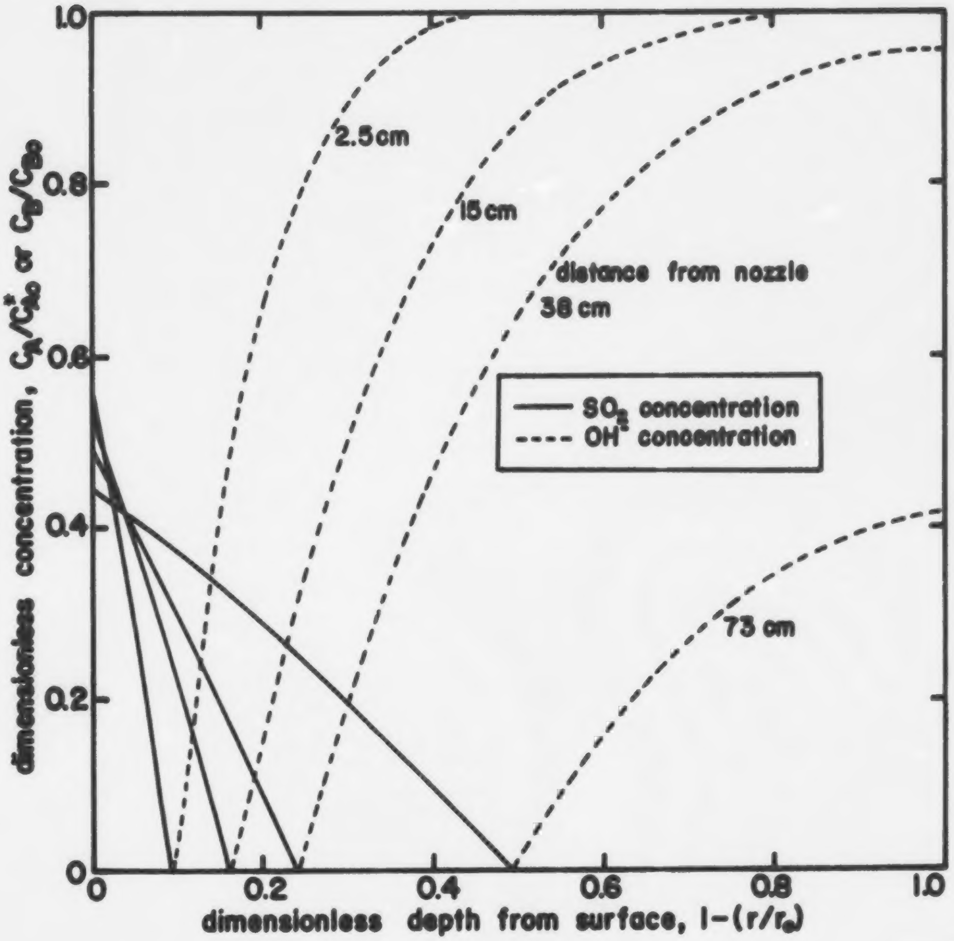

Figure 24. Concentration Profiles of SO_2 and NaOH in a Droplet (EPA Venturi: NaOH - SO_2 - H_2O System)

a liquid drop are shown in a case of the SO_2 - NaOH - H_2O system.

Finally the calculated SO_2 removal percentages are summarized and compared in Figure 25 with the experimental data obtained from different venturi scrubbers under different experimental conditions. The agreement between the calculated values and the data is quite satisfactory.

B. Simulation of the Holding Tank Performance

In this section, the simulation of the holding tanks for the lime and the limestone slurry processes will be be discussed. Only a few data on the performance of holding tanks for the lime and the limestone slurry processes are available. The operating conditions under which these data were taken are summarized in Table 4.

(1) Holding tank for the lime slurry process

Only one series of experiments performed by Gleason et al. (50) fed lime directly to the mixing/holding tank. They measured the values of pH at the inlet and outlet points of the holding tank. The value of pH is related to the concentration of $Ca(OH)_2$ in the solution as shown in Figure D-1 in APPENDIX D. The model for the dissolution of lime proposed in the last chapter has been used to simulate the holding tank used by Gleason et al. The results are compared with experimental data in Figure 26, showing good agreement.

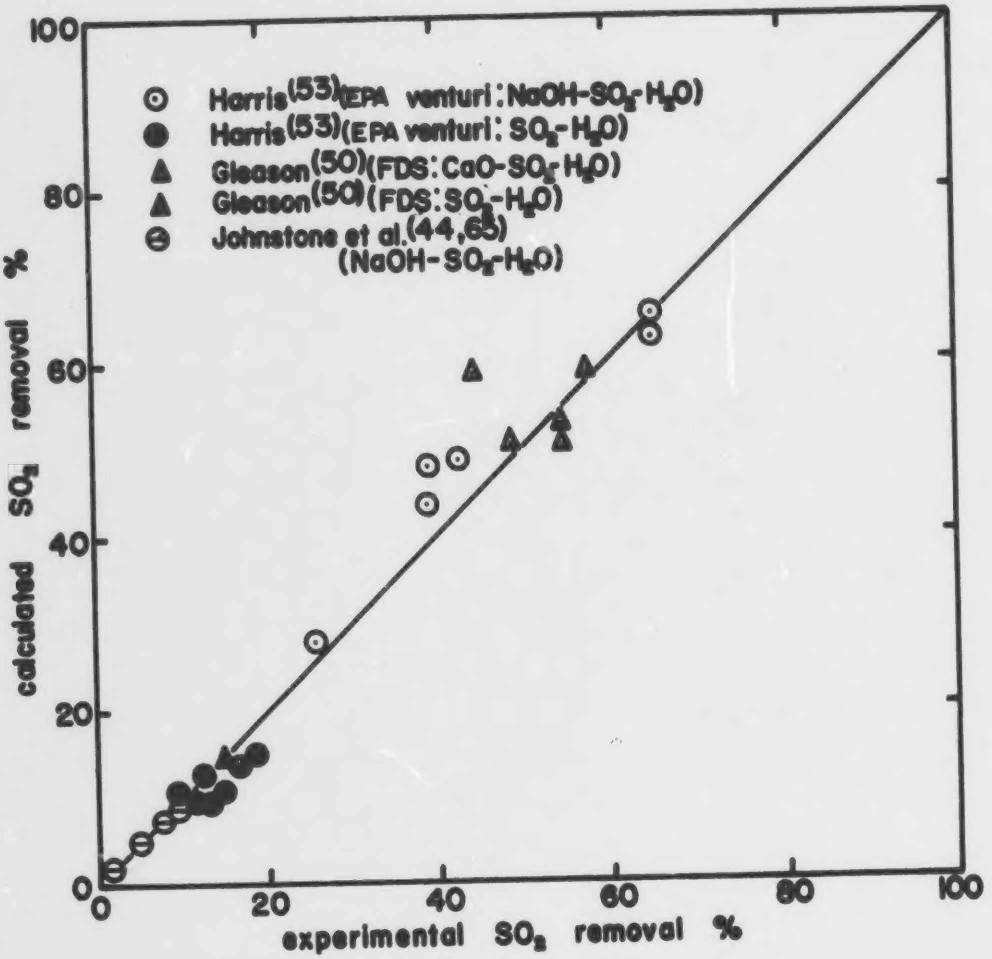

Figure 25. Comparison of Calculated SO$_2$ Removal % with Experimental Data

Table 4. Experimental Conditions of Holding Tanks Used in Four Experiments

Experiment	Gleason(50)	Borgwardt(13)	Burklin and Phillips(23)	Skloss et al. (117)
alkali	lime	limestone	limestone	limestone
volume, ℓ (volume, gallon)	1900 ~ 5600 (500 ~ 1500)	1,300 (350)	22,700 (6,000)	2,350 (620)
liquid rate, ℓ/min (liquid rate, GPM)	30 ~ 60 (8 ~ 16)	32.2 (8.5)	570 ~ 1,840 (150 ~ 485)	435 (115)
residence time, min	30 ~ 150	4 ~ 40	12 ~ 40	5.4
liquid temp. ^{o}C	40 ~ 50	43	50	50

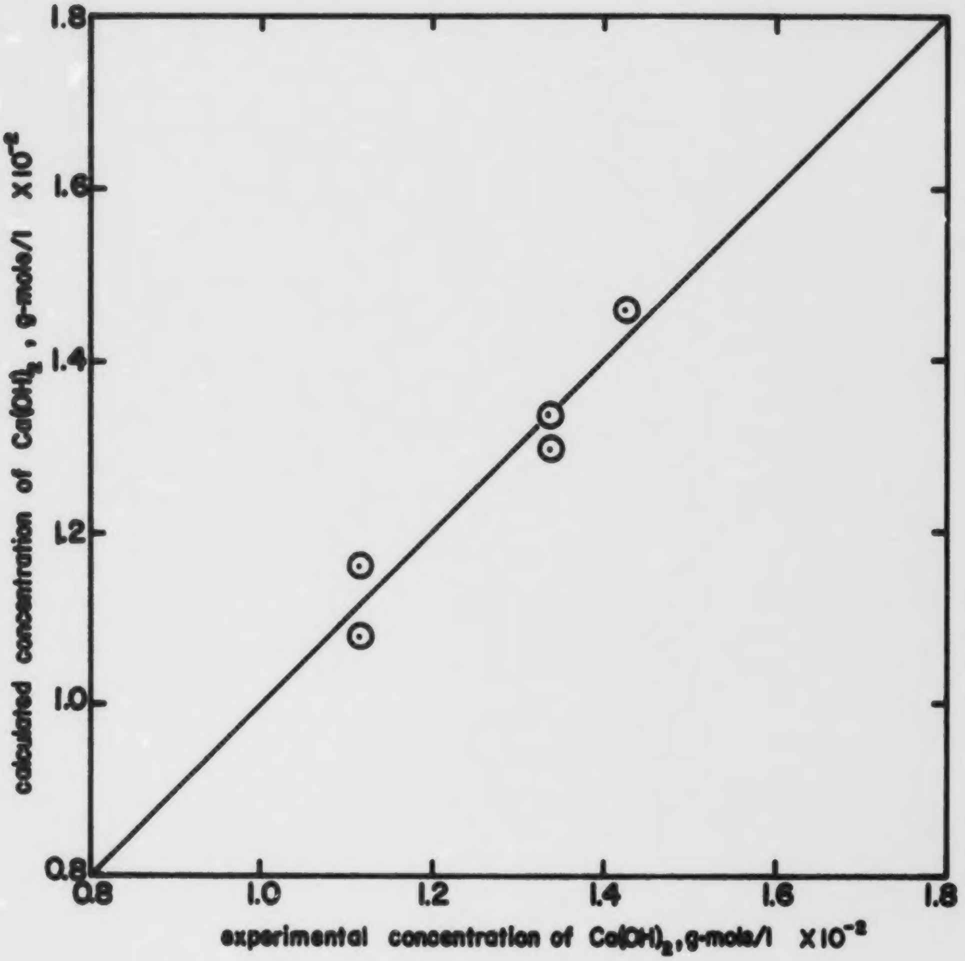

Figure 26. Comparison of Calculated Concentration of $Ca(OH)_2$ in Solution from Holding Tank with Data Obtained by Gleason et al. (50)

(2) Holding tank for the limestone slurry process

The amount of data available on the performance of holding tanks in the limestone slurry processes is substantially greater than that available on the holding tanks in the lime slurry processes. The holding tanks in the limestone slurry processes are simulated based on the data obtained by Borgwardt (13), Burklin and Phillips (23), and Skloss et al. (117). The comparisons of calculated results with the experimental data are shown in Figures 27, 28, and 29.

In Figure 27, the values of the pH of the outlet liquor are shown. Although some scatter of the points is seen, the agreement between the experimental and calculated outlet pH is satisfactory within the errors of the data.

In Figures 28 and 29, the calculated concentrations of the key components in the outlet solutions, such as total calcium, total sulfite, total sulfate, and total carbonate, are compared with the measured values. Total sulfite and carbonate concentrations are somewhat scattered but the calculated and experimental values are within the same order of magnitude. The experimental and calculated total calcium and total sulfite concentrations are in good agreement.

In the above simulations of the holding tank in the limestone slurry process, it is assumed that the holding

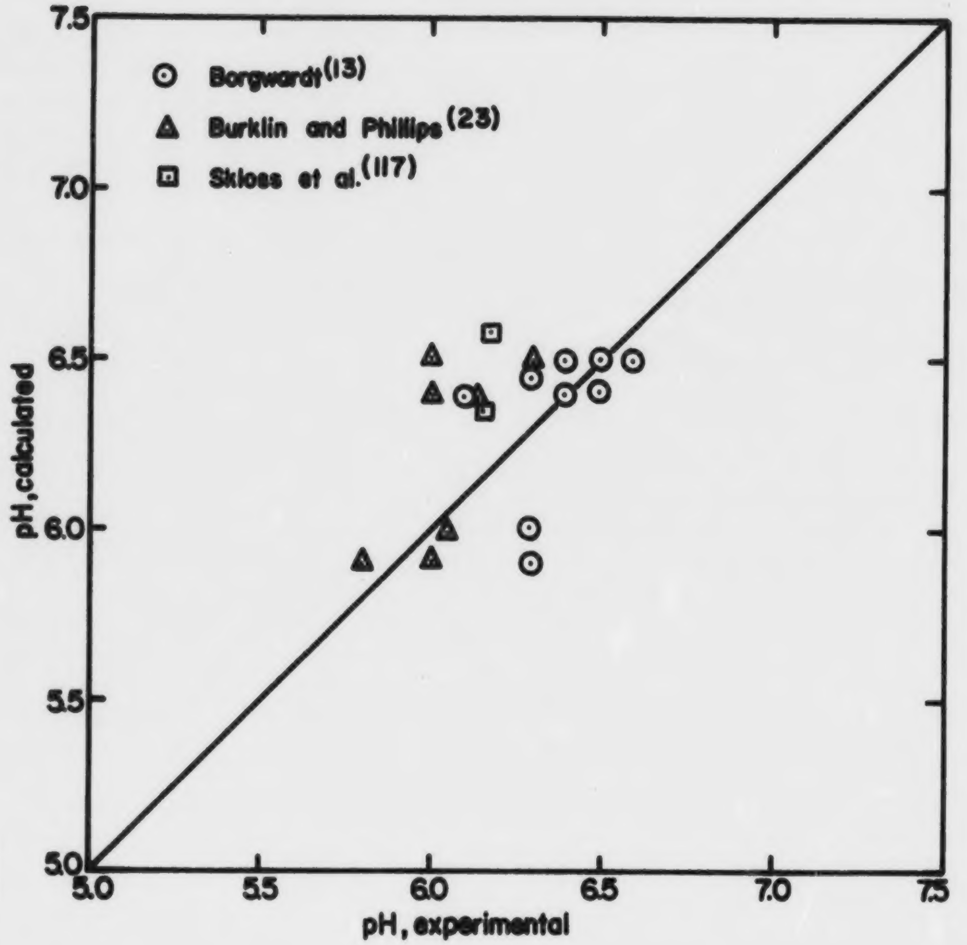

Figure 27. Comparison of the Values of Calculated pH of Outlet Liquor from Holding Tank with Experimental Data. (Limestone Slurry Process)

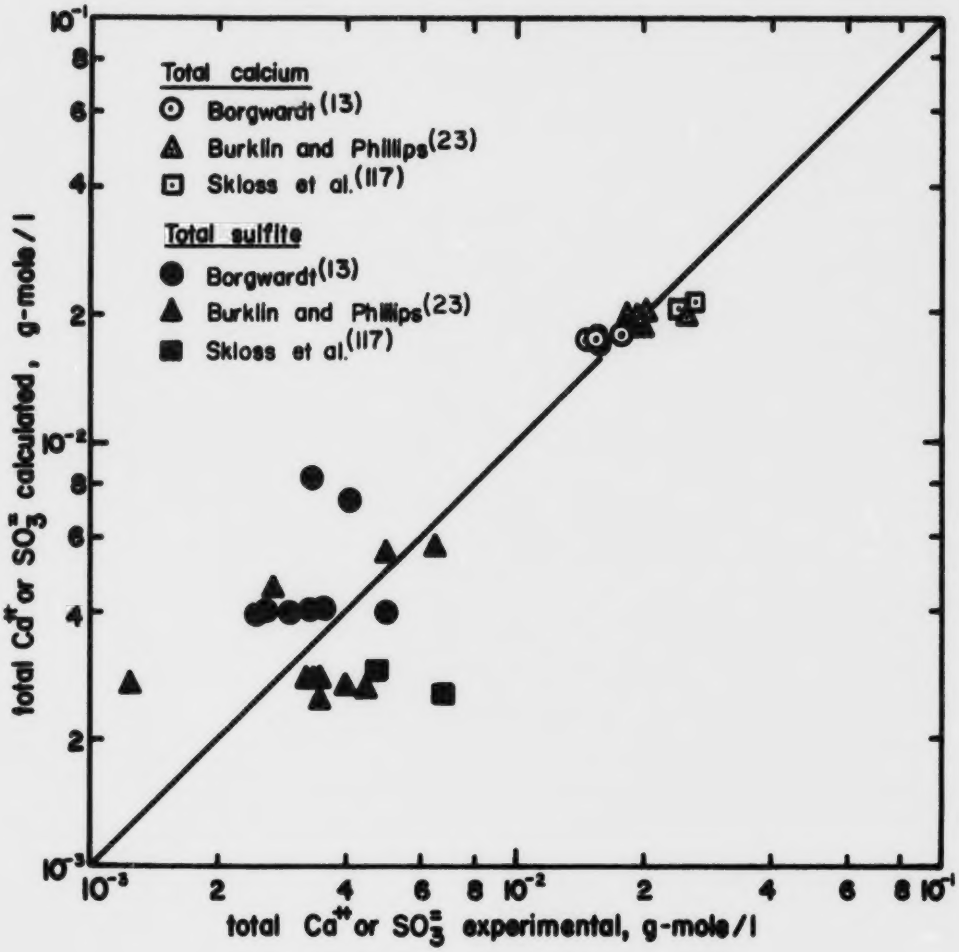

Figure 28. Comparison of Calculated Values of Concentrations of Total Calcium and Sulfite in Outlet Liquor from Holding Tank with Experimental Data (Limestone Slurry Process)

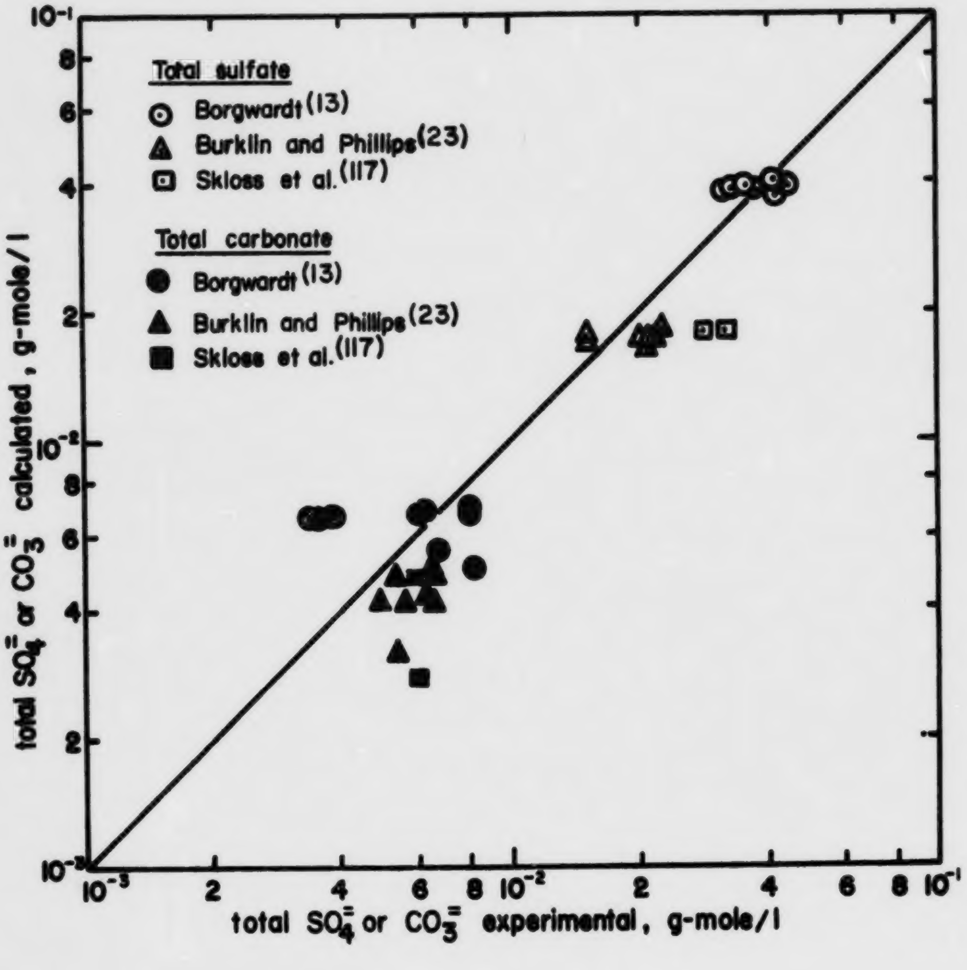

Figure 29. Comparison of Calculated Values of Concentrations of Total Sulfate and Carbonate in Outlet Liquor from Holding Tank with Experimental Data (Limestone Slurry Process)

tank is an equilibrium stage. Based on the favorable comparison of the calculated pH and concentrations of key components with the experimental data, this assumption appears to be very reasonable. A model based on the equilibrium stage assumption will be used to simulate the holding tank of a scrubber-holding tank system in which the scrubbing liquor is recycled.

C. Performance of Venturi-Holding Tank Systems with Closed-Loop Recycle of the Scrubbing Slurry

In this section the calculated results for venturi-holding tank systems based on the conditions described in Section D of CHAPTER III are discussed and the sensitivities of operating variables are investigated. For more detailed information see the references (42, 50, 104).

(1) Lime slurry process with a closed-loop recycle of the scrubbing liquor.

The momentum, heat and mass balances describing the lime slurry process based on Gleason's experiment (50) were solved. The dependence of the alkali efficiency (defined as the percentage of consumed alkali to make-up alkali), and the SO_2 removal percentage on the liquid flow rate and the alkali feed rate is shown in Figure 30. From this figure, the following can be concluded:

1. At low alkali feed rate, the percent SO_2 removal increases proportionally with the alkali feed rate.

2. An increase in the liquid flow rate reduces SO_2 removal and alkali efficiency since the residence time in

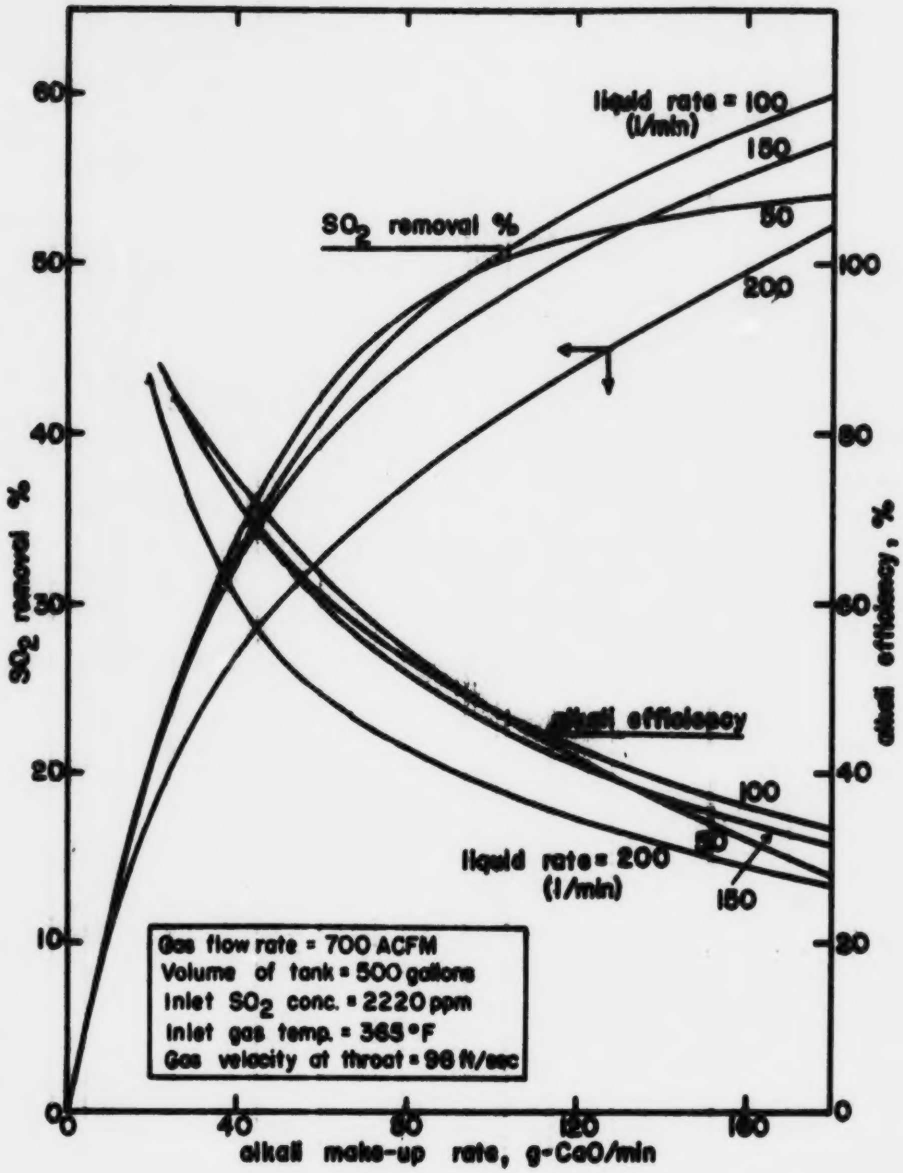

Figure 30. Performance of a Venturi-Holding Tank System with a Closed-Loop Recycling of Slurry (Lime Slurry Process)

the holding tank under the constant volume condition decreases. An increase in liquid flow rate also produces in a larger diameter droplet resulting in more alkali in the outlet liquid.

3. The pressure drop (which is not in this figure) increases with the liquid flow rate from 17 cm-H_2O at 50 l/min of liquid rate to 47 cm-H_2O at 200 l/min.

4. At low liquid rates, and the alkali feed rates above 80 [g-CaO/min], the percentage of SO_2 removal does not improve as rapidly with increase in alkali flow rate as in the case where the alkali feed rate is less than 80 [g-CaO/min]. The reason for this is that at this flow rate the solubility limit of CaO in the recycling liquor is reached. Therefore, the alkali efficiency goes down rapidly from this point.

5. Taking into consideration the pressure drop, SO_2 removal % and alkali efficiency, there will be an optimum operating condition for this lime slurry process.

(2) Limestone slurry process with a closed-loop recycle of the scrubbing liquor

An overall simulation of a scrubber-holding tank system is based on the experimental conditions used by Princiotta and Epstein (42, 104).

In addition to the assumptions made in Section D of Chapter III, the following assumptions are made in this calculation.

a) Alkali sulfur ratio (mole ratio of alkali to sulfur dioxide in the scrubbinggas) is high enough so that the liquor leaving the holding tank is in equiligrium with solid limestone present in the liquid phase.

b) From the relation of the overall reaction (30), one mole of SO_2 absorbed produces one mole of CO_2. The amount of CO_2 evolved in the holding tank is equal to the amount of SO_2 absorbed in the scrubber.

The calculated results in typical cases are shown and compared with experimental data (42) in Figure 31. The agreement between the calculated values and the data seems quite fair.

The dependence of SO_2 removal percentage and the pH of the liquor in the holding tank on the flow rate of the recycling liquor is shown in Figure 32. Some other operating conditions are listed in the same figure. Examination of this figure reveals the following:

1. The SO_2 removal percentage increases with the liquid rate and the decrease in pH of the inlet liquor to the scrubber has little effect on the absorption efficiency.

2. An increase in the liquor flow rate causes a decrease in pH of the liquor leaving the holding tank since CO_2 evolution per unit of liquor from the holding tank decreases with the liquor rate. The pH of the

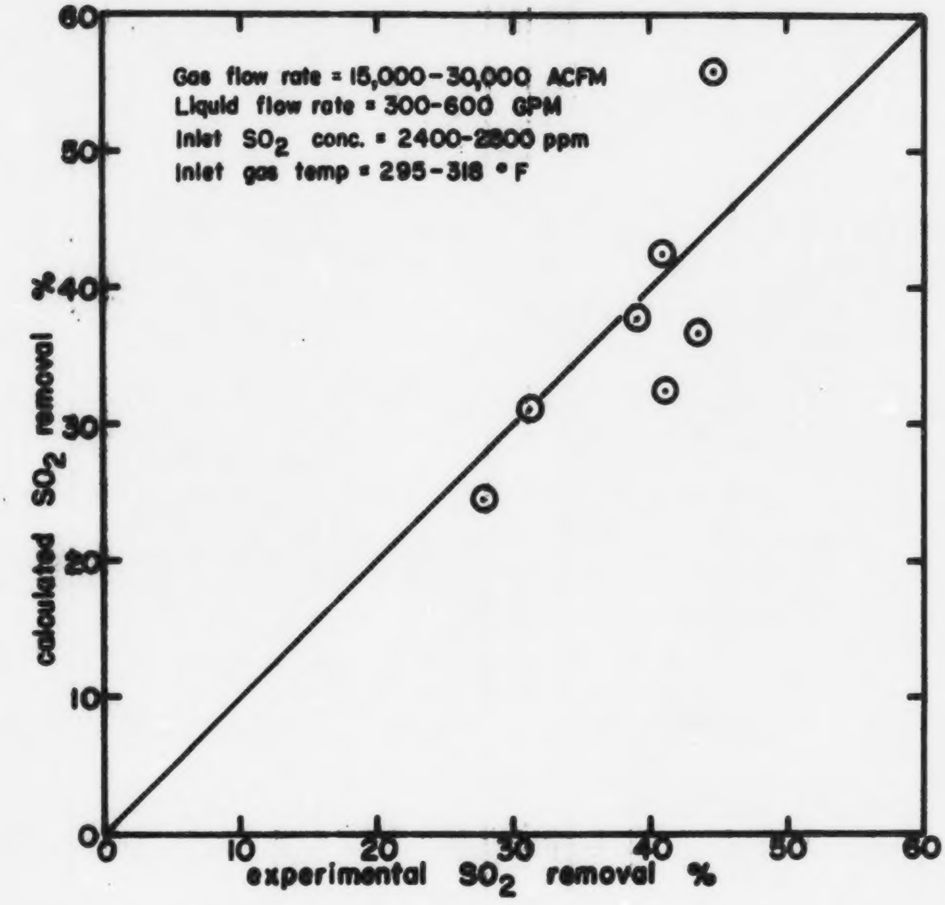

Figure 31. Comparison of Calculated SO_2 Removal % with Experimental Data Obtained by Epstein et al. (42) (Limestone Slurry Process)

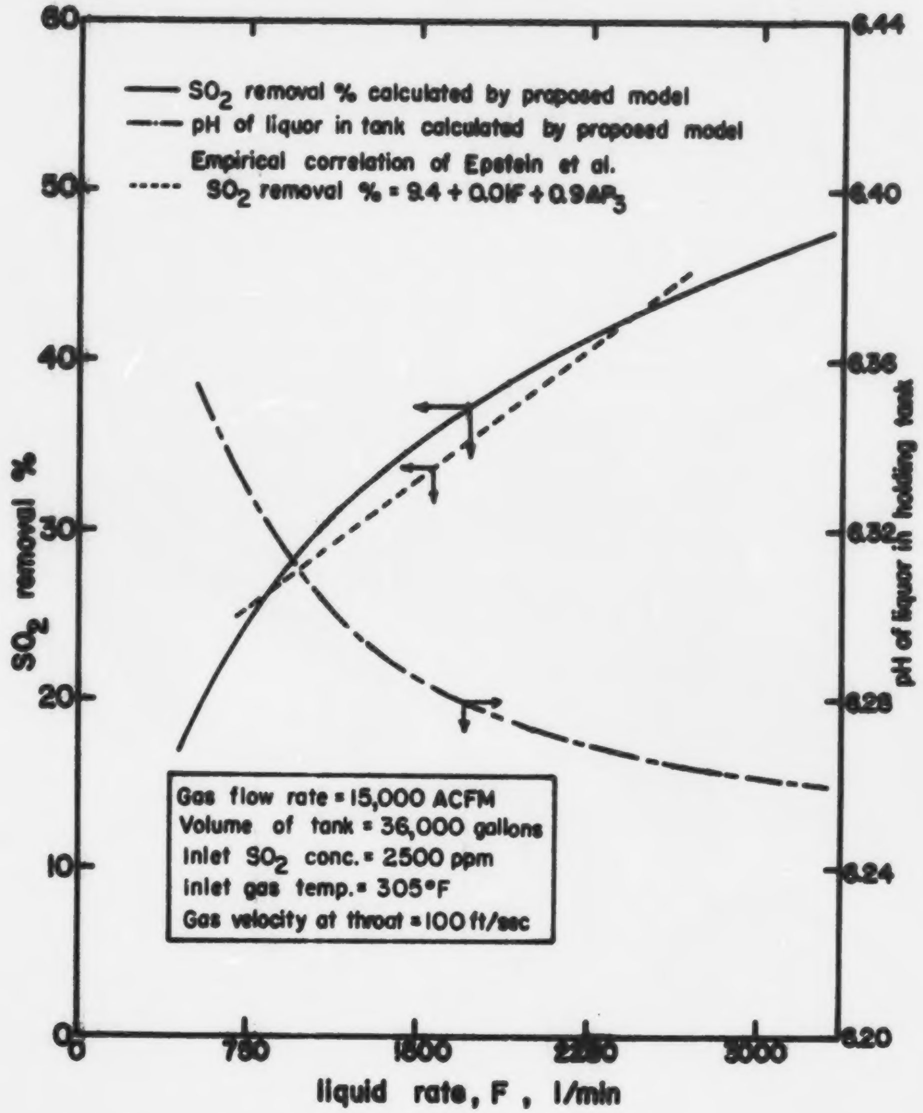

Figure 32. Performance of a Venturi-Holding Tank System with a Closed-Loop Recycling of Slurry (Limestone Slurry Process)

recycling liquor increases with the CO_2 evolution.

3. The calculated SO_2 removal percentages are compared with the values calculated by the correlation obtained by Epstein et al. (42). Two show similar trends with respect to the change in liquid flow rate.

D. Scaling and Oxidation in Lime/Limestone Processes

Some of the problems encountered in the practical operation of a lime/limestone process are scaling, erosion, corrosion and pH instability. Of these scaling in the scrubber and other parts of the scrubber-holding tank system is one of the major problems encountered in removing SO_2 from acid gases by a lime or limestone scrubbing process. This has consistantly been the main problem in the operation of lime/limestone scrubbing systems starting from the ICI-Howden work (70, 95) in England in the 1930's to the current pilot plant tests.

Hence, the study of the mechanism of scale formation and related problems has been an active area of research since the 1930's (7, 8, 13, 23, 43, 50, 77, 98, 100, 103, 111, 116, 118, 119). In the following section, reviews of the work on the scaling in the lime/limestone processes are given and some comments pertinent to the operation of venturi scrubbers are made.

Scaling in a scrubber-holding tank system is due mainly to the fact that the operating condition of recycling liquor is usually near saturation or above saturation with respect to the concentrations of calcium sulfite and calcium sulfate. Therefore, the production of these compounds resulting from SO_2 absorption in the scrubber increases the tendency for crystallization of calcium salts to take place on exposed surfaces, not only on crystals already present in the slurry but also on the scrubber walls and packing.

The mechanism of scaling in a scrubber system appears to be much more complex than for scaling in boilers and desalination equipments. Factors related to scaling are:

(i) degree of oxidation in the scrubber
(ii) pH levels at various points in the scrubber
(iii) type of the scrubber
(iv) type of alkali
(v) amount of SO_2 absorbed per unit of slurry
(vi) concentration of calcium sulfite and calcium sulfate crystals (seeds) in the recirculated slurry.

When SO_2 is absorbed in lime or limestone slurry, crystalline $CaSO_3 \cdot \frac{1}{2}H_2O$ is produced in the system. If oxygen is present in the gas, as it is in most situations, oxygen is also absorbed simultaneously with SO_2. The oxygen absorbed will be partially consumed in the oxidation of sulfite or bisulfite existing in the solution to sulfate.

There is evidence that the degree of sulfite oxidation in the system has an important effect on absorption, scaling (or precipitation of calcium salts), and corrosion. Since there are several offsetting considerations, it is not yet clear whether oxidation should be promoted, inhibited, or left alone. There are several ways for either promoting or inhibiting oxidation but their relative merits have not been studied adequately.

There are both advantages and disadvantages of sulfite oxidation. The following presents a few of the major advantages and disadvantages (103, 111, 118, 119).

1. Under upset scrubber conditions, which promotes low pH, and an increased sulfite concentration in the solution (see Figure 8), sulfite crystallization on limestone surfaces may occur. This process is called blinding. An increase in the oxidation rate could reduce the sulfite content, which perhaps would decrease the blinding effect.

2. The degree of oxidation in scrubber and its supporting system increase the sulfate to sulfite ratio in the solid phase. This ratio is important in solid settling since the sulfate crystals grow larger and thus settle better.

3. Oxidation of sulfite throughout the scrubber system, including the waste pond, reduces the possibility of water pollution by sulfite.

4. If a recovery process were operated with $CaO-CaCO_3$ as the absorbent, oxidation of the sulfite to sulfate would not be desirable because it is more difficult to thermally regenerate calcium oxide from the sulfate than to regenerate CaO from $CaSO_3$.

In what is to follow some of the conclusions reached in kinetic studies of the sulfite oxidation reaction is reviewed.

The sulfite oxidation reaction which is thought to take place in the liquid phase is

$$SO_3^{=} + \frac{1}{2} O_2 \rightarrow SO_4^{=} \qquad (109)$$

This reaction has been investigated since 1897 (33) and a chain reaction mechanism with typical radical intermediates has been suggested.

Reaction (109) can be accelerated by a trace of heavy metal ions such as cuprous, nickel and cobaltous ions and retarded strongly by the addition or organic metals such as carbohydrates, and benzoic, phthalic and glycolic acid (33). The sulfite oxidation reaction is also affected by several other factors such as temperature, light intensity, solute concentration, pH value, etc. The reaction has also very complex kinetics (33); for instance when the reaction is catalyzed by cobalt, it is zero-th order with respect to O_2 for sulfite concentrations of 0.06 g-mole/l, 1st-order for sulfite concentrations of 0.25 g-mole/l, and 2nd-order with respect to O_2 for sulfite concentration between 0.25 and 1.0 g-mole/l. Linek and Mayrhoferova (76) do not recommend taking the rate data for the reaction from the literature because the quoted rate constants may depend strongly on the purity of the sulfite solution. Linek (75) showed the effect of impurities using the experimental data.

There are many other studies on the absorption of oxygen into a sulfite solution and suggested reaction mechanisms (26, 30, 36, 64, 67, 74, 75, 76, 130) including an experimental study by Anderson and Johnstone (3) in which a venturi scrubber was used in the presence of a copper or cobalt catalyst and considerable oxidation was observed. A study reported by Yagi and Inoue (130) shows that the absorption rate of oxygen into sulfite solution without catalyst may be represented by the absorption of O_2 into the liquid phase accompanied by rapid, 2nd-order reaction.

The situation in regard to the various promoters (fly ash, NO_2, limestone constituents) and inhibitors (phenolics, etc.) is somewhat confused (119). More work must be done before the relative importance of these factors can be determined.

The type of the scrubber is an important consideration when scaling is prevalent. Scrubber types differ in the amount of slurry hold up. Unfortunately, those with the largest hold up appear to be the ones most subject to scaling: packed beds of the standard type, for example, give good hold up, but the fixed packing expecially if it has horizontal surfaces where solids can settle and convert to adherent sulfite or sulfate, is more likely to scale than a moving bed, spray tower, turbulent bed contactor, or venturi scrubber. The venturi scrubber is mechanically simple and thus it is easy to clean even if solid scale deposits on the equipment. Therefore, venturi scrubbers are considered to be superior in scaling resistance even though SO_2 removal efficiency in venturi scrubbers may be lower than some other scrubbers and therefore are suitable for scrubbing high SO_2 content gases. Although scaling in the main body of the venturi scrubber can be avoided, at the wet-dry interface, such as at the nozzle where liquid may stagnant, a "mud" tends to collect and stick to the surfaces. Careful design with regard to the irrigation of the surfaces with slurry or a special spray, or soot blowers at critical points will probably be required at the wet-dry interface to prevent scale build up.

The type of alkali affects the degree of scaling. Lime gives more scaling than limestone, but no conclusive reasons for this observation have been found. The generally lower pH in limestone system appear to be a factor, at least with regard to sulfite scaling. At the present level of development, lime system must be operated with recycle liquor diluted by adding water, or the stoichiometric amount of lime must be reduced to maintain a lower pH. It appears possible, in a venturi scrubber system, to use slightly higher stoichiometric ratios of lime to compensate for the relatively lower SO_2 absorption efficiency of the venturi scrubber.

In order to have adequate SO_2 removal, in closed-loop scrubbing operation with limestone, the slurry circulation rate and slurry solids content must be much higher for limestone scrubbing process than for lime scrubbing process. Since this operating condition should also reduce scaling, the limestone process may be superior to lime process with regard to scaling. However, in the venturi scrubber where scaling poses no serious problems and the pressure drop is relatively high, lime is a better absorbent for SO_2 removal with a low liquor rate.

As mentioned above the scaling mechanisms are not simple and it is impossible to draw any definite conclusions about the process of scaling based on the present information concerning scaling. However, it can be concluded that the venturi scrubber presents less scaling problems than other types of conventional scrubbers. More studies are required to avoid this problem completely in the lime/limestone slurry processes.

V. CONCLUSIONS AND RECOMMENDATIONS

The mechanism of sulfur dioxide absorption into water and various alkaline solutions in a venturi-holding tank system have been investigated. The data in the literature on the reaction kinetics accompanying sulfur dioxide absorption in alkaline solutions and water serve as the foundation to build a mathematical model for the mechanical and hydrodynamic characteristics of the venturi scrubber as well as heat and mass transfers. The model of the venturi scrubber developed can predict performances that compare favorably with the experimental data for the SO_2-H_2O and the SO_2-NaOH systems.

For lime or limestone slurry scrubber systems, the dissolution mechanisms of lime and limestone into a weak acid solution such as the recycle liquor become important. It was possible to explain these mechanisms by a kinetic model based on the dissolution of lime, and an equilibrium model in the limestone slurry process for the performance of the holding tank. These models are used to simulate the performances of the holding tanks and compared with the available experimental data.

Finally, the model for SO_2 absorption in a venturi scrubber has been combined with the model for the holding tank to simulate a closed-loop operation in which the scrubbing liquor is recycled. This combined model for a venturi-holding tank system has been used to investigate the sensitivity of the operating variables on the SO_2 removal efficiency in lime and limestone slurry process.

In addition, practical problems such as scaling and oxidation were briefly discussed.

In developing mathematical equations for simulation, assumptions and simplification were made to reduce mathematical difficulties and to provide realistic but convenient and practical models. In spite of the simplification, the comparison between the calculated results based on the model and the experimental data shows good agreement.

The specific conclusions and recommendations resulting from this study are as follows:

Conclusions

(1) A significantly large amount of mass and heat transfer takes place near the liquid nozzle in the venturi scrubber. This is primarily due to small transfer resistances, large driving forces, and relatively long residence time of the liquid droplets in this region.

(2) The operation of the venturi scrubber is practically isothermal except in the zone extending a few

centimeters from the liquid injection nozzle.

(3) Liquid-phase SO_2 concentration is observed to be close to the equilibrium concentration in the case of the SO_2-H_2O system at the exit of the scrubber.

(4) The dissolution mechanism of lime into a weak acid solution can be explained by a kinetic model which expresses the rate of dissolution of lime by the shrinking core model.

(5) The performance of a holding tank in the limestone slurry process can be approximated by the "equilibrium stage model" in which the holding tank liquor is assumed to be in a "dynamic equilibrium" with the gaseous phase above the tank. The rate of CO_2 evolution in the holding tank plays an important role in the dissolution process and may control the attainable pH value of the limestone slurry in the holding tank.

Recommendations

(1) The effect of the solid phase in a liquid on the absorption rate of a gas may be negligible in the venturi-type scrubber. This is because the residence time of the liquid is so short that very little dissolution can take place. However, the presence of a solid phase affects the rate of dissolution of limestone in the holding tank and in scrubbers which have a relatively long residence time. It is necessary, therefore,

to have a better understanding of the mechanisms of the dissolution of limestone into acid solutions. More fundamental studies on the mechanism of the limestone dissolution are required.

(2) The formation of the scale, particularly around the nozzle mouth, during the scrubbing operation affects the diameter of the droplet, and is one of the major causes for the decrease in absorption efficiencies in the venturi scrubbers. Studies to elucidate the cause of scale formation and to develop a means of reducing scale are needed.

(3) The reaction kinetics of oxidation of sulfite to sulfate in the liquid phase must be studied. The effects of oxidation on absorption, equilibrium between gas and liquid, scaling and corrosion, must be investigated in more detail. Oxidation may be important in improving the settling rate of calcium salts and in increasing the efficiency of the lime or limestone scrubbing processes.

(4) The effects of the presence of magnesium species in the liquid phase on the equilibrium relation appear to be very important. To use the equilibrium stage model for a holding tank successfully, an accurate estimate of the concentration of magnesium components accumulating in the liquid phase is needed.

(5) To improve the mathematical models proposed in this study, more accurate information on the total concentrations of the key components and pH values of the liquor at various points in the scrubber process should be developed.

NOMENCLATURE

A	component of gas absorbed
a	contact area per unit volume, cm^2/cm^3
B	reactant in liquid-phase
C_A	concentration of component A in liquid-phase, g-mole/cm^3
$[Ca]_i$	total concentration of calcium in liquid-phase of recycling liquor, $i = 1 \sim 3$, g-mole/l
$\overline{C}_A$	mean concentration of component A in liquid-phase with respect to radial direction in venturi scrubber, g-mole/cm^3
$\overline{C}'_A$	dimensionless mean concentration of component A in liquid-phase with respect to radial direction in venturi scrubber, -
C_{Ai}	concentration of component A at interface, g-mole/cm^3
C_{Ao}	concentration of component A at $t=0$ or in bulk liquid-phase, g-mole/cm^3
C_A^*	concentration of component A in equilibrium with partial pressure of gas A in bulk gas-phase, g-mole/cm^3
$\hat{C}_A$	concentration of component A defined by equation (A-12), g-mole/cm^3
C_B	concentration of component B in liquid-phase, g-mole/cm^3

C_{Bi}	concentration of component B in inlet liquor to holding tank, g-mole/cm^3
C_{Bo}	concentration of component B at t=0 or in bulk liquid-phase, g-mole/cm^3
C_{Bs}	concentration of component B at liquid-solid interface, g-mole/cm^3
C_{CO_2i}	concentration of CO_2 at gas-liquid interface, g-mole/cm^3
C_d	drag coefficient defined by equation (38)
C_F	concentration of component F in liquid-phase, g-mole/cm^3
$[CO_3]_i$	total concentration of carbonate in liquid-phase of recycling liquor, i = 1 ~ 3, g-mole/l
C_{OH}	concentration of hydroxyl ion in liquid-phase, g-mole/cm^3
C_{Pg}	specific heat of gas, cal/g-mole · °C
C_{PL}	specific heat of liquid, cal/g-mole · °C
C_{SO_2i}	concentration of SO_2 at gas-liquid interface, g-mole/cm^3
D	mean diffusivity of gas and reactant in liquid-phase, cm^2/sec
D_A	diffusivity of component A in liquid-phase, cm^2/sec
D_B	diffusivity of component B in liquid-phase, cm^2/sec

D_{Ag}	diffusivity of component A in gas-phase, cm^2/sec
D_e, d_e	effective diameter, cm
D_m	mass median diameter of droplet, micron
D_n	diameter of nozzle, cm
d_p	diameter of liquid droplet, cm
dp_f	differential pressure drop due to friction, atm
dV	differential volume of venturi scrubber, cm^3
D_{32}	surface-volume mean diameter of liquid droplet, micron
E	enhancement factor for gas absorption with chemical reaction
E_i	enhancement factor for gas absorption with instantaneous reaction
E(t)	exit age distribution function
F	volumetric liquid flow rate, l/min
f	friction factor
G	component of gas absorbed
g	acceleration due to gravity, cm/sec^2
g_c	unit conversion factor, g/sec^2·cm·atm or g·cm/sec^2·G
G_m	molar flow rate of gas, g-mole/sec
G_o	volumetric gas flow rate, cm^3/sec
H_A	Henry's law constant for component A, g-mole/cm^3·atm
h_G	heat transfer coefficient in gas-phase, cal/cm^2·sec·^{o}C

k	thermal conductivity, cal/cm·sec·^{o}C
K_G	overall mass transfer coefficient, g-mole/cm^2·sec·atm
k_G	mass transfer coefficient in gas phase, g-mole/cm·sec·atm
$k'_G a$	mass transfer coefficient for CO_2 evolution, g-mole/l·min·atm
k_{Gw}	mass transfer coefficient for H_2O evaporation, g-mole/cm^2·sec·atm
K_L	overall mass transfer coefficient, cm/sec
k_L	mass transfer coefficient in liquid-phase, cm/sec
$k_L{}^o$	mass transfer coefficient in liquid-phase without reaction, cm/sec
k_{Lp}	instantaneous mass transfer coefficient in liquid-phase, cm/sec
k_s	mass transfer coefficient for solid dissolution, cm/sec
k'_s	mass transfer coefficient for solid dissolution with reaction, cm/sec
k_2, k'_2	reaction rate constant for second-order reaction, l/g-mole·sec
L	length of throat, mm
L_m	molar liquid flow rate, g-mole/sec
L'_m	dimensionless molar liquid flow rate, -
L_o	volumetric liquid flow rate, cm^3/sec

M	make up rate of lime or limestone, g-mole/min
M_g	mass flow rate of gas, g/sec
M_L	mass flow rate of liquid, g/sec
m	liquor to gas mass ratio, g-liquid/g-gas
m_o	specific wetting, l -liquid/ m^3-gas
N_A	rate of absorption of component A, g-mole/ $cm^2 \cdot sec$
N_A^o	rate of absorption of component A without reaction, g-mole/$cm^2 \cdot sec$
N_{Ac}	acceleration group, $(d_p/v_r^2)(dv_r/dt)$, -
N_B	number of moles of component B, g-mole
N_{Gr}	Grashof number, $gd_p^3(\rho_L-\rho_g)\rho_g/\mu_g^2$, -
N_{CO_2}	rate of CO_2 evolution, g-mole/min
N_{Re}	Reynolds number, $d_p v_r \rho_g/\mu_g$, -
N_{Sc}	Schmidt number, $\mu_g/\rho_g D_{Ag}$, -
N_{Sh}	Sherwood number, $d_p k_G R T'_g/D_{Ag}$ or $d_p h_G/k$
N_{Su}	surface tension group, $g_c \sigma d_p \rho_L/\mu_g^2$, -
N_{Wt}	gravity group, $dp[4g\rho_g(\rho_L-\rho_g)/3\mu_g^2]^{1/3}$, -
P	dimensionless total pressure, -
p	total pressure, atm
P_A	dimensionless partial pressure of gas A in gas-phase, -
p_A	partial pressure of gas A in gas-phase, atm
p_{Ai}	partial pressure of gas A at gas-liquid interface, atm

$P^*_{CO_2}$	equilibrium partial pressure of CO_2 at gas-liquid interface, atm
$P^o_{CO_2}$	partial pressure of CO_2 in bulk gas-phase, atm
q	liquid to gas ratio, liter-liquid/m^3-gas
R	gas constant, = 82.06 $cm^3/g\text{-mole}\cdot{}^oK$
R_p	radius of solid particle, cm
r	distance from center of droplet, cm
r_A	rate of reaction expressed by equation (A-7),
r_o	radius of liquid droplet, cm
r_p	radius of solid particle, cm
S	cross-sectional area of venturi, cm^2
S_i	flow rate of solid with recycling liquor, $i = 1 \sim 2$, g-mole/min
$[S]_i$	total concentration of sulfur in liquid-phase of recycling liquor, $i=1 \sim 3$, g-mole/l
$[SO_3]_i$	total concentration of sulfite in liquid-phase of recycling liquor, $i=1 \sim 3$, g-mole/l
$[SO_4]_i$	total concentration of sulfate in liquid-phase of recycling liquor, $i=1 \sim 3$, g-mole/l
S_o	flow area for atomizing air, cm^2
T	dimensionless time, -
t	time, sec
$\bar{t}$	mean residence time, sec
T_g	dimensionless gas temperature, -
T'_g	gas temperature, ^oK

T_i	flow rate of solid calcium salts with recycling liquor, $i = 1 \sim 3$, g-mole/min
t_g	gas temperature, ^{o}C
T_L	dimensionless liquid temperature, -
t_L	liquid temperature, ^{o}C
v	velocity, cm/sec
V_g	dimensionless gas velocity, -
v_g	gas velocity, cm/sec
v_{go}	gas velocity at nozzle, cm/sec
v_{g1}	gas velocity at entrance to venturi or at downstream, cm/sec
v_{g2}	gas velocity at exit from venturi, cm/sec
v_L	liquid velocity or velocity of liquid drop, cm/sec
v_r	relative velocity of gas and liquid, cm/sec
v_{ro}	relative velocity of gas and liquid at throat, cm/sec
V_L	dimensionless velocity of liquid droplet, -
V_t	volume of holding tank, l
w	gas velocity at throat, m/sec
x	mole fraction of component A in liquid-phase, -
X_B	fraction of dissolution of solid particle, -
$\bar{X}_B$	mean fraction of dissolution of solid, -
X_i	flow rate of solid limestone with recycling liquor, $i = 1 \sim 3$, g-mole/min

Y_i	flow rate of solid calcium sulfite in recycling liquor, $i = 1 \sim 3$, g-mole/min
y_w	mole fraction of H_2O in gas-phase, -
y_{wi}	mole fraction of H_2O at gas-liquid interface, -
Z	dimensionless distance from nozzle in venturi, -
Z_i	flow rate of solid calcium sulfate in recycling liquor, $i = 1 \sim 3$, g-mole/min
z	distance from nozzle along axial direction of venturi, cm

Greek Letters

β	heat of vaporization, cal/g-mole
γ	stoichiometric factor, -
ΔC_A	driving force for gas absorption, g-mole/cm^3
$\Delta C_A'$	dimensionless driving force for gas absorption, -
ΔM_L	difference of mass flow rate at entrance and at exit of venturi, g/sec
ΔP	total pressure drop across venturi scrubber, atm
ΔP_a	pressure drop due to acceleration of liquid, atm
ΔP_{ag}	pressure drop due to acceleration of gas, cm-H_2O

ΔP_{as}	pressure drop due to acceleration of solid, cm-H_2O
ΔP_c	pressure drop due to contraction, atm
ΔP_d	pressure drop due to friction, N/m^2
ΔP_e	pressure drop due to expansion, atm
ΔP_f	pressure drop due to friction, atm
ΔP_m	measured pressure drop across test section, cm-H_2O
ΔP_{oz}	pressure drop at generalized position, cm-H_2O
$\Delta P_{\rho g}$	pressure drop across test section due to gas and gravity, cm-H_2O
$\Delta P_{\rho s}$	pressure drop across test section due to solids and gravity, cm-H_2O
ΔP_t	pressure drop due to composite fluid friction, cm-H_2O
ΔP_1	pressure drop across venturi, N/m^2
ΔP_2	pressure drop across venturi, mm H_2O
ΔP_3	pressure drop across venturi, in H_2O
ΔP_4	pressure drop across flooded disc scrubber, in H_2O
Δv_g	difference of gas velocity at entrance and at exit of scrubber, cm/sec
Δv_L	difference of liquid velocity at entrance and at exit of scrubber, cm/sec
ε	void fraction in venturi scrubber, -

θ	time
μ_g	viscosity of gas, poise
μ_L	viscosity of liquid, poise
ξ	stoichiometric factor, -
ξ_i	dimensionless coefficient, $i = 1 \sim 12$, -
ρ_g	density of gas, g/cm^3
ρ_L	density of liquid, g/cm^3
ρ_M	molar density of liquid, g-mole/cm^3
ρ_{MB}	molar density of solid particle, g-mole/cm^3
ρ_m	mean density of gas mixed with liquid, g/cm^3
σ	surface tension, dyne/cm
τ	time required for complete dissolution, sec

BIBLIOGRAPHY

1. Adams, F. W., Ind. Eng. Chem., 19, 589 (1927)

2. Allen, H. S., Phil. Mag. (5), 50, 323, 519 (1900)

3. Anderson, L. B. and Johnstone, H. F., A.I.Ch.E.J., 1, 135 (1955)

4. Antoine, T. E., VAPOR-PRESSURE OF ORGANIC COMPOUNDS, Interscience, New York (1954)

5. Astarita, G., Ind. Eng. Chem. Fundamentals, 2, 294 (1963)

6. Bechtel Corporation, Progress Report, EPA Alkali Scrubbing Test Facility at the TVA Shawnee Power Plant (Nov. Dec., 1972, Jan. 1973)

7. Berkowitz, J. B., paper presented at the 2nd International Lime/Limestone Wet Scrubbing Symposium, New Orleans, La. (Nov. 1971)

8. Berkowitz, J. B., Progress Reports, A. D. Little Inc.

9. Beuschlein, W. L. and Conrad, H., Paper Trade J., Tech. Assoc. Sec., 63rd yr., 119 (September 20, 1934)

10. Bjerle, I., Bengtsson, S., and Färnkvist, K., Chem. Eng. Sci., 27, 1853 (1972)

11. Boll, R. H., Ind. Eng. Chem. Fundamentals, 12, 40 (1973)

12. Boothroyd, R. G., Trans. Instn. Chem. Engrs., 44, T306, (1966)

13. Borgwardt, R. H., Progress Reports No. 1-4, 6, Environmental Protection Agency (Aug., Sept., Oct., Nov. 1972, Jan., 1973)

14. Boyadzhiev, K. H., Int'l. Chem. Eng., 4, 22 (1964)

15. Boynton, R. S., CHEMISTRY AND TECHNOLOGY OF LIME AND LIMESTONE, Interscience, New York (1966)

16. Brian, P. L. T., A.I.Ch.E.J., 10, 5 (1964)

17. Brian, P. L. T., Baddeur, R. F. and Matiatos, D. C., A.I.Ch.E.J., 10, 727 (1964)

18. Brian, P. L. T. and Beaverstock, M. C., Chem. Eng. Sci., 20, 47 (1965)

19. Brian, P. L. T., Hurley, J. F. and Hasseltine, E. H., A.I.Ch.E.J., 7, 226 (1961)

20. Brink, J.A., Jr. and Contant, C. E., Ind. Eng. Chem., 50, 1157 (1958)

21. Brunson, R. J. and Wellek, R. M., Chem. Eng. Sci., 25, 904 (1970)

22. Brunson, R. J. and Wellek, R. M., A.I.Ch.E.J., 17 1123 (1971)

23. Burklin, C. E. and Phillips, J. L., Technical Note 200-014-10, Radian Corporation (November 1972)

24. Calvert, S., A.I.Ch.E.J., 16, 392 (1970)

25. Cameron, F. K., and Ball, J. M., Bulletin of Bureau of Solids, U. S. Dept. of Agriculture, No. 33, 47 (1906)

26. Chen, T. and Barron, C. H., Ind. Eng. Chem. Fundamentals, 11, 466 (1972)

27. Comings, E. W., Adams, C. H. and Shippe, E. D., Ind. Eng. Chem., 40, 75 (1948)

28. Comstock, C. S. and Dodge, B. F., Ind. Eng. Chem., 29, 520 (1937)

29. Cook, G., Phil. Mag. (6), 39, 350 (1920)

30. Cooper, C. M., Fernstrom, G. A. and Miller, S. A., Ind. Eng. Chem., 36, 504 (1944)

31. Danckwerts, P. V., Ind. Eng. Chem., 43, 1460 (1951)

32. Danckwerts, P. V., Trans. Faraday Soc., 46, 712 (1950)

33. Danckwerts, P. V., GAS-LIQUID REACTIONS, McGraw Hill, New York, (1970)

34. Danckwerts, P. V. and Kennedy, A. M., Chem. Eng. Sci., 8, 201 (1958)

35. Danckwerts, P. V. and Sherma, M. M., Chem. Engr., Oct., CE244 (1966)

36. de Waal, K. J. A. and Okeson, J. C., Chem. Eng. Sci., 21, 559 (1966)

37. Drehmel, D. C., paper presented at 2nd Int'l Lime/Limestone Wet Scrubbing Symposium, New Orleans, La. (November 1971)

38. Drehmel, D. C., paper presented at 65th Annual Meeting of APCA, (June 1972)

39. Ekman, F. O. and Johnstone, H. F., Ind. Eng. Chem., 43, 1358 (1951)

40. Elenkov, D. and Boyadzhiev, L., Int'l Chem. Eng., 5, 31 (1965); 7, 191 (1967)

41. Emmert, R. E. and Pigford, R. L., A.I.Ch.E.J., 8, 171 (1962)

42. Epstein, M. et al., Progress Report, EPA Alkali Scrubbing Test Facility at the TVA Shawnee Power Plant, Bechtel Corporation (Nov., Dec. 1972, Jan., Feb., 1973)

43. Fabuss, B. M., paper presented at 2nd Int'l Lime/Limestone Wet Scrubbing Symposium, New Orleans, La. (November, 1971)

44. Feild, R. B., M.S. thesis in chemical engineering, University of Illinois (1950)

45. Friedlander, S. K. and Litt, M ., Chem. Eng. Sci., 7, 229 (1952)

46. Froessling, N., Gerland's Beit zur Geophs., 52, 170 (1938)

47. Fujita, S., KAGAKU KOGAKU I, Iwanami, Tokyo, (1959)

48. Fujita, S., Editor in Chief, CHEMICAL ENGINEER'S HANDBOOK, 3rd ed., Maruzen, Tokyo (1968)

49. Gieseke, J. A., Ph.D. Dissertation, Univ. of Washington, Seattle, Washington (1963)

50. Gleason, R. J. and McKenna, J. D., paper presented at the 69th National Meeting of A.I.Ch.E., Cincinnati, Ohio (1971): Final Rept. of Pilot Scale Investigation of a Venturi-type Contactor for Removal of SO_2 by the Limestone Wet-scrubbing Process, Cottrell Environmental Systems, Inc. (1971)

51. Gretzinger, J. and Marshall, W. R., Jr., A.I.Ch.E.J., 7, 312 (1961)

52. Harriot, P., Chem. Eng. Sci., 17, 149 (1962)

53. Harris, D. B., Private Communication (1971)

54. Haslam, R. T., Adams, F. W. and Kean, R. H., Ind. Eng. Chem., 18, 19 (1926)

55. Hatta, S., Techol. Repts. Tohoku Imp. Iniv., 8, 1 (1928-1929); 10, 119 (1932)

56. Higbie, R., Trans. Amer. Inst. Chem. Engrs., 35, 365 (1935)

57. Hikita, H., Asai, S. and Tsuji, J., paper presented at the 34th Annual Meeting of the Society of Chemical Engineers, Japan, A202 (1969)

58. Himmelblau, D. M., Chem. Rev., 64, 527 (1946)

59. Hrubeckey, H. F., J. Appl. Physics, 29, 572 (1958)

60. Huang, C. J. and Kuo, C. H., A.I.Ch.E.J., 9, 161 (1963)

61. Hughes, R. R. and Gilliland, E. R., Chem. Eng. Progr., 48, 497 (1952)

62. Ingebo, R. D., NACA Tech. Note, 3762 (Sept. 1956)

63. Johnson, A. I., Hamielec, A. E. and W. T. Houghton, A.I.Ch.E.J., 13, 379 (1967)

64. Johnstone, H. F. and Coughanowr, D. R., Ind. Eng. Chem., 50, 1169 (1958)

65. Johnstone, H. F., Feild, R. B. and Tassler, M. C., Ind. Eng. Chem., 46, 1601 (1954)

66. Johnstone, H. F. and Robert, M. H., Ind. Eng. Chem., 41, 2417 (1949)

67. Johnstone, H. F. and Singh, A. D., Ind. Eng. Chem., 32, 1037 (1940)

68. Kim, K. Y. and Marshall, W. R., Jr., A.I.Ch.E.J., 17, 575 (1971)

69. Kuznetsov, M. D. and Oratovskii, V. I., Int'l Chem. Eng., 2, 185 (1962)

70. Lessing, R., J. Soc. Chem. Ind., November, 373 (1938)

71. Levenspiel, O., CHEMICAL REACTION ENGINEERING, Wiley & Sons, New York (1962)

72. Lewis, H. G., Edwards, D. G., Goglia, M. J., Rice, R. I. and Smith, L. W., Ind. Eng. Chem., 40, 67 (1948)

73. Lewis, W. L. and Whitman, W. G., Ind. Eng. Chem., 16, 1215 (1924)

74. Linek, V., Chem. Eng. Sci., 21, 777 (1966)

75. Linek, V., Chem. Eng. Sci., 26, 491 (1971)

76. Linek, V. and Mayrhoferova, J., Chem. Eng. Sci., 25, 787 (1970)

77. Lowell, P. S., paper presented at the 2nd Int'l Lime/Limestone Wet Scrubbing Symposium, New Orleans, La. (November, 1971)

78. Lynn, S., Straatemeir, J. R. and Kramers, H., Chem. Eng. Sci., 4, 49 (1955)

79. Marangozis, J. and Johnson, A. I., Can. J. Chem. Engg., 39, 152 (1961)

80. Markant, H. P., Mclory, R. A. and Matty, R. E., Tappi, 45, 849 (1962)

81. Marshall, W. R., Jr., Chem. Eng. Progr. Symposium Ser. No. 2, 50 (1954)

82. Matrozov, V. I., Soobscheniya o Nauchno-Tekhnicheskikh Rabotakh NIUIF, Nos. 6/7, 152 (1953)

83. Moody, L. F., Trans. A.S.M.E., 66, 671 (1944)

84. Mugele, R. A., A.I.Ch.E.J., 6, 3 (1960)

85. Murthy, B. N., Harris, D. B. and Phillips, J. L., paper presented at the 2nd Int'l Lime/Limestone Wet Scrubbing Symposium, New Orleans, La. (November 1971)

86. Nijsing, R. A. T. O., Hendriksz, R. H. and Kramers, H., Chem. Eng. Sci., 10, 88 (1959)

87. Nilsson, G., Rengemo, T. and Sillén, L. G., Acta. Chem. Scand., 12, 868 (1958)

88. Norman, W. S., ABSORPTION, DISTILLATION AND COOLING TOWERS, Longmans, London (1961)

89. Nukiyama, S. and Tanasawa, Y., Trans. Soc. Mech. Engrs. (Japan), 4 (14), 86 (1938), 4 (15), 138 (1938), 5 (18), 68 (1939), 6 (22), II-7 (1940)

90. Olander, D. R., A.I.Ch.E.J., 6, 233 (1960)

91. Onda, K., Sada E., KAGAKU-KOJO, (Japan), 9 111 (1966)

92. Onda, K., Sada, E. and Maeda, Y., Kagaku Kogaku (Japan), 35, 345 (1971)

93. Parkison, R. V., Tappi, 39, 517 (1956)

94. Pearson, J. R. A., Appl. Sci. Rec., All, 321 (1963)

95. Pearson, J. L., Nonhebel, G. and Ulander, P. H., J. Inst. Fuel, VIII, 39, 119 (Feb. 1935)

96. Perry, J. H., Editor in Chief, CHEMICAL ENGINEER'S HANDBOOK, 4th edition, McGraw-Hill, New York (1963)

97. Perry, R. H. and Pigford, R. L., Ind. Eng. Chem., 45, 1247 (1953)

98. Phillips, J. L. and Ottmers, D. M., Monthly Work Report, Radian Corporation (Feb. 1972-Jan. 1973)

99. Phillips, J. L., Final Reports for No. CPA-22-69-138, 1 and 2, Radian Corporation (June 1970)

100. Phillips, J. L. et al., Tech. Note, 200-014-05 ~ 09, Radian Corporation (Feb. 1972-Jan. 1973)

101. Pigford, R. L. and Pyle, C., Ind. Eng. Chem., 43, 1649 (1951)

102. Potter, O. E., Trans. Instn. Chem. Engrs., 36, 415 (1958)

103. Potts, J. M., Slack, A. V. and Hatfield, J. D., paper presented at 2nd Int'l Lime/Limestone Wet Scrubbing Symposium, New Orleans, La. (November, 1971)

104. Princiotta, F. T. and Epstein, M., paper presented at 65th Annual Meeting of the A.I.Ch.E., New York (November, 1972)

105. Ramachandran, P. A., and Sherma, M. M., Trans. Instn. Chem. Engrs., 49, 253 (1971)

106. Ramm, V. M., ABSORPTION OF GASES, Israel Program for Scientific Translation, Jerusalem (1968)

107. Ranz, W. E. and Marshall, W. R., Chem. Eng. Progr., 48, 141, 173 (1952)

108. Rehm, T. R., Moll, A. J. and Babb, A. L., A.I.Ch.E.J., 9, 760 (1963)

109. Roberts, D. and Danckwerts, P. V., Chem. Eng. Sci., 17, 961 (1962)

110. Roper, G. H., Hatch, T. F., Jr. and Pigford, R. L., Ind. Eng. Chem. Fundamentals, 1, 144 (1962)

111. Saleem, A., J. Air Pollution Control Assoc., 22, 172 (1972)

112. Sazhin, V. I. and Matrozov, V. I., The Societ Chem. Ind., No. 7, 51 (1969)

113. Seidell, A., SOLUBILITIES OF INORGANIC AND METAL ORGANIC COMPOUNDS, Am. Chem. Soc., 538 (1958)

114. Sherwood, T. K. and Pigford, R. L., ABSORPTION AND EXTRACTION, McGraw-Hill, New York (1952)

115. Sherwood, T. K. and Ryan, J. M., Chem. Eng. Sci., 11, 81 (1959)

116. Simpson, H. G., Final Report No. B.120488/2,4, Imperial Chem. Industry (February 1951)

117. Skloss, J. L., Wells, R. M. and Mekrole, F. B., Phillips, N. P., Thompson, C. M. and Hawn, W. C., Technical Note 200-010-02, Radian Corporation (October 1971)

118. Slack, A. V., Falkenberry, H. L. and Harrington, R. E., J. Air Pollution Control Assoc., 22, 159 (1972)

119. Slack, A. V. and Hatfield, J. O., paper presented at the 2nd Int'l Lime/Limestone Wet Scrubbing Symposium, New Orleans, La. (November 1971)

120. Steinberger, R. L. and Treybal, R. E., A.I.Ch.E.J., 6, 227 (1960)

121. Tassler, M. C., Ph.D. Dissertation, Univ. of Illinois, Illinois (1952)

122. Teramoto, M., Hashimoto, K. and Nagata, S., Kagaku Kogaku (Japan), 34, 1296 (1970)

123. Tillman, E. S., Jr., paper presented at the 64th Annual Meeting of the Air Pollution Control Assoc., Atlantic City, N. J. (1971)

124. Treybal, R. E., LIQUID EXTRACTION, McGraw-Hill, New York (1955)

125. Volgin, B. P., Efimova, T. F. and Gofman, M.S., Int'l Chem. Eng., 8, 113 (1968)

126. Walker, A. B. and Hall, R. M., J. Air Pollution Control Assoc., 18, 319 (1968)

127. Wetzel, H., Ph.D. Dissertation, Univ. of Wisconsin, Madison (1951)

128. Whitney, R. P. and Vivian, J. E., Chem. Eng. Prgr., 45, 323 (1949)

129. Wigg, L. D., J. Inst. Fuels, 37, 286, 500 (1964)

130. Yagi, S. and Inoue, H., Chem. Eng. Sci., 17, 411 (1962)

APPENDIX A

Enhancement Factor for Gas Absorption with Instantaneous Chemical Reaction into a Liquid Drop

When mass transfer is accompanied by a chemical reaction, its rate is accelerated and becomes faster than that without the chemical reaction. This effect may be expressed in terms of an enhancement factor, defined as follows:

$$E = \frac{k_L}{k_L^o} \qquad \text{(A-1)}$$

where, k_L^o = mass transfer coefficient without reaction
k_L = mass transfer coefficient with chemical reaction

If a gas A and a reactant B in the liquid phase react very rapidly according to the following stoichiometric equation,

$$A + \gamma B \longrightarrow \text{Product} \qquad \text{(A-2)}$$

the liquid film at the phase boundary is rapidly depleted of reactants A and B. Thus, the reaction can proceed only as fast as the reactants can diffuse to the reaction surface. A diffuses from the interface to the reaction surface and B diffuses from the bulk of the liquid to this surface. A semiquantitative plot of the concentration profiles in and around the liquid film is shown in Figure A-1. The dashed line indicates an

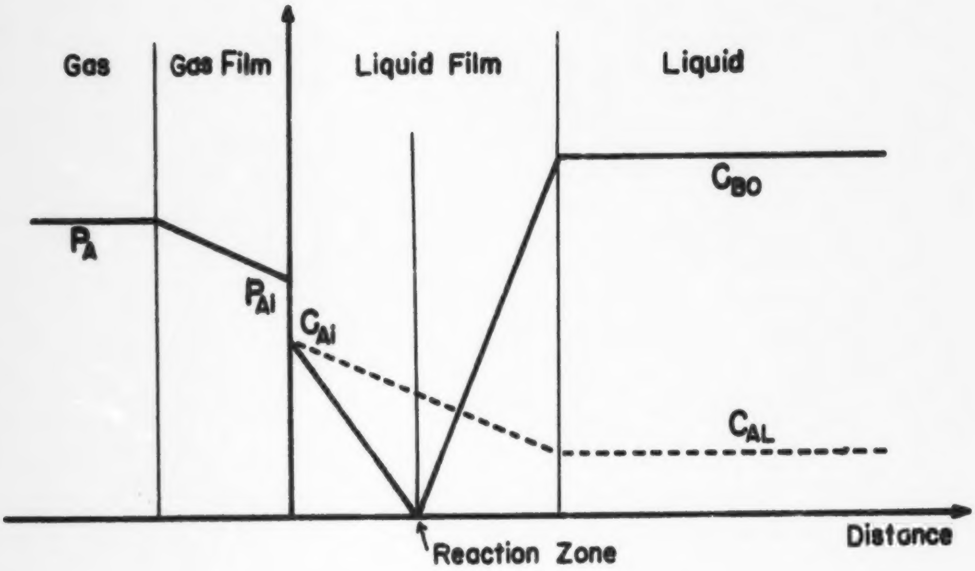

Figure A-1: Concentration Profile Across the Gas-Liquid Interface with Instantaneous Reaction. The Dashed Line Indicates the Approximate Concentration Gradient across the Fluid Film in the Absence of Chemical Reaction.

approximate concentration across the liquid film in the case of physical absorption. It can be noted that with the chemical reaction, the concentration gradient of A is steeper. Thus, the enhancement factor, E, should be greater than 1.

Hatta (55) first derived an expression for E_i based on the assumption of a completely stagnant fluid film and found:

$$E_i = 1 + \frac{D_B C_{Bo}}{\gamma D_A C_{Ai}} \qquad \text{(A-3)}$$

Of course, the assumption of a stagnant fluid film with an abrupt transition to the bulk of the liquid is not very realistic, but equation (A-3) fits many experimental data very well.

Two other theories for predicting E_i for very fast reaction lead to similar results. Higbie's penetration theory, (56) which is based on unsteady state diffusion into a laminar fluid stream, leads to the following expression (34) for the enhancement factor:

$$E_i = \left(1 + \frac{D_B C_{Bo}}{\gamma D_A C_{Ai}}\right) \sqrt{\frac{D_A}{D_B}} \qquad \text{(A-4)}$$

This differs from equation (A-3) only by the factor $\sqrt{D_A/D_B}$, which is often nearly unity. A derivation based on the boundary layer theory results in the expression (45, 79, 102, 115).

$$E_i = \left(1 + \frac{D_B C_{Bo}}{\gamma D_A C_{Ai}}\right) \left(\frac{D_A}{D_B}\right)^{1/3} \qquad \text{(A-5)}$$

If the diffusivities of components A and B are equal, equations (A-3), (A-4) and (A-5) become:

$$E_i = 1 + \frac{C_{Bo}}{\gamma C_{Ai}} \qquad (A-6)$$

The above expression for the enhancement factor is for gas absorption into semi-infinite plane of liquid. The following is a demonstration that for gas absorption into a droplet with an instantaneous reaction, the enhancement factor always reduces to equation (A-6) if the diffusivities of the gas and the reactant in the liquid phase are equal $^{(21)}$.

Suppose that the reaction rate for reaction (A-2) can be expressed as a function of the concentration of A and B as follows:

$$r_A = k_2 f\ (C_A, C_B) \qquad (A-7)$$

Then, equations of continuity for the two components are generally given as:

$$\frac{\partial C_A}{\partial t} + v\cdot\nabla C_A = D_A\ \nabla^2 C_A - k_2 f\ (C_A, C_B) \qquad (A-8)$$

$$\frac{\partial C_B}{\partial t} + v\cdot\nabla C_B = D_B\ \nabla^2 C_B - \gamma\, k_2 f\ (C_A, C_B) \qquad (A-9)$$

If $D_A = D_B = D$, the above set of equations can be simplified. Multiplying equation (A-8) by γ and subtracting equation (A-9) from this product gives:

$$\frac{\partial(\gamma C_A - C_B)}{\partial t} + v\cdot\nabla(\gamma C_A - C_B) = D\,\nabla^2(\gamma C_A - C_B) \qquad (A-10)$$

or

$$\frac{\partial \hat{C}_A}{\partial t} + v \cdot \nabla \hat{C}_A = D\nabla^2 \hat{C}_A \qquad (A\text{-}11)$$

where,

$$\hat{C}_A = \left(\frac{\gamma C_A - C_B + C_{Bo}}{\gamma C_{Ai} + C_{Bo}}\right) \cdot C_{Ai} \qquad (A\text{-}12)$$

The boundary conditions for equations (A-8) and (A-9) are:

$$\left.\begin{array}{lll} t = o, \ r > o & : & C_A = o \ , \ C_B = C_{Bo} \\ r = o, \ t > o & : & \dfrac{\partial C_A}{\partial r} = o \ , \ \dfrac{\partial C_B}{\partial r} = o \\ r = r_o, \ t > o & : & C_A = C_{Ai} \ , \ \dfrac{\partial C_B}{\partial r} = o \end{array}\right\} (A\text{-}13)$$

When these conditions are substituted into equation (A-12), the following initial and boundary conditions on C_A result:

$$\left.\begin{array}{lll} t = o \ , \ r > o & : & \hat{C}_A = o \\ r = o \ , \ t > o & : & \dfrac{\partial \hat{C}_A}{\partial r} = o \\ r = r_o, \ t > o & : & \hat{C}_A = C_{Ai} \end{array}\right\} \qquad (A\text{-}14)$$

The rate of gas absorption from the gas phase to the liquid phase is obtained as the product of the diffusivity of the gas and its concentration gradient at the interface. That is,

$$N_A = D \left(\frac{\partial C_A}{\partial r}\right)_{r=r_o} \qquad (A\text{-}15)$$

Since equation (A-11) does not contain the reaction term, this equation expresses the gas absorption without chemical reaction, i.e., physical absorption. The rate of physical absorption will be expressed as follows:

$$N_A^o = D \left(\frac{\partial \hat{C}_A}{\partial r}\right)_{r=r_o} \tag{A-16}$$

For equal diffusivities of A and B, the enhancement factor is reduced to the ratio of the concentration gradient of C_A at interface.

$$E_i = \frac{N_A}{N_A^o} = \left(\frac{\partial C_A}{\partial r}\right)_{r=r_o} \Big/ \left(\frac{\partial \hat{C}_A}{\partial r}\right)_{r=r_o} \tag{A-17}$$

Taking the derivative of equation (B-12) with respect to r,

$$\left(\frac{\partial \hat{C}_A}{\partial r}\right)_{r=r_o} = \frac{C_{Ai}}{\gamma C_{Ai}+C_{Bo}} \left[\gamma \left(\frac{\partial C_A}{\partial r}\right)_{r=r_o} - \left(\frac{\partial C_B}{\partial r}\right)_{r=r_o} \right] \tag{A-18}$$

Applying boundary condition (A-13), $(\partial C_B/\partial r)_{r=r_o} = 0$, gives

$$\left(\frac{\partial \hat{C}_A}{\partial r}\right)_{r=r_o} = \frac{\gamma C_{Ai}}{\gamma C_{Ai}+C_{Bo}} \left(\frac{\partial C_A}{\partial r}\right)_{r=r_o} \tag{A-19}$$

Therefore, from equations (A-17) and (A-19), the enhancement factor for gas absorption with an instantaneous chemical reaction into a droplet is also given by the same equation as equation (A-6). That is:

$$E_i = 1 + \frac{C_{Bo}}{\gamma C_{Ai}} \tag{A-20}$$

When a second gas whose diffusivity is the same as that of the first gas is absorbed and reacts with the same liquid component, B, irreversibly and instantaneously according to the following chemical reaction,

$$G + \xi B \longrightarrow \text{Product} \qquad \text{(A-21)}$$

it can be shown also that the enhancement factors for both gases are equal to: (110)

$$E_i = 1 + \frac{C_{Bo}}{\gamma C_{Ai} + \xi C_{Gi}} \qquad \text{(A-22)}$$

If a gas which contains SO_2 and CO_2 is treated with an alkaline solution, the rates of absorption of these two gases will be accelerated by the factor:

$$E_i = 1 + \frac{C_{OH^-}}{2(C_{SO_2 i} + C_{CO_2 i})} \qquad \text{(A-23)}$$

APPENDIX B

Derivation of Equation (105)

As discussed in Section (4) of CHAPTER III, if the holding tank can be considered as an equilibrium stage, the following set of nine simultaneous equations is obtained from the material balance.

$$X_2+T_2 = S_2 \qquad \text{(B-1)}$$

$$X_3+T_3= M \qquad \text{(B-2)}$$

$$X_3/M = X_2/S_2 \qquad \text{(B-3)}$$

$$F[Ca]_1+S_1+M = F[Ca]_2+S_2+M \qquad \text{(B-4)}$$

$$F[S]_1+T_1 = F[S]_2+T_2+ T_3 \qquad \text{(B-5)}$$

$$F[CO_3]_1+X_1+M = F[CO_3]_2+X_2+X_3+N_{CO_2} \qquad \text{(B-6)}$$

$$[Ca]_2 = f_1(pH) \qquad \text{(B-7)}$$

$$[S]_2 = f_2(pH) \qquad \text{(B-8)}$$

$$[CO_3]_2 = f_3(pH) \qquad \text{(B-9)}$$

It will be shown that the pH of the liquor in the holding tank must satisfy a consistency condition and that the pH can be calculated without solving the entire set of equations.

Assume that the pH of the liquor leaving the tank is known. Then $[Ca]_2$, $[S]_2$ and $[CO_3]_2$ are given by equations (B-7), (B-8), and (B-9). Substituting these relations into the rest of the equation, we obtain:

$$S_2 = F\{[Ca]_1-[Ca]_2\}+S_1 \qquad \text{(B-10)}$$

$$T_2+T_3= F\{[S]_1-[S]_2\}+T_1 \qquad \text{(B-11)}$$

$$X_2+X_3 = F\{[CO_3]_1-[CO_3]_2\}+X_1+M-N_{CO_2} \qquad \text{(B-12)}$$

$$X_3+T_3= M \qquad \text{(B-13)}$$

$$X_2+T_2 = S_2 \qquad \text{(B-14)}$$

$$X_2/S_2-X_3/M = 0 \qquad \text{(B-15)}$$

Equation (B-11) through (B-14) can be written:

$$T_2+T_3+0+0= F\Delta S+T_1 \equiv b_1 \qquad \text{(B-16)}$$

$$0+0+X_3+X_2 = F\Delta CO_3+X_1+M-N_{CO_2} \equiv b_2 \qquad \text{(B-17)}$$

$$0+T_3+X_3+0= M \equiv b_3 \qquad \text{(B-18)}$$

$$T_2+0+0+X_2 = S_2 \equiv b_4 \qquad \text{(B-19)}$$

The augmented coefficient matrix of the above set of the equations is given as:

$$\left|\begin{array}{cccc|c} 1 & 1 & 0 & 0 & b_1 \\ 0 & 0 & 1 & 1 & b_2 \\ 0 & 1 & 1 & 0 & b_3 \\ 1 & 0 & 0 & 1 & b_4 \end{array}\right| = \left|\begin{array}{cccc|c} 1 & 1 & 0 & 0 & b_1 \\ 0 & 1 & 1 & 0 & b_3 \\ 0 & 0 & 1 & 1 & b_2 \\ 0 & -1 & 0 & 1 & b_4-b_1 \end{array}\right|$$

$$= \left|\begin{array}{cccc|c} 1 & 0 & -1 & 0 & b_1-b_3 \\ 0 & 1 & 1 & 0 & b_3 \\ 0 & 0 & 1 & 1 & b_2 \\ 0 & 0 & 1 & 1 & b_4-b_1+b_3 \end{array}\right|$$

Therefore, in order for equations (B-1) through (B-9) to be consistent and have a solution,

$$b_2 = b_4 - b_1 + b_3$$

or in terms of the definitions of the b's,

$$F\Delta CO_3 + X_1 + M - N_{CO_2} = S_2 - F\Delta S - T_1 + M$$

Substituting equation (B-10) and $S_1 = X_1 + T_1$ into the above equation gives

$$\Delta C_a - \Delta S - \Delta CO_3 + N_{CO_2}/F = 0 \qquad \text{(B-20)}$$

This is the condition for the existence of a solution to equations (B-1) through (B-9).

APPENDIX C

The Rate of Gas Absorption Accompanied by Instantaneous Irreversible Reactions in a Liquid Droplet in a Venturi Scrubber-- A Numerical Solution

As discussed in Section A of CHAPTER III, absorption of SO_2 (and CO_2) by alkaline solutions and limestone slurries may be treated as gas absorption accompanied by an instantaneous reaction. Numerical methods have been used by many investigators to solve the equations describing mass transfer under similar situations. Perry and Pigford (97) numerically solved the simultaneous partial differential equations for the penetration model of gas absorption into a liquid accompanied by a second-order reversible reaction. Brian et al. (19) also solved the penetration model for an irreversible chemical reaction and presented results for a wide range of parameters.

In this appendix, the equations describing gas absorption into a spherical liquid drop with instantaneous irreversible reaction in the liquid phase are presented. Also the equations describing mass transfer in the gas phase surrounding the liquid sphere are given along with the initial and boundary conditions appropriate for the description of gas absorption in a venturi scrubber.

When SO_2 (and CO_2) is absorbed into a liquid drop which contains an alkali reactant, instantaneous reactions such as reactions (A-2) and (A-21) in APPENDIX A will take place. Material balances on the absorbed gases and alkali reactant in the liquid sphere yield the following set of partial differential equations.

$$\frac{\partial C_A}{\partial t} = D_A\left(\frac{\partial^2 C_A}{\partial r^2} + \frac{2}{r}\cdot\frac{\partial C_A}{\partial r}\right) - k_2 C_A C_B \qquad \text{(C-1)}$$

$$\frac{\partial C_B}{\partial t} = D_B\left(\frac{\partial^2 C_B}{\partial r^2} + \frac{2}{r}\cdot\frac{\partial C_B}{\partial r}\right) - \gamma k_2 C_A C_B - \xi k_2' C_B C_G \qquad \text{(C-2)}$$

$$\frac{\partial C_G}{\partial t} = D_G\left(\frac{\partial^2 C_G}{\partial r^2} + \frac{2}{r}\cdot\frac{\partial C_G}{\partial r}\right) - k_2' C_B C_G \qquad \text{(C-3)}$$

$$\left.\begin{array}{llll} \text{I.C.} \quad : t=0\ ,\ r>0; & C_A = 0 \ , & C_B = C_{Bo}, & C_G = 0 \\ \text{B.C. I} : r=0\ ,\ t>0; & \dfrac{\partial C_A}{\partial r}=0 \ , & \dfrac{\partial C_B}{\partial r}=0\ , & \dfrac{\partial C_G}{\partial r}=0 \\ \text{B.C.II} : r=r_o,\ t>0; & C_A=C_{Ai} \ , & \dfrac{\partial C_B}{\partial r}=0\ , & C_G=C_{Gi} \end{array}\right\} \text{(C-4)}$$

In the derivation of these equations it is assumed that the reactions taking place in liquid are all second-order reactions.

The concentrations of the absorbed gases at the gas-liquid interface are not constant but change with position in the venturi scrubber. Usually the interfacial concentration of G, C_{Gi}, which is carbon dioxide in this case can be approximated by a constant since its solubility is much lower than sulfur dioxide and its partial pressure in the gas-phase is nearly constant.

If the resistance to mass transfer in the gaseous phase around the liquid drop is not negligible, boundary condition II has to be replaced by:

B.C.II′ : $r = r_o, \qquad t > 0;$

$$D_A\left(\frac{\partial C_A}{\partial r}\right) = k_G(p_A - p_{Ai}) = \frac{k_G}{H_A}(C_A^* - C_{Ai}), \quad \frac{\partial C_B}{\partial r} = 0 \qquad \text{(C-5)}$$

and the rate of absorption of species A into the liquid is given by:

$$N_A = D_A\left(\frac{\partial C_A}{\partial r}\right)_{r=r_o} \qquad \text{(C-6)}$$

The set of partial differential equations, equations (C-1) through (C-3), combined with appropriate boundary conditions can be solved numerically as described below.

Equations (C-1) through (C-3), boundary conditions (C-4) or (C-5), and equation (C-6) were approximated by an explicit finite difference discretization of these equations utilizing forward differences to approximate the time derivatives and the central differences to approximate space derivatives. By choosing $k_2 \rightarrow \infty$ and $k_2 \rightarrow \infty$, equations (C-1) through (C-3) are made to represent the case of instantaneous, irreversible reactions occurring in the liquid. For the case of constant interfacial concentration, $C_{Ai}=C_{Gi}$=constant, analytical solutions are available and the numerical solution can be checked against them. It was soon discovered, through trial and error, that an exceedingly small "net" size was necessary to ensure convergence of the numerical method to the correct solution.

APPENDIX D

Comments on the Physical and Chemical Properties used in the Mathematical Models of the Scrubbing Processes

The values of physical and chemical properties used in the simulation of the processes described in this study were evaluated as follows.

The density and viscosity of the gas and liquid phases, surface tension of liquid, thermal conductivity of the gas, diffusivities of SO_2 and CO_2 in the gas and the liquid phases were approximated by the values for air in the case of the gas phase and water in the case of the liquid phase. This is reasonable since the temperature and the pressure in the system are moderate and the concentration of dissolved components in the liquid phase are dilute. The data on these properties are quoted from standard correlations which appear in the literature (4, 48, 58, 124).

Some of the other important properties in mass transfer processes are shown below:

Diffusivities of NaOH, $Ca(OH)_2$, and HCO_3^-

The diffusion of an electrolyte is complicated by the dissociation of the molecule into ions. Conductivity measurements indicate that the various ions have different mobilities, and consequently, it might be expected that the various ions might diffuse at different rates. This would lead, however, to high local concentrations of positively and negatively charged ions, and the resulting electro-static forces would slow down the fast ions and increase the speed of slow ions. As a result, the ions actually diffuse at equal speeds, and the solution remains electrically neutral. Since the ions are smaller than the undissociated molecules, they diffuse at a greater rate.

In this study, diffusivities of NaOH, $Ca(OH)_2$, and HCO_3^- (approximated by H_2CO_3) are calculated by Nernst's equation (124) as follows:

$$D = \frac{R\ T\ U^+U^-}{U^+ + U^-}\left(\frac{1}{Z^+} + \frac{}{Z^-}\right) \qquad \text{(D-1)}$$

where U^+ and U^- = absolute velocity of the cation and anion, respectively, cm/sec, under a force of 1 dyne at infinite dilution.

Z^+ and Z^- = values of the cation and anion, respectively.

R = the gas constant, 8.314×10^7 ergs/g-mole °K.

D = diffusivity at infinite dilution, cm^2/sec

T = temperature, °K

Table D-1

Ionic Velocities U at Infinite Dilution, 18°C (124)

Cation or anion	Na+	H^+	$\frac{1}{2}Ca^{++}$	OH^-	$\frac{1}{2}CO_3^=$
U^+ or U^-	46.6	337	55.7	187	64.5

In the actual absorption calculations, the liquid phase diffusivities of the absorbed gases and the alkali reactant were assumed to be the same and equal to the mean value of the individual diffusivities.

The properties of solid lime are also important for the simulation of the holding tank in a lime slurry process.

Solubility of lime

The solubility of lime in water has been measured in many investigations and the values of the solubility are in reasonably good agreement (15). The following table provides solubility data in tabular form expressed as CaO equivalent or as $Ca(OH)_2$:

Table D-2

Solubility of Lime in Water Expressed as CaO or $Ca(OH)_2$ at Different Temperatures (15)

temperature, °C	CaO, g/l	$Ca(OH)_2$, g/l
0	0.140	0.185
20	0.125	0.165
40	1.106	0.140
60	0.088	0.116
80	0.070	0.092
100	0.054	0.071

pH of Lime Solution

The pH of $Ca(OH)_2$ solutions at 25°C has been measured (15) and this pH as a function of CaO equivalent is shown in Figure D-1. The data are also presented in tabular form below in Table D-3.

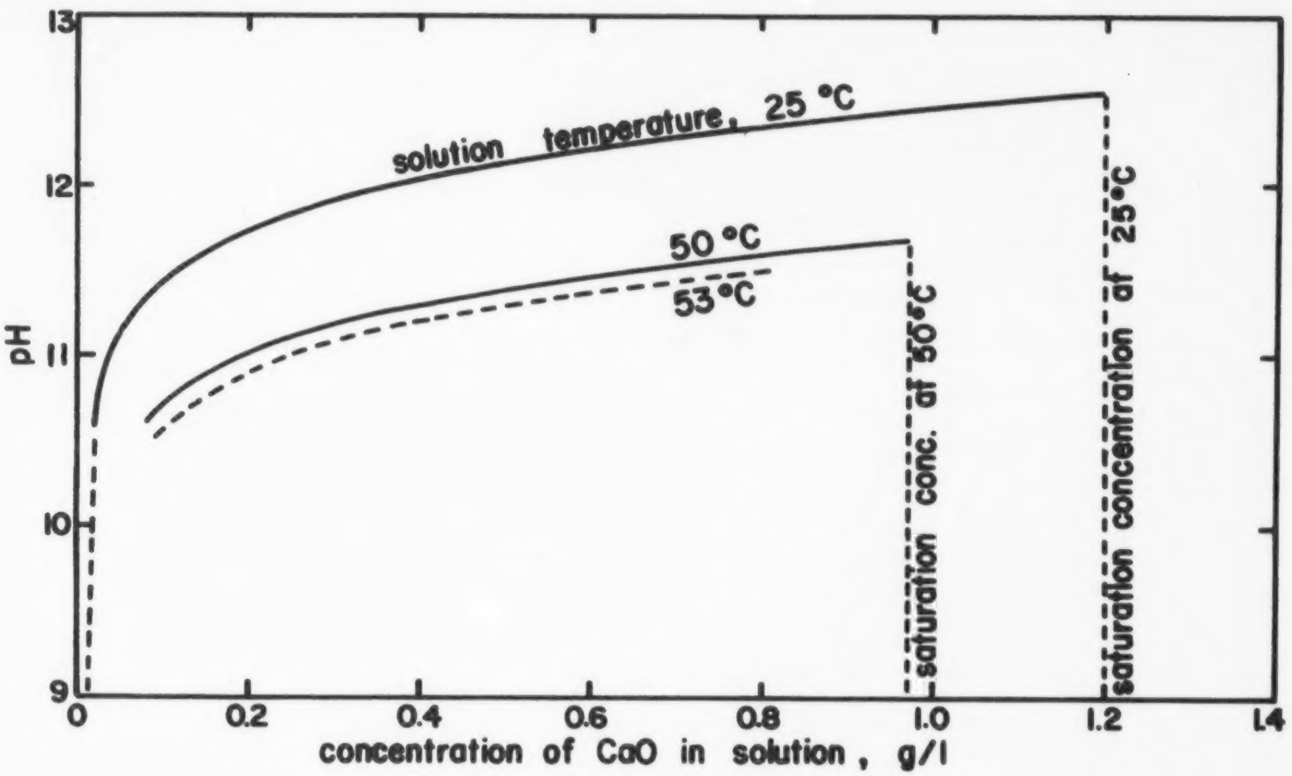

Figure D-1. pH Values of $Ca(OH)_2$ Solutions of Varying Concentration and Temperature

Table D-3

pH of Lime Solution at 25°C (15)

Concentration of CaO, g/l	pH of the solution
0.06	11.27
0.122	11.54
0.271	11.89
0.680	12.29
0.975	12.44
1.160	12.53

Examination of this table reveals that the lime in the solution is almost completely dissociated into its ionic forms. The lines for 50°C and 53°C in Figure D-1 are calculated from the ion product of water at these temperatures.